Novel pharmaceutical approaches for the promotion of dermal wound healing

PhD Thesis

Döníz Degovics, M.D.

Supervisor:

Gábor Erős, M.D. Ph.D.

University of Szeged

Faculty of Medicine

Department of Dermatology and Allergology

Doctoral School of Clinical Medicine

Szeged, Hungary

2022

LIST OF PUBLICATIONS

Full papers included in this thesis

I. Degovics D, Hartmann P, Németh IB, Árva-Nagy N, Kaszonyi E, Szél E, Strifler G, Bende B, Krenács L, Kemény L, Erős G.: A novel target for the promotion of dermal wound healing: Ryanodine receptors.

Toxicol Appl Pharmacol. 2019;366:17-24. doi: 10.1016/j.taap.2019.01.021.
IF: 3.347

II. Nguyen CM, Tartar DM, Bagood MD, So M, Nguyen AV, Gallegos A, Fregoso D, Serrano J, Nguyen D, **Degovics D**, Adams A, Harouni B, Fuentes JJ, Gareau MG, Crawford RW, Soulika AM, Isseroff RR.: Topical Fluoxetine as a Novel Therapeutic That Improves Wound Healing in Diabetic Mice.

Diabetes. 2019;68(7):1499-1507. doi: 10.2337/db18-1146.
IF: 7.720

Abstracts related to the subject of the dissertation

I. Degovics D, Hartmann P, Németh IB, Árva-Nagy N, Kemény L, Erős G: A rianodin receptorok szerepe a sebgyógyulásban. Bőrgyógy Vener Szle 89(6):p.165, 2013. (A Magyar Dermatológiai Társulat 86. Nagygyűlése, Budapest, 2013. december 12-14.)

II. Degovics D, Hartmann P, Németh I, Árva-Nagy N, Kemény L, Erős G: The effect of ryanodine receptors on dermal wound healing. Journal of Investigative Dermatology 134 (Suppl 2):S102, 2014

III. Degovics D, Hartmann P, Németh IB, Árva-Nagy N, Kemény L, Erős G: The role of ryanodine receptors in wound healing. European Surgical Research 52:178, 2014.

Other full papers

I. Szél E, Danis J, Sőrés E, Tóth D, Korponyai Cs, **Degovics D**, Prorok J, Acsai K, Dikstein S, Kemény L, Erős G: Protective effects of glycerol and xylitol in keratinocytes exposed to hyperosmotic stress.

Clin Cosmet Investig Dermatol. 2019;12:323-331. doi: 10.2147/CCID.S197946
IF: 1.970

II. Szél E, Polyánka H, Szabó K, Hartmann P, **Degovics D**, Balázs B, Németh IB, Korponyai C, Csányi E, Kaszaki J, Dikstein S, Nagy K, Kemény L, Erős G: Anti-irritant and anti-inflammatory effects of glycerol and xylitol in sodium lauryl sulphate-induced acute irritation.

J Eur Acad Dermatol Venereol. 2015;29(12):2333-41. doi: 10.1111/jdv.13225
IF: 3.029

III. Szolnoky Gy, Erős G., **Degovics D**., Németh I., Kui R., Paschali E, Vasas J, Korom E, Varga M, Kemény L: Novel aspects of lymphedema-, and venous leg ulcer-related pathomechanism and therapy
Bőr és Vener Szemle. 2019;95(2):65–68. doi 10.7188/bvsz.2019.95.2.6

Other abstracts

I. Degovics D, Erős G, Hartmann P, Gati K, Nemeth IB, Czobel M, Korponyai C, Nagy K, Kemeny L. The effects of oxygen- and hydroxyproline-containing solutions on the healing of acute wounds. Clinical Hemorheology and Microcirculation 2013; 54(2):193-194.

II. Szél E, Erős G, Hartmann P, Németh IB, **Degovics D**, Korponyai C, Dikstein S, Boros M, Nagy K, Kemény L: Anti-irritant and anti-inflammatory effects of polyols in irritant contact dermatitis. Clinical Hemorheology and Microcirculation 54(2):205, 2013.

III. Szél E, Erős G, Hartmann P, **Degovics D**, Korponyai C, Boros M, Dikstein S, Nagy K, Kemény L: Poliolok antiirritáns és gyulladáscsökkentő hatása irritatív kontakt dermatitiszben. Bőrgyógy Vener Szle 89(6):p.179, 2013. (A Magyar Dermatológiai Társulat 86. Nagygyűlése, Budapest, 2013. december 12-14.)

IV. Szél E, Erős G, Hartmann P, Németh I, **Degovics D**, Korponyai C, Kaszaki J, Polyánka H, Szabó K, Dikstein S, Nagy K, Kemény L: Poliolok antiirritáns és gyulladáscsökkentő hatása irritatív kontakt dermatitiszben. Bőrgyógy Vener Szle 90(6):p.261, 2014. (A Magyar Dermatológiai Társulat 87. Nagygyűlése, Budapest, 2014. november 27-29.)

Patent applications

I. Erős, G; Degovics, D; Hartmann, P; Kemény, L: Pharmaceutical composition comprising a ryanodine receptor antagonist for facilitating wound healing
US20160303085A1, Benyújtás éve (szabadalom): 2016, Benyújtás száma: 15/103,374, Benyújtás országa: Amerikai Egyesült Államok

II. Degovics, D; Erős, G; Hartmann, P; Kemény, L: Pharmaceutical composition comprising dantrolene analogues for treating skin wounds
HU1300720A2, Benyújtás éve (szabadalom): 2013, Benyújtás száma: P1300720, NSZO: A61K 31/4178, A61P 17/02, Ügyszám: P1300720, Benyújtás országa: Magyarország

III. Erős, G; Degovics, D; Hartmann, P; Kemény, L: Pharmaceutical compositions for facilitating wound healing
WO2015087097A2, Benyújtás éve (szabadalom): 2014, Benyújtás száma: PCT/HU2014/000124, NSZO: A61K 31/4178

IV. Erős, G; Degovics, D; Hartmann, P; Kemény, L: Pharmaceutical composition comprising a ryanodine receptor antagonist for facilitating wound healing
Benyújtás éve (szabadalom): 2016, Benyújtás száma: 201647023609, Ügyszám: 201647023609, Benyújtás országa: India

V. Erős, G; Degovics, D; Hartmann, P; Kemény, L: Pharmaceutical composition comprising a ryanodine receptor antagonist for facilitating wound healing
Benyújtás éve (szabadalom): 2016, Benyújtás száma: 201480075392.6, Ügyszám: 201480075392.6, Benyújtás országa: Kína

VI. Erős, G; Degovics, D; Hartmann, P; Kemény, L: Pharmaceutical composition comprising a ryanodine receptor antagonist for facilitating wound healing
Benyújtás éve (szabadalom): 2016, Benyújtás száma: 14837102.4, Ügyszám: 14837102.4, Benyújtás országa: Hollandia

VII. Erős, G; Degovics, D; Hartmann, P; Kemény, L: Pharmaceutical composition comprising a ryanodine receptor antagonist for facilitating wound healing
Benyújtás éve (szabadalom): 2017, Benyújtás száma: 17103927.3, Ügyszám: 17103927.3, Benyújtás országa: Hongkong

Table of contents

List of abbreviations

4-CMC: 4-chloro-m-cresol

5-HT: serotonin

5HTR: serotonin receptor

DA: dantrolene

ER: endoplasmic reticulum

FLX: Fluoxetine

Glut: glutamate

H_2O_2: hydrogen peroxide

HTR: serotonin receptor

IP3R: inositol 1,4,5-triphosphate receptor

IVM: intravital videomicroscopy

KET: ketanserin

KGM: keratinocyte growth medium

MAPK: mitogen-activated protein kinase

MPO: myeloperoxidase

NHK: neonatal human keratinocyte

NMDA: N-methyl-D-aspartate receptor

NOR: novel object recognition

P2X: P2X purinergic receptor

PEG: polyethylene glycol

RBCV: red blood cell velocity

ROS: reactive oxygen species

RyR: ryanodine receptor

SERT: serotonin reuptake transporter

SR: sarcoplasmic reticulum

SSRI: selective serotonin reuptake inhibitor

VD: vessel diameter

XOR: xanthine-oxidoreductase

1. Introduction

The skin represents the largest organ of the human body, which functions as the first line of protection from a range of external stress factors that can lead to injury. Restoration of skin integrity is a fundamental process that ensures survival. The repair response is a complex, dynamic interplay of multiple cell types. This process is divided into three overlapping phases: inflammation, proliferation, and remodeling **(Singer AJ et al., 1999)**.

The initial step that occurs after injury is hemostasis. The injured blood vessels constrict, and platelets become activated to form a fibrin clot, which serves not only as a hemostatic plug, but also provides a scaffold for incoming inflammatory cells **(Clark RA 2003)**. Neutrophil cells are immediately recruited at the wound site to destroy infectious threats. Macrophages are recruited within 24–48 h after injury **(He L et al., 2013)**. In the early stages of wound healing, pro-inflammatory macrophages phagocyte pathogens and also contribute to eliminating expended neutrophils within a few days after wounding **(Slauch JM 2011, Martin P 1997, Savill J et al., 2000)**. The adaptive immune system (T cells, dermal dendritic cells, and Langerhans cells) is activated, as well. With the resolution of inflammation, anti-inflammatory macrophages occur and contribute to angiogenesis **(Galli SJ et al., 2011, Leibovich SJ et al., 1987)**. In the phase of proliferation, activated endothelial cells break down the fibrin/fibronectin-rich clot, which serves as a scaffold for infiltrating cells, while proliferate, migrate, form new cell-cell junctions, and branch out to form new capillaries **(Eilken HM et al., 2010)**. The resident fibroblasts also invade the clot, proliferate and deposit extracellular matrix replacing the provisional matrix by contractile granulation tissue that draws the wound margins together **(Martin P 1997)**. Re-epithelialization simultaneously occurs and involves the proliferation and migration of epidermal cells from the wound edges to restore the barrier function **(Rodrigues M et al., 2019)**. The last phase of wound healing is remodeling, which lasts for several months or even years. This phase is characterized by the regression of the neovasculature, and reconstitution of granulation tissue to scar tissue, in which collagen III is partially replaced by the stronger collagen I **(Gurtner GC et al., 2008)**.

Impairment of the wound healing process can lead to chronic wounds, which is defined as a barrier defect that has not healed in 6 weeks **(Fonder MA et al., 2008)**. The most common types are diabetic foot ulcers, venous or arterial leg ulcers and pressure ulcers. Chronic wounds represent a significant source of morbidity, with more than 6 million people suffering in the U.S. alone and expenditures of ~$9.7 billion annually **(Powers JG et al., 2016)**.

Diabetes impairs each phase of wound healing. Diabetic wounds exhibit a persistent inflammatory phase, due to altered neutrophil and monocyte phenotypes, abnormalities in the expression and activity of cytokines and growth factors, the proliferation phase is characterized by endothelial cell dysfunction, impaired angiogenesis, decreased keratinocyte migration and proliferation, resulting in inadequate granulation tissue formation and reduction in wound tensile strength **(Pradhan L et al., 2007)**. Although, there has been exponential growth of research in the field of wound management over the past years, with standard of care, still only 50% of patients with diabetic foot ulcers heal, and to date, no single therapeutic agent has been successful in improving the healing rate above 50– 60% **(Otero-Viñas M et al., 2016)**. Hence, understanding of the cellular and molecular mechanisms responsible for delayed wound healing is essential to find new therapeutic approaches to promote wound healing.

Immediately after injury several damage signals are released, such as Ca^{2+} waves and hydrogen peroxide (H_2O_2) gradients **(Cordeiro JV et al., 2013)**. As a major secondary messenger, intracellular Ca^{2+} is involved in various intracellular signaling pathways e.g., excitation-contraction coupling. The main intracellular Ca^{2+} stores are the endoplasmic reticulum (ER)/sarcoplasmic reticulum (SR) and the mitochondrion. There are two major receptors regulating the Ca^{2+} release from the SR/ER, the inositol 1,4,5-triphosphate receptors (IP3Rs) **(Nixon GF et al., 1994)** and the ryanodine receptors (RyRs) **(Otsu K et al., 1990)**. In mammalian tissues, three genes encode three RyR isoforms and many types of cells express each of them. RyR1 (skeletal muscle type) and RyR2 (cardiac type) are primarily expressed in the skeletal and the cardiac muscle and they are pivotal for excitation–contraction coupling, whereas RyR3 (brain type) contributes to the intracellular calcium regulation in the brain **(Zucchi R et al., 1997, Kushnir A et al., 2010).** Recently the functional existence of RyR in epidermal keratinocytes has been demonstrated **(Denda S et al., 2012)**.

Intracellular Ca^{2+} signaling in keratinocytes is essential for cellular processes, including migration, proliferation, differentiation, barrier homeostasis and release of proinflammatory cytokines **(Graham DM et al., 2013, Tu CL et al., 2013, Denda M et al., 2003)**. It has been previously shown that activation of excitatory receptors, such as N-methyl-D-aspartate receptor (NMDA), nicotinic acetylcholine receptor, P2X purinergic receptor, and RyR induces elevation of intracellular calcium concentration and delays barrier recovery of the skin **(Denda M et al., 2002, Denda M et al., 2003, Fuziwara S et al., 2003)**. On the other hand, the inhibition of calcium channels, such as voltage-gated calcium channel, P2X receptor, and RyR accelerate barrier recovery **(Denda M et al., 2002, Denda M et al., 2006, Denda S et al., 2012)**. However,

no information is available concerning the effects of RyRs on the healing of full-thickness dermal wounds.

In addition to the above-mentioned receptors, serotonin receptors (5HTRs) and serotonin reuptake transporters (SERT), which are responsible for the uptake of serotonin from the extracellular space to the intracellular space, decreasing the extracellular serotonin concentrations, are also widely expressed on many tissues, including cells present within the skin (**Slominski A et al., 2003**). Serotonin or 5-hydroxytryptamine (5-HT) is a monoamine neurotransmitter and cytokine. Although it is mostly synthesized in the gastrointestinal mucosa and the central and peripheral nervous system, the biosynthetic pathways of serotonin have also been found in cells playing key roles in all phases of wound healing such as inflammatory cells (neutrophil granulocytes, macrophages, T lymphocytes), cutaneous human fibroblasts and keratinocytes **(Slominski A et al., 2002, Slominski A et al., 2005, Ahern GP 2011)**. There has been growing evidence that serotonin has an important role in the promotion of cutaneous wound healing **(Shah A et al., 2017)**. The importance of 5-HT in hemostasis has been well-established. In the inflammatory phase platelets release 5-HT, which enhances the recruitment of neutrophil cells and macrophages **(Duerschmied D et al., 2013)**. While in the early stages, pro-inflammatory M1 macrophages predominate, later the number of anti-inflammatory M2 macrophages increase contributing to the resolution of inflammatory responses. 5-HT modulates macrophage functions by skewing macrophages towards an anti-inflammatory M2 phenotype **(de Las Casas-Engel M et al., 2014)**. Interestingly, 5-HT has been known to promote fibroblast proliferation in vitro, and also promotes myofibroblast differentiation **(Lofdahl A et al., 2016, Mann DA et al., 2013*)***, which suggests the important role of the serotoninergic pathway in wound healing **(Slominski A et al., 2003)**. Prior studies have shown that selective serotonin reuptake inhibitors (SSRIs), for example fluoxetine (FLX) have anti-inflammatory effects such as suppression of T cell activation, cytokine secretion and proliferation **(Gobin M et al., 2013)**. The underlying mechanism is likely due to that FLX suppresses intracellular Ca^{2+} signaling by decreasing IP3- and RyR mediated Ca^{2+} release **(Gobin M et al., 2015)**. Therefore, examining SSRI local effects on chronic wounds, characterized by stalled inflammatory phase is reasonable.

These data guided the design of our studies.

2. Aims

Our principal goal was to study the effects of locally applied drugs in the process of wound healing. For this aim, *in vitro* and *in vivo* experiments were designed. The entire study was divided into 2 parts (mentioned as Study I and Study II, respectively).

In Study I, the major objectives were:

- to examine the effect of induction and inhibition of RyRs on full-thickness wounds in SKH-1 mice,
- to evaluate the rate of wound closure by means of photographic imaging and histological analysis,
- to examine the effects of 4-chloro-m-cresol (4-CMC), a RyR agonist and dantrolene (DA), a RyR antagonist on keratinocyte proliferation and monitor different parameters of the microcirculation in the wound edges with intravital videomicroscopy and laser Doppler flowmetry,
- to study the effects of the topical agents (4-CMC and DA) on the inflammation process of the healing,
- to monitor the effect of induction and inhibition of RyRs on wound closure of HaCaT cells with scratch test.

The goals of Study II were:

- to examine the effect of FLX as a topically applied drug on wound healing in db/db diabetic mice, a model for impaired wound healing,
- to evaluate the effect of FLX on keratinocyte migration using an in vitro scratch assay,
- to monitor if topical FLX treatment induces psychological effects, behavioral experiments on wounded diabetic mice treated with topically applied FLX were performed.

3. Methods

3.1. Materials

In study I. a ryanodine receptor (RyR) agonist, 4-chloro-m-cresol (4-CMC, 0.5 mM), or a RyR antagonist, dantrolene sodium salt (DA, 100 μM) was applied on the wounds of the animals. The drugs were dissolved in sterile saline. Immortalized human keratinocytes from the HaCaT-cell line after scratching were treated with 4-CMC (0.3 mM) or DA (45 μM). The drugs were dissolved in purified water before added to the culture medium. The solutions were vortexed and sonicated until DA and 4-CMC were completely dissolved. 4-CMC and DA were purchased from Sigma-Aldrich.

In study II. full-thickness excisional wounds in db/db diabetic mice were treated with either 0.02% fluoxetine (FLX) or 2% serotonin (5-HT) dissolved in 5% w/v polyethylene glycol (5% PEG). Neonatal human keratinocytes (NHKs) isolated from human foreskin after scratching were treated with different concentrations of 5-HT (1 μmol/L 5-HT, 10 μmol/L 5-HT, 100 nmol/L 5-HT) in keratinocyte growth medium (KGM).

3.2. Animals

In study I. the experiments were performed on 12-15-week-old male SKH-1 hairless mice (body weight: 36-44 g). The animals were housed in plastic cages in a thermoneutral environment with a 12 h light-dark cycle and had access to standard laboratory chow and water *ad libitum*. All interventions were in full accordance with the NIH guidelines. The procedures and protocols applied were approved by the Ethical Committee for the Protection of Animals in Scientific Research at the University of Szeged. (Permit number: V./145/2013.) Animal studies are reported in compliance with the ARRIVE guidelines **(Kilkenny C et al., 2010, McGrath JC et al., 2015)**.

In study II. the genetically diabetic male mice (db/db; BKS.Cgm+/+ *Leprdb*) were obtained from Jackson Laboratories (Bar Harbor, ME). Four animals were housed per cage presurgery and alone postsurgery, and they were maintained in an animal care facility with a 12-hour light/dark cycle throughout the acclimation (4 weeks) and test periods. The animals were 11 weeks old at the time of surgical wounding. The protocol for this experiment was approved by the Institutional Animal Care and Use Committee of University of California, Davis.

3.3. Study design

Study I.

The mice were divided into 3 treatment groups: (1) wounds were treated with sterile saline (pH=7.4); (2) wounds were treated with 4-CMC (0.5 mM, pH=6.5); (3) wounds were treated with DA (100 μM, pH=7.1). Photographs were taken every 4 days (4, 8, 12, 16 and 20), then the animals were euthanized with an overdose of ketamine and tissue samples were taken for histological analysis.

Monitoring of the microcirculation with intravital videomicroscopy (IVM) was performed on days 4, 8 and 12. In a separate group of mice laser Doppler flowmetry was performed on wounds treated with either 4-CMC or DA.

Xanthine-oxidoreductase (XOR) and myeloperoxidase (MPO) activity were measured during the inflammatory phase on days 1 and 4. 6 mice were assigned to each group and time point.

Concerning treatments, the mice were restrained with a plastic cylinder into which they were inserted. The titanium frames were fixed to an aperture on the cylinder, hereby free access was provided to the wounds. The covering glasses were removed, and sterile saline, the formulation of 4-CMC or the solution of DA was administered to the wounds with micropipette (100 μL). The covering glasses were then rapidly returned. Daily one treatment was applied in all groups. The experimental setup is shown in **Figure 1**. Groups and treatments are summarized in **Table 1**. This part of our investigation also involved *in vitro* wound-healing assays (these are described in chapter 3.11.)

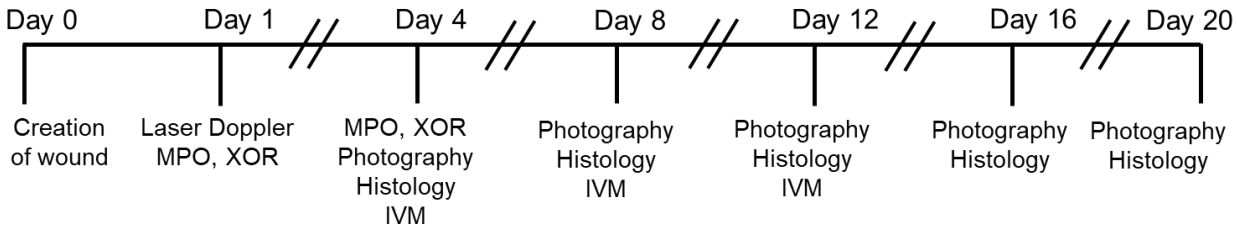

Figure 1. Experimental protocol in study I.

Group	Treatment	Observation period (days)	Method	n
1	4-CMC	1	laser Doppler	6
2	DA			6
3	NaCl	1	MPO, XOR	6
4	4-CMC			6
5	DA			6
6	NaCl	4	MPO, XOR photography histology IVM	6
7	4-CMC			6
8	DA			6
9	NaCl	8	photography histology IVM	6
10	4-CMC			6
11	DA			6
12	NaCl	12	photography histology IVM	6
13	4-CMC			6
14	DA			6
15	NaCl	16	photography histology	6
16	4-CMC			6
17	DA			6
18	NaCl	20	photography histology	6
19	4-CMC			6
20	DA			6

Table 1. Summary of research methods. DA, dantrolene; 4-CMC, 4-chloro-m-cresol; MPO, myeloperoxidase; XOR, xanthine-oxidoreductase; IVM, intravital videomicroscopy.

Study II.

Diabetic mice were randomly assigned to control or treatment groups to limit bias. Diabetic (db/db) mice (age 11 weeks, blood glucose 300 mg/dL) received two full-thickness 8-mm splinted circular excisional wounds as previously described **(Park SA et al., 2014)**. The mice were divided into 3 treatment groups: (1) wounds were treated with topically applied FLX; (2) wounds were treated with serotonin; (3) wounds were treated with vehicle control 5% w/v polyethylene glycol (PEG). Daily treatments were applied topically. On day 9, behavioral

experiments were performed. The time mice spent in light versus dark chambers was quantified, and percent time not spent in the light chamber is a measure of anxiety. Exploration ratio was used to evaluate cognitive ability in mice. On day 10 the animals were euthanized with an overdose of CO_2, wound tissue was fixed, sectioned, and stained for hematoxylin-eosin or immunohistochemistry. In this part of our investigation *in vitro* wound-healing assays were performed as well (these are described in chapter 3.12.). Groups and treatments are summarized in **Table 2**.

Group	Treatment	Observation period (days)	Method	n
1	0.02% FLX	10	behavioral experiment photography histology	9
2	2% 5-HT			9
3	5% PEG			9

Table 2. Summary of research methods. FLX, fluoxetine; 5-HT, serotonin; 5% PEG, 5% w/v polyethylene glycol.

3.4. Implantation of dorsal skin fold chamber (Study I.)

The animals were carefully examined. Mice with any type of injury or apparent sign of disorder were discarded. Prior to intervention the animals were anesthetized with a mixture of ketamine (90 mg/kg body weight) and xylazine (25 mg/kg body weight) administered intraperitoneally. The surgery was performed as described elsewhere **(Sorg H et al., 2007)**. Briefly, two holding stitches were inserted in the dorsal midline and moderate tension was exerted in order to form a skin fold. Two symmetrical titanium frames (IROLA GmbH, Schonach, Germany) were then applied to sandwich the extended double layer of the skin. The skin fold was fixed to the metal frames with sutures and sandwiched securely between the frames by means of three nuts and bolts. A circular full-thickness wound was formed on one side of the skin fold. A stamp with a diameter of 4 mm was used to determine the line of incision. The complete skin and the musculus panniculus carnosus were removed. The non-wounded skin of the opposite side still consisted of epidermis, dermis and striated skin muscle. The wounded side was treated topically with one or other of the test solutions and was then covered with a removable glass coverslip incorporated in the titanium frame. The covering glasses were removed only for the times of treatments and measurements.

3.5. Measurement of wound area (Study I.)

The animals were anesthetized before measurement, as described above. They were placed on a heating pad in a lateral position and the covering glass was removed. Photographs were taken with a camera (DiMage A200, KonicaMinolta). Photographing was performed under standard circumstances: the same light sources were used in a dark room and the camera was fixated to a stand in order to standardize the distance. The resolution of the images was 3264x2448. Planimetric analysis of the images was performed by means of a software (modification of the ImageJ) (DermAssess©) developed by our working group. This software can be utilized for the determination of an area and for the quantification of colour intensity (e.g. grade of erythema), as it has been reported in a recent study **(Erős G et al., 2014)**. The area of the wound was measured by two investigators independently and referred to the area determined on day 0 in order to calculate the rate of wound closure.

3.6. Intravital videomicroscopy (IVM) (Study I.)

The microcirculation was visualized with a fluorescence intravital videomicroscope equipped with a 100 W mercury lamp (Axiotech vario, Zeiss, Jena, Germany). The anesthetized mice received a retrobulbar injection of 80 μL 2% fluorescein isothiocyanate-labeled dextran (molecular weight 150 kD; Sigma Chemicals, USA). After this injection, a blue (450-490 nm) filter set allowed analysis of the microcirculation by the epi-illumination technique, using an Acroplan 20x water immersion objective. During examinations, the tissue was superfused with 37 °C saline. The intravital microscopic images were recorded with a charge-coupled device video camera (AVT-BC 12, AVT Horn, Aalen, Germany) attached to an S-VHS video recorder (Panasonic AG-MD830) and a personal computer. Quantitative assessment of the microcirculatory parameters was performed offline with frame-to-frame analysis, using image analysis software (IVM, Pictron Ltd., Budapest, Hungary). The following parameters were examined: the red blood cell velocity (RBCV, μm/s) was measured in the capillaries of wound edges. At least 2 separate fields of view were visualized in all quadrants of the circular wound and measurements were performed in at least 6 capillaries of all fields of view. Vessel diameter (VD, μm) was assessed by measuring of all vessels in the given fields or view except those of less than 6 μm.

3.7. Microcirculatory measurements by means of laser Doppler flowmetry (Study I.)

A non-invasive laser Doppler tissue flowmeter (PeriFlux System 5000, Perimed, Järfälla, Sweden) was used to evaluate the cutaneous microvascular blood flow. A standard pencil probe

producing laser beam was placed on the surface of the wound edge. The method is based on the reflection of a beam of laser light (780 nm). The coherent, monochromatic laser beam penetrates into the tissues and scattered by moving and stationary tissue cells. The photons scattered by red blood cells are Doppler-shifted, and the reflected light is collected by fibers coupled to a photodetector. The number of blood cells and their velocities within the measured skin volume are linearly correlated with the skin blood flow and expressed in perfusion unit (P.U.) **(Jarabin J et al., 2015, Zografos GC et al., 1992)**. We formed circular wounds as big as the probe head. We measured the flow 24 h after the surgery. First, we measured the baseline flow, and then the wounds were treated. 10 minutes later we repeated the measurements. The signal was registered for 20 seconds.

3.8. Tissue XOR activity (Study I.)

Skin biopsies kept on ice were homogenized in phosphate buffer (pH 7.4) containing 50 mM Tris–HCl (Reanal, Budapest, Hungary), 0.1 mM EDTA, 0.5 mM dithiotreitol, 1 mM phenylmethylsulfonyl fluoride, 10 μg/mL soybean trypsin inhibitor and 10 μg/mL leupeptin. The homogenate was centrifuged at 4 °C for 20 min at 24,000 g and the supernatant was loaded into centrifugal concentrator tubes. The activity of XOR was determined in the ultrafiltered supernatant by fluorometric kinetic assay based on the conversion of pterine to isoxanthopterine in the presence (total XOR) or absence (XO activity) of the electron acceptor methylene blue **(Beckman JS et al., 1989)**.

3.9. Tissue MPO activity (Study I.)

The activity of MPO, a marker of tissue leukocyte infiltration, was measured from homogenized skin biopsies by the modified method of Kuebler *et* al **(Kuebler WM et al., 1996)**. Briefly, the pellet was resuspended in K_3PO_4 buffer (0.05 mol L^{-1}; pH 6.0) containing 0.5% hexa-1,6-bisdecyltriethylammonium bromide. After 3-times repeated freeze-thaw procedures, the material was centrifuged at 4 °C for 20 min at 24,000 g and the supernatant was used for MPO determination. During the measurements, 0.15 mL of 3,3',5,5'-tetramethylbenzidine (dissolved in DMSO; 1.6 mmol L^{-1}) and 0.75 mL of hydrogen peroxide (dissolved in K_3PO_4 buffer; 0.6 mmol L^{-1}) were added to 0.1-mL samples. The reaction causes the hydrogen peroxide-dependent oxidation of tetramethylbenzidine, which can be detected spectrophotometrically at 450 nm (UV-1601 spectrophotometer; Shimadzu, Kyoto, Japan). The MPO activities of the samples were measured at 37 °C; the reaction was stopped after 5 min with 0.2 mL of H_2SO_4 (2 mol L^{-1}) and the data were referred to the protein content **(Varga G et al., 2010)**.

3.10. Routine histology and immunohistochemistry (Study I.)

The tissue in the window of the titanium chamber was excised. The biopsies were fixed in a 4% buffered solution of formaldehyde and embedded in paraffin. One slide was stained with haematoxylin-eosin (H&E), while the other was used for immunohistochemical detection of Ki-67 (Biocare Medical, Cat#: PRM 325 AA, rabbit monoclonal, prediluted) positive cells. Retrieval was performed at pH = 6 at 100°C for 20 min. The antibody was applied overnight. A Bond Polymer Refine Detection Kit (Leica Biosystems) was then used; the sections were exposed to 3,3'-diaminobenzidine (DAB) for 10 min, followed by counterstaining with haematoxylin.

The sections were subjected to histological examination with the Pannoramic Viewer software (3DHISTECH Ltd., Budapest, Hungary). In the H&E-stained sections, we measured the diameter of the wound and the length of the growing epithelial tissue on both sides. The sum of the growing epithelial tissue was referred to the initial diameter of the wound. In the Ki-67-stained slides, tissue samples were separated into 100 μm long regions. The wound area was divided into 1-4 regions, depending on the length of the growing epithelial tissue, whereas unwounded areas surrounding the wound were divided into 4 regions at each side of the wound. To analyze the epidermal proliferation in response to the treatments, we calculated the epidermal proliferation index; the amount of Ki-67-expressing basal keratinocytes were divided by the whole number of basal keratinocytes, to determine the percentage of proliferating cells as an indicator for proliferative activity **(Safferling K et al., 2013)**.

3.11. Cell culture and scratch test (Study I.)

Human HaCaT keratinocytes, kindly provided by Dr N. E. Fusenig (Heidelberg, Germany), were cultured in Dulbecco's modified Eagle's medium (DMEM) containing 10% foetal bovine serum (FBS) until reaching confluency. HaCaT keratinocytes were grown at 37°C in a 5% CO_2 atmosphere. For the experiments, cells were seeded into 24-well plates. 3 different treatments were applied by using 6 samples for each case.

Scratch wounding was performed with a cell scraper of 4 mm width, according to a well-established *in vitro* wound-healing assay **(Matsuura K et al., 2007)**. The cells were treated once daily with either 4-CMC (0.3 mM), or DA (45 μM), while the control group was left untreated. The entire area of a well was imaged using a Nikon Eclipse TS100 inverted routine microscope (Nikon Incorporation, Melville, USA) fitted with a Nikon Coolpix 4500 camera (Nikon Incorporation, Melville, USA) at the time of wounding (time 0), at 24 h, 48 h, and 72 h post-wounding. DermAssess© software was used to measure the width of the scratch.

3.12. Cell culture and scratch test (Study II.)

Keratinocyte Growth: Human keratinocytes were isolated from neonatal foreskins as we have reported previously **(Isseroff RR et al., 1987)**, under an approved exemption granted by the Internal Review Board at University of California, Davis, and cultured using a modification of the method of Rheinwald and Green **(Rheinwald JG et al., 1975**). The cells were grown in keratinocyte growth medium (KGM) (Epilife, 0.06 mM Ca^{2+}), supplemented with human keratinocyte growth supplement (0.2 ng/ml epidermal growth factor, 5 μg/ml insulin, 5 μg/ml transferrin, 0.18 μg/ml hydrocortisone, and 0.2% bovine pituitary extract) (Cascade Biologics, Inc., Portland, OR) and antibiotics (100 units/ml penicillin, 100 μg/ml streptomycin, and 0.25 μg/ml amphotericin) (Gemini Bio-Products, Inc., Calabasas, CA) at 37 °C in a humidified atmosphere of 5% CO_2. Cell strains isolated from at least three different foreskins were used in all of the experiments, performed with subcultured cells between passages 3 and 7.

Scratch Assay: Three different strains of keratinocytes were grown to confluence in KGM on 35-mm culture dishes (Fisher). The cells were either untreated (control) or treated with different concentrations of 5-HT (1 μmol/L 5-HT, 10 μmol/L 5-HT, 100 nmol/L 5-HT) in KGM at time 0. A sterile pipette tip was used to scratch three 500-μm-wide to 1-mm-wide wounds around the center of the dish, The rate of healing scratch wounds made in confluent NHK cultures was examined by previously reported techniques **(Pullar CE et al., 2006)**.

Time-lapse images of wounded cultures were every 30 min for 6 h. Healing was calculated as follows:

$$\% \text{ healed} = \frac{SAt_{=0} - SA_{t=6}}{SA_{t=0}}$$

SA represents surface area of the scratch wound gap at the 0-h (t = 0) or 6-h time point.

3.13. Splinted wound model (Study II.)

In Study II. mice were anesthetized with isofluorane using a multicircuit anesthesia system for rodents (SAA2–3, Viking Medical, Minneapolis, MN). Buprenorphine HCl (0.05 mg/kg, buprenorphine HCl injection, Ben Venue, Bedford, OH) was administered subcutaneously prior to wounding. For surgery, the dorsal surface was shaved, sterilely prepped, and draped for aseptic surgery. All wounding procedures and postoperative treatments were performed by one surgeon. Two donut-shaped splints (inner diameter of 10 mm, outer diameter of 14 mm) fabricated from a 1.6-mm thick silicone sheet (Press-to-Seal Silicone Sheet JTR-S-2.0, Grace Bio-Labs, Bend, OR) were placed bilaterally at the designated locations (centers of the wounds were located 40 mm cranial from the tail head and 10 mm lateral from the spine**)** and adhered

with cyanoacrylate adhesive (Krazy glue, Elmer's product, Inc., Columbus, OH) plus eight interrupted sutures using 6-0 nylon sutures (6-0 Ethilon Nylon Suture, Ethicon L.L.C., Cornelia, GA). A full-thickness wound including the *panniculus carnosus* layer was created within the circumference of each splint by using an 8-mm sterile skin biopsy punch and Westcott scissors (model e3322; Bausch Lomb Storz, Manchester, MO). A trimmed plastic cover slip (Fisher Scientific, Pittsburgh, PA) was placed on top of the splint, and a semi-occlusive dressing (Tegaderm Film 9506W, 3 M Health Care, St. Paul, MN) was applied circumferentially around the trunk of the animal**.** All splints and cover slips used in this study were sterilized using a hydrogen peroxide sterilization system (Sterrad 100S system, Advanced Sterilization Products, Irvine, CA) **(Park SA et al., 2014)**.

Daily treatments as indicated were applied topically. Day 10 wound tissue was fixed, sectioned, and stained for hematoxylin-eosin or immunohistochemistry. To limit potential bias in scoring results of scratch wound assays and histological evaluation of wound re-epithelialization, images were captured, coded, and scored by investigators blinded to the treatment group. To limit potential bias in the measurement of wound re-epithelialization, wounds were bisected through the center of the lesion and multiple sections obtained in order to score the section with the largest wound diameter.

3.14. Behavioral experiments (Study II.)

3.14.1. Light/dark box test

Anxiety-like behavior was tested using light/dark box test. The model is based on observations that, although rodents naturally tend to explore a novel environment, mild stressors, that is, open fields and light, inhibit their exploratory behavior. Thus, a drug-induced increase in time spent in the illuminated compartment versus the dark compartment is suggested as an index of anxiolytic activity **(Crawley JN et al., 1980, Bourin M et al., 2003)**. The test was conducted in a large cage lined with bedding containing a light (2/3) and a dark (1/3) compartment. The mouse was introduced to the light compartment to initiate the test session. The number of transitions from one compartment to the other, and the total amount of time the mouse spent in the light box were assessed. Mice were individually tested in ten-minute sessions, recorded by a video camera.

3.14.2. Novel object recognition task

The Novel Object Recognition (NOR) task is one of the most commonly used behavioral test for rodents to evaluate cognition, particularly recognition memory. This test is based on the

innate preference of rodents for novelty **(Ennaceur A 2010, Berlyne D 1950)**. It consists of three phases: training, resting and testing. During the training phase the mouse was presented with two different objects in an open field arena. Mice were videotaped for 5 min, and video records were analyzed for the number of times the mouse sniffed or touched the object while looking at it. Following the training phase, the animal was returned to his home cage for a resting period. In the testing phase the mouse was returned to the open field arena and one of the familiar objects was replaced with a novel object. Recognition memory was expressed as an exploration ratio, calculated as the frequency of exploration of a novel versus a known object **(Gareau MG 2011)**.

3.15. Statistical analysis

3.15.1. Statistical analysis of study I.

Data analysis was performed with SigmaStat for Windows (Jandel Scientific, Erkrath, Germany). Since the normality test (Shapiro-Wilk) failed in few cases, nonparametric test was chosen. Differences between groups were analyzed with Kruskal-Wallis one-way analysis of variance on ranks, followed by Dunn method for pairwise multiple comparison. In the Figures, median values with 25^{th} and 75^{th} percentiles are given, $P < 0.05$ was considered statistically significant. The data and statistical analysis comply with the recommendations on experimental design and analysis in pharmacology **(Curtis MJ et al., 2015)**.

3.15.2. Statistical analysis of study II.

Data analysis was performed using GraphPad Prism version 5.0 software (GraphPad Software, San Diego, CA). Kolmogorov-Smirnov tests were performed to verify normal distribution of each data set. For data that do not deviate from normal distribution, Student t test was used to compare each individual treatment group to the control; ANOVA was used to determine statistical significance when there were three or more groups of treatment. For data that did not pass the normality test, the nonparametric Mann-Whitney test was used to assess statistical significance. P values #0.05 were considered significant.

4. Results

4.1. Study I.

4.1.1. Inhibition of RyRs accelerates wound closure in vivo

Planimetric analysis of the wound area on digital images showed a continuous increase in epithelialization with approximately 20% wound coverage on day 4, 50% on day 8, and 80% on day 12 in the group treated with DA **(Figure 2A, 2B)**. At the end of the experiment, on day 20 all of the calcium antagonist treated wounds achieved a complete wound closure, while the 4-CMC treated animals did not.

The macroscopic finding of increased rate of wound closure in the group treated with DA was confirmed by routine histology. The growing epithelial tongues of the edges of the wounds were found significantly longer on days 4 and 8, compared to the control animals. From day 12 to 20, no significant difference was found between the groups **(Figure 3A, 3B)**.

To determine whether the accelerated wound closure can be attributed to increased proliferation, the proliferative activity of the epidermis was quantified by analyzing Ki-67-stained sections. The epidermal proliferation index was calculated on days 4, 8, 12, 16 and 20 but our results did not show significant difference temporally or spatially between the groups **(Figure 4A, 4B)**.

Fig. 2A

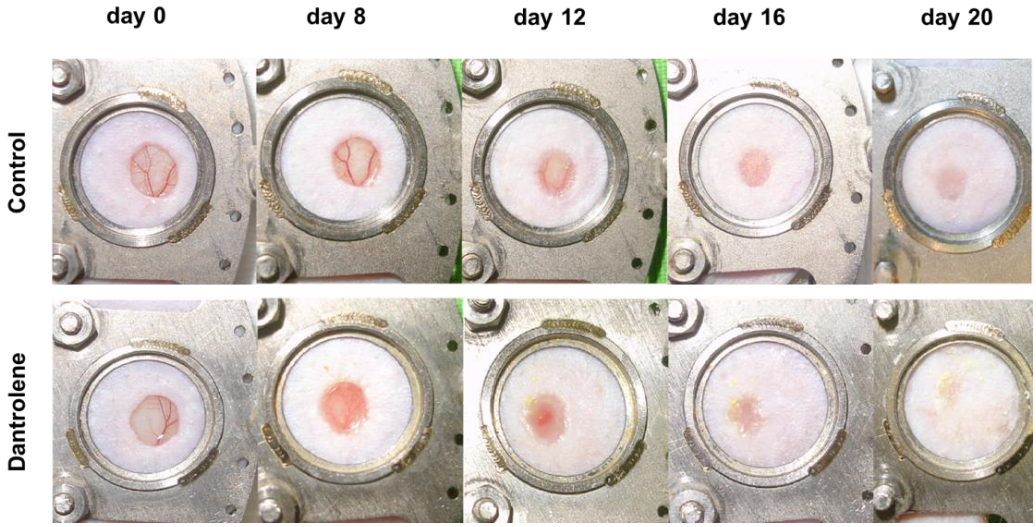

Fig. 2B

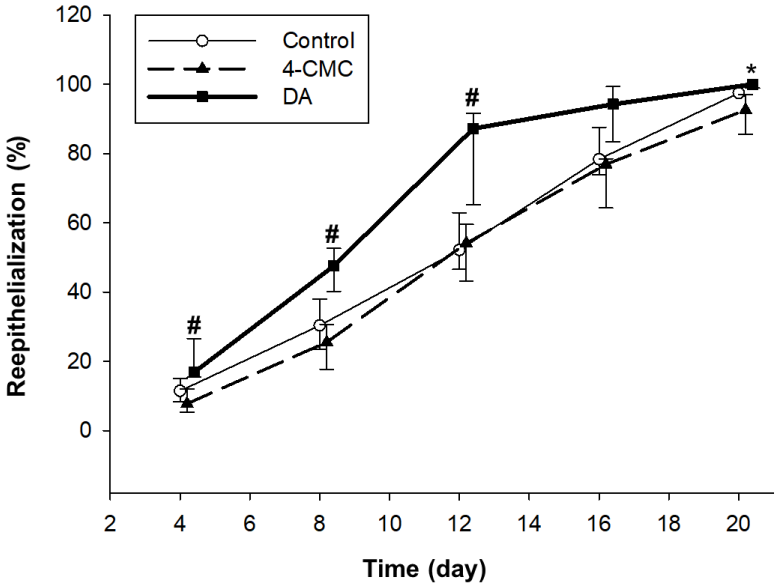

Figure 2. Inhibition of ryanodine receptors accelerates wound closure in vivo. Full-thickness excisional skin wounds were created on the backs of SKH-1 mice, topically treated with DA or 4-CMC or saline daily. Wounds were digitally photographed every 4 days. Image is representative of a healing wound in the control and the DA-treated groups (A). The extent of wound closure was expressed as the increasing coverage of the wound area referred to the size of the wound on day 0 (B). # $p<0.05$ vs control, * $p<0.05$ vs 4-CMC, n=6 (median values with 25th and 75th percentiles are given, $p<0.05$ was considered statistically significant)

Fig. 3A

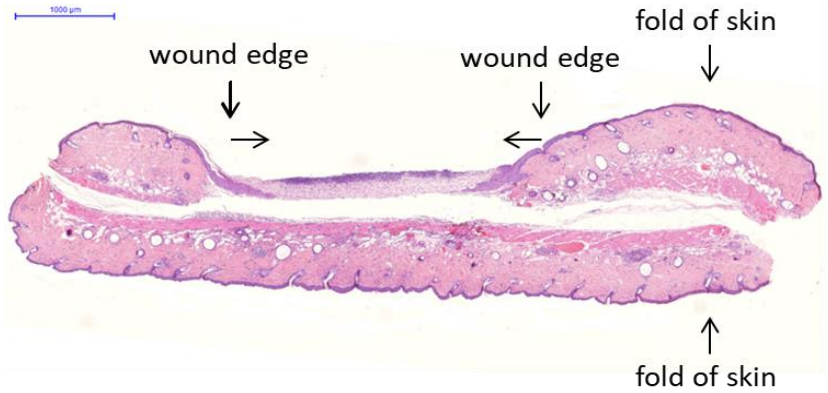

Fig. 3B

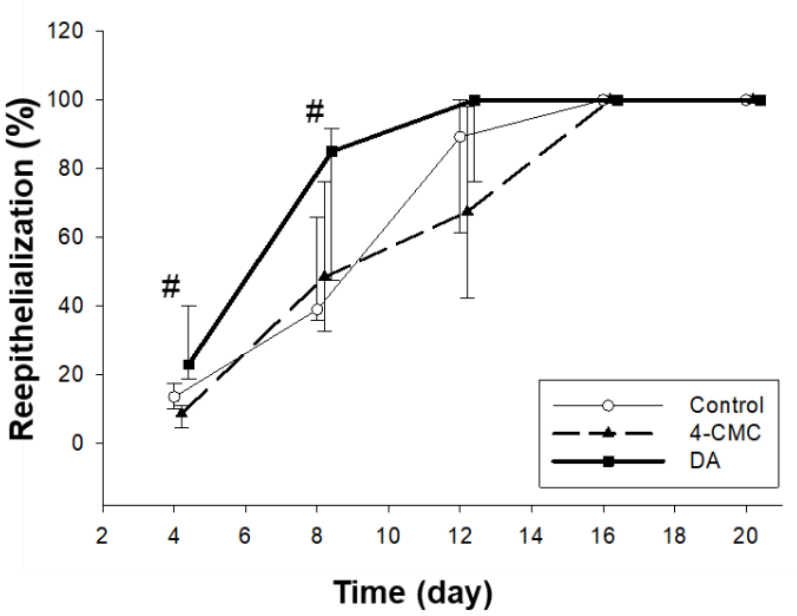

Figure 3. Analysis of histological sections shows accelerated re-epithelialization after DA treatment. Image is representative of a histological section stained with haematoxylin and eosin at day 4. Scale bar is 1000 µm, and arrows indicate the two folds of the sandwiched skin, the wound edges and the growing epithelial tissue (A). Wound closure rate during 20 days was calculated as a percentage of that at 0 h (0%) until total closure of the wound (100%) and is shown in (B). # $p<0.05$ vs control, n=6 (median values with 25th and 75th percentiles are given, $p<0.05$ was considered statistically significant)

Fig. 4A

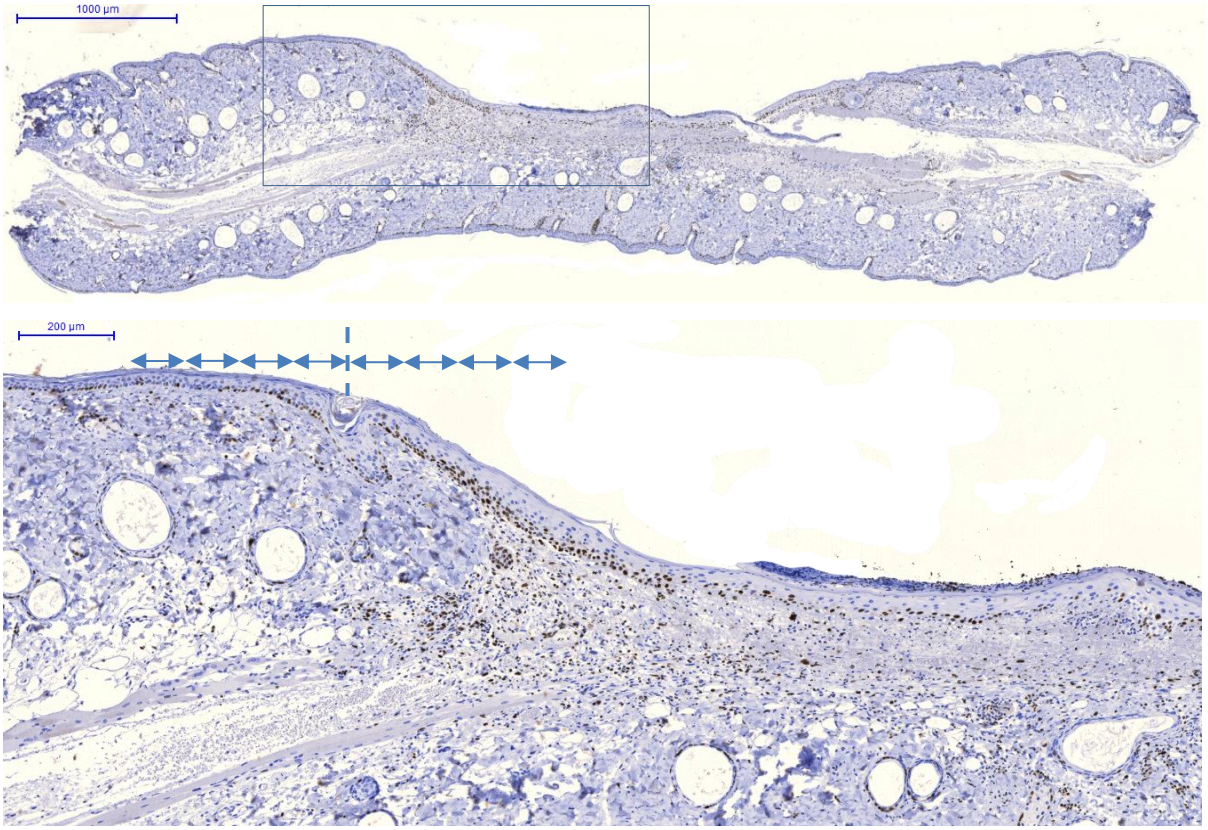

Fig. 4B

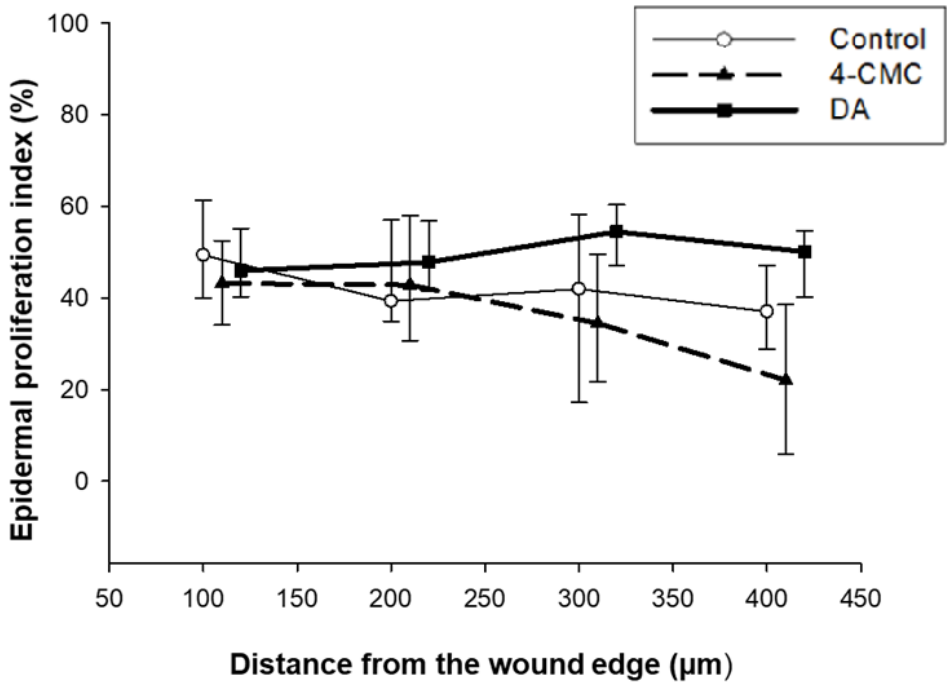

Figure 4. Representative images of Ki-67-stained wound bed sections. The wound area was divided into four regions, whereas unwounded areas surrounding the wound were also divided into four regions at each side of the wound. Broken line denotes the wound margin (A). Quantification of proliferation

by Ki-67 image processing of virtual slides on day 8. The epidermal proliferation index was calculated on days 4, 8, 12, 16 and 20 but our results did not show significant difference temporally or spatially between the groups (B). n=6 (median values with 25th and 75th percentiles are given, $p<0.05$ was considered statistically significant)

4.1.2. Wound closure of HaCaT cells is accelerated by dantrolene

We investigated the effect of DA and 4-CMC on wound closure in HaCaT cell monolayers. **Figure 5A** shows the evolution of the scratch on the cell culture. The experimental results showed that the scratch closure occurred at a significantly faster rate in the presence of DA compared to the control, and the scratch area was completely closed after 72-hour culture. In contrast, in cultures treated with 4-CMC the gap closure was delayed by 72 h **(Figure 5B)**.

Fig. 5A

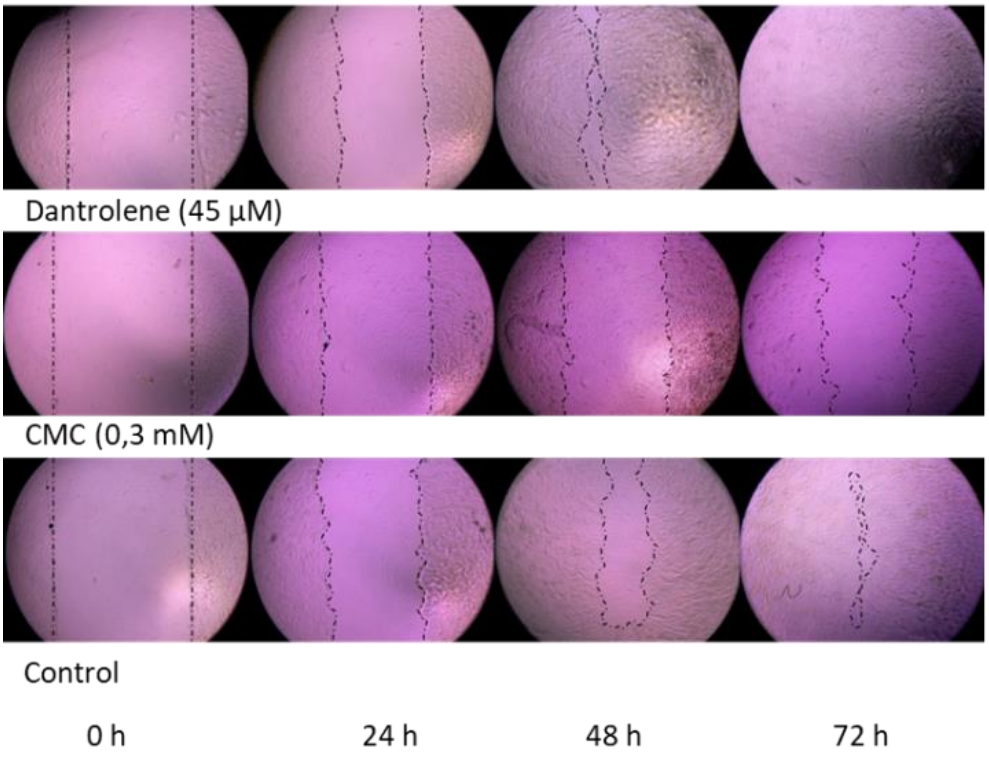

Fig. 5B

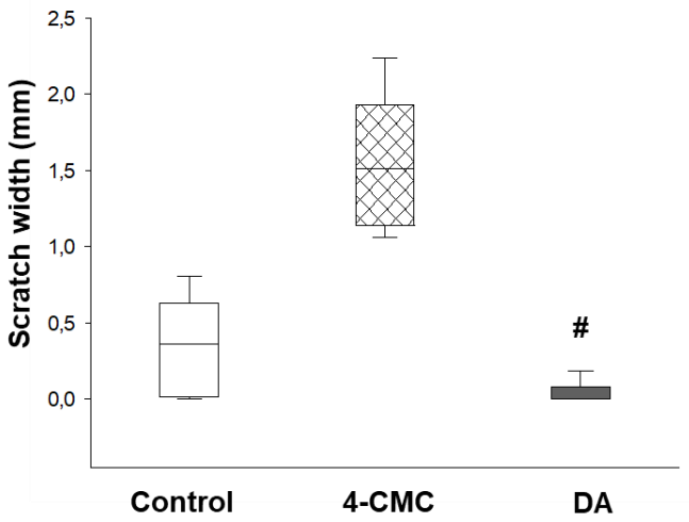

Figure 5. Wound closure of HaCaT cells is accelerated by DA. Representative microscopic images of scratch wounds at 0 hour, 24, 48, and 72 hours. The migrating edges were outlined using black dashed/dotted lines (A). The gap width was measured in mm at the time of wounding (time 0 h), at 24 h, 48 h, and 72 h post-wounding. Epithelialization rate of cultures treated with DA is significantly higher than those treated with sterile saline at 72 h (B). All data are representative of three independent experiments with n=6 per group. # $p<0.05$ vs control (median values with 25th and 75th percentiles are given, $p<0.05$ was considered statistically significant)

4.1.3. Dantrolene elevates the vessel diameter and the red blood cell velocity

The analysis of the IVM video records revealed that the vessel diameters did not display a change within the 4-CMC and the control groups during the observation period, while the calcium channel antagonist increased the vessel diameters by 25% on day 4 compared to the control group. This significant difference was also observed on day 8 (17%) and on day 12 (22%) as well **(Figure 6A)**.

It has also been shown that inhibition of the RyRs increased the red blood cell velocity in the capillaries at all times of measurements by approximately 25%, while there was no difference between the 4-CMC and the control group **(Figure 6B)**. The findings of laser Doppler flowmetry have confirmed the data obtained from IVM. The flow curves demonstrated consistent significant increases in the blood flow from baseline levels to posttreatment levels with an average of 15-fold increase in the group treated with DA **(Figure 7)**.

Fig. 6A

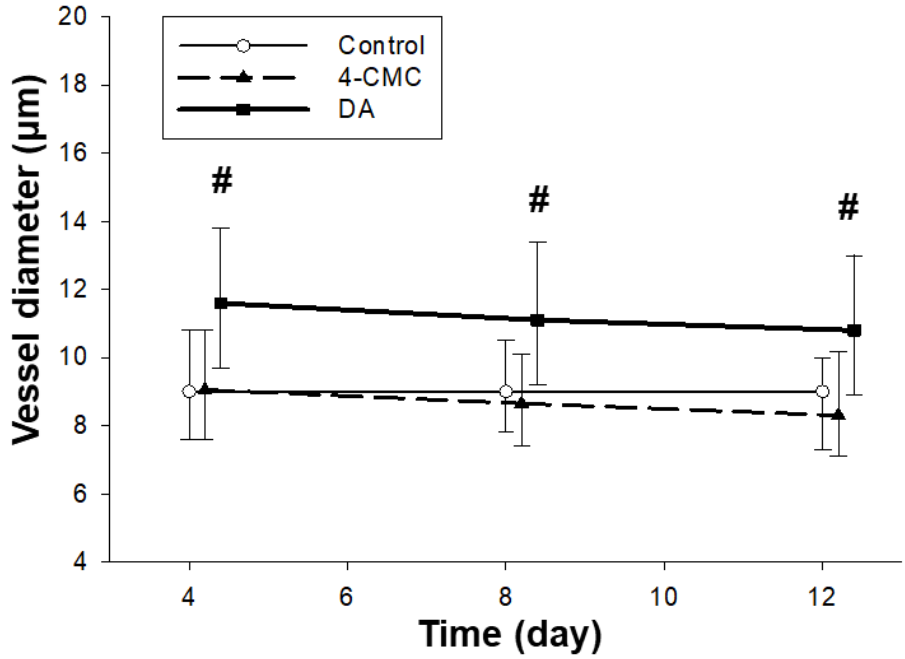

Fig. 6B

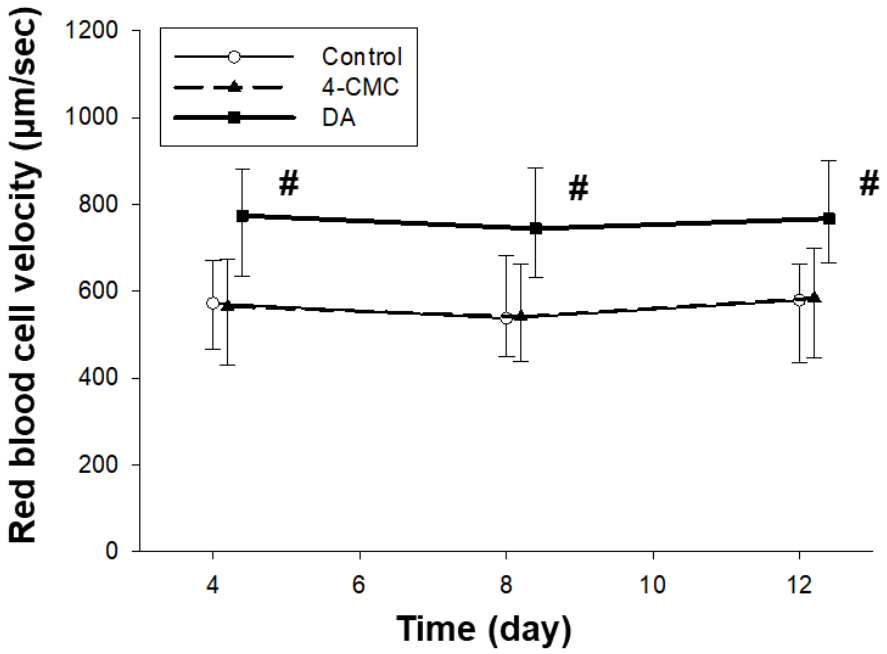

Figure 6. DA elevates the vessel diameter and the red blood cell velocity. Microcirculatory parameters were determined from fluorescein isothiocyanate-labeled dextran perfused vessels in the dorsal skin-fold. Quantitative analysis of their diameters (µm) during regeneration at days 4, 8, and 12 post wounding shows a significant increase in caliber in the DA treated mice compared to the control group (A). Red blood cell velocity in the microvasculature of calcium antagonist treated mice reached 800 µm/sec significantly differ to values in the control group (B). # $p<0.05$ vs control, n=6 (median values with 25th and 75th percentiles are given, $p<0.05$ was considered statistically significant)

Fig. 7

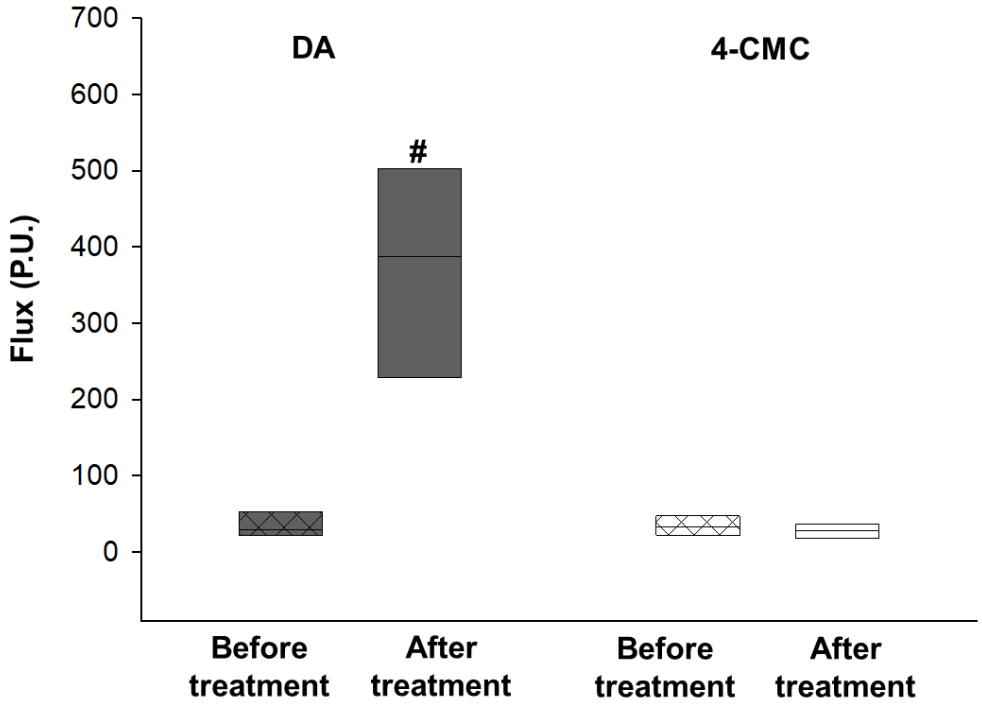

Figure 7. Laser-Doppler microvascular measurements show increased flow after DA treatment. Blood flow in the calcium antagonist treated mice 10 min post-treatment ranged between 200 P.U. and 500 P.U. significantly differ to baseline values, ranging between 20 P.U. and 30 P.U. # $p<0.05$ vs before treatment, n=6 (median values with 25th and 75th percentiles are given, $p<0.05$ was considered statistically significant)

4.1.4. Inhibition of RyRs decreases XOR activity thereby diminishing ROS production, while does not affect MPO activity and leukocyte accumulation

MPO activity, a commonly used index of inflammatory cell accumulation, was measured during the inflammatory phase of wound healing on the first and the fourth days post-wounding. According to our results no significant difference was found between the groups **(Figure 8)**. In contrast, significant reductions of XOR activity, a critical source of ROS production, were observed in the group treated with DA on days 1 and 4 as compared with the control group, while 4-CMC did not alter the enzyme activity **(Figure 9)**.

Fig. 8

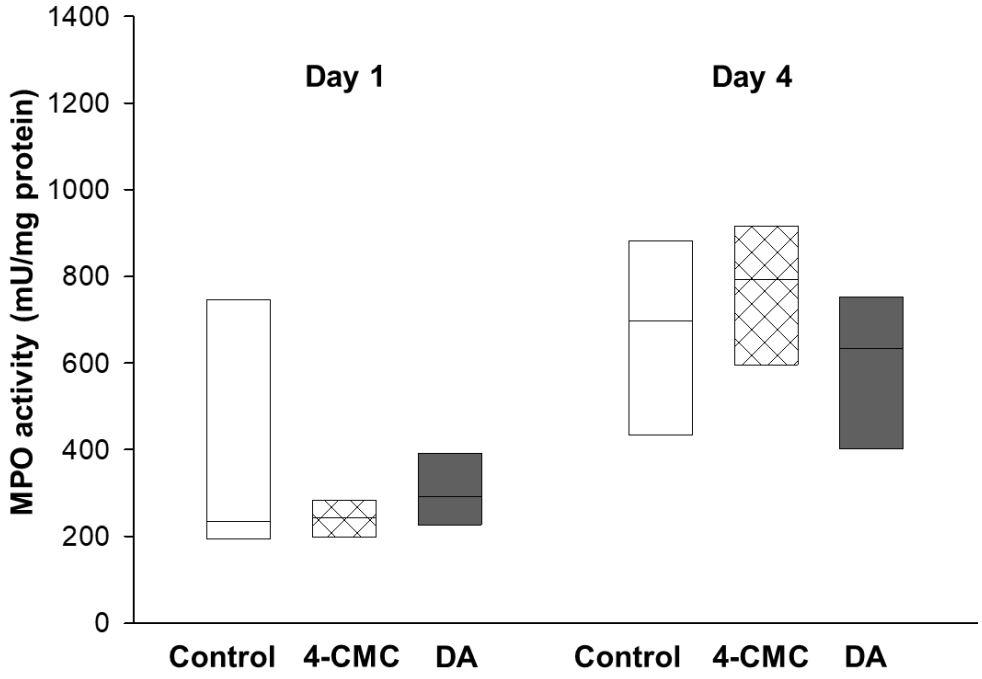

Figure 8. Inhibition of RyRs does not affect MPO activity and leukocyte accumulation. The level of MPO, a lysosomal protein highly expressed in neutrophil granulocytes and macrophages, which is used as a marker of inflammatory cell accumulation was not affected by application of DA during the inflammatory phase. n=6 (median values with 25th and 75th percentiles are given, $p<0.05$ was considered statistically significant)

Fig. 9

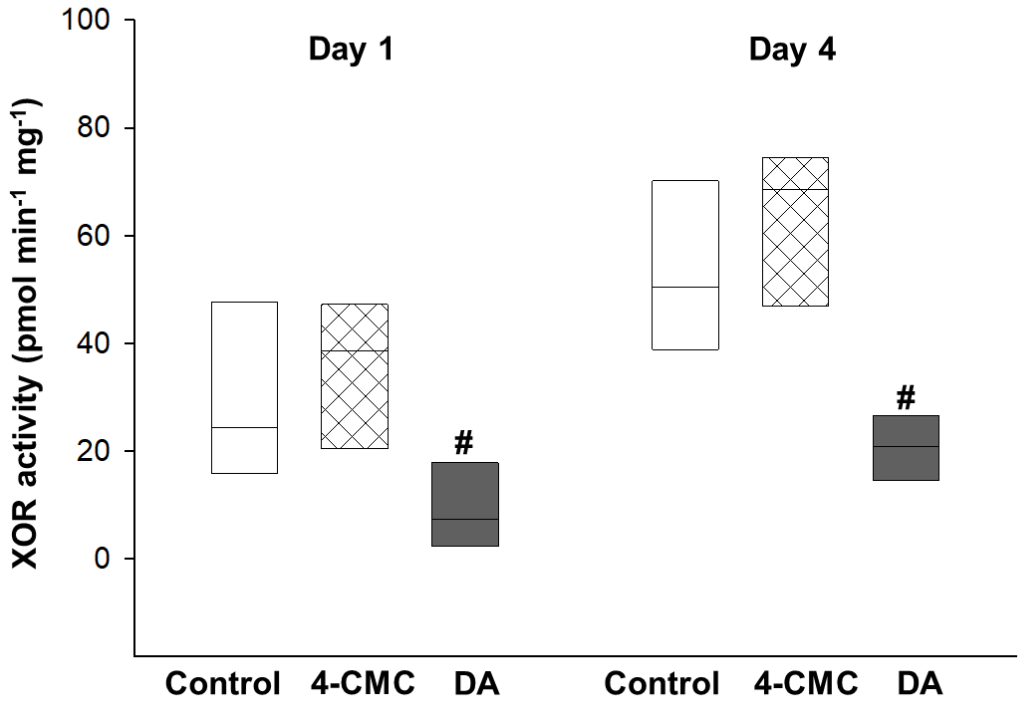

Figure 9. Inhibition of RyRs decreases XOR activity. Wounds were harvested on days 1 and 4 post-wounding. Animals were treated once a day with 4-CMC (0.5 mM, pH=6.5) or DA (100 μM, pH=7.1) or saline (control). Compared to the control group, DA produced a significant decrease in XOR activity during the inflammatory phase of wound healing in all six tissues studied at each time point. # $p<0.05$ vs control, n=6 (median values with 25th and 75th percentiles are given, $p<0.05$ was considered statistically significant)

4.2. Study II.

4.2.1. Wound closure of NHK cells is accelerated by fluoxetine in the presence of serotonin

Although human keratinocytes have been shown to express tryptophan hydroxylase gene **(Slominski A et al., 2003)**, an enzyme in the rate-limiting step in 5-HT synthesis, we did not find any 5-HT produced by keratinocytes above our lower limit of detection of 9.8 nmol/L. Thus, endogenous generation of 5-HT by keratinocytes may be too low to enhance migratory speed in FLX-treated keratinocytes in the absence of exogenous 5-HT. In the presence of 5-HT, however, FLX improved healing in treated cultures: 60.6% in the 10 nmol/L treatment group, 62.0% in the 100 nmol/L treatment group ($P = 0.01$), and 67.0% healed wound area in the 1 μmol/L FLX group ($P = 0.001$), relative to the 52.2% healing in the control cultures. To

provide further evidence that FLX is working through 5-HT-dependent pathways, scratch wound assays were repeated in the presence of the HTR2A blocker ketanserin (KET). The HTR2A blocker KET reversed the effects of FLX on wound healing in vitro, again returning wound healing to the level of the untreated control group (P = 0.948). These data demonstrate not only that FLX increases keratinocyte migration in vitro but that this is dependent upon 5-HT signaling through HTR **(Figure 10).**

Fig. 10

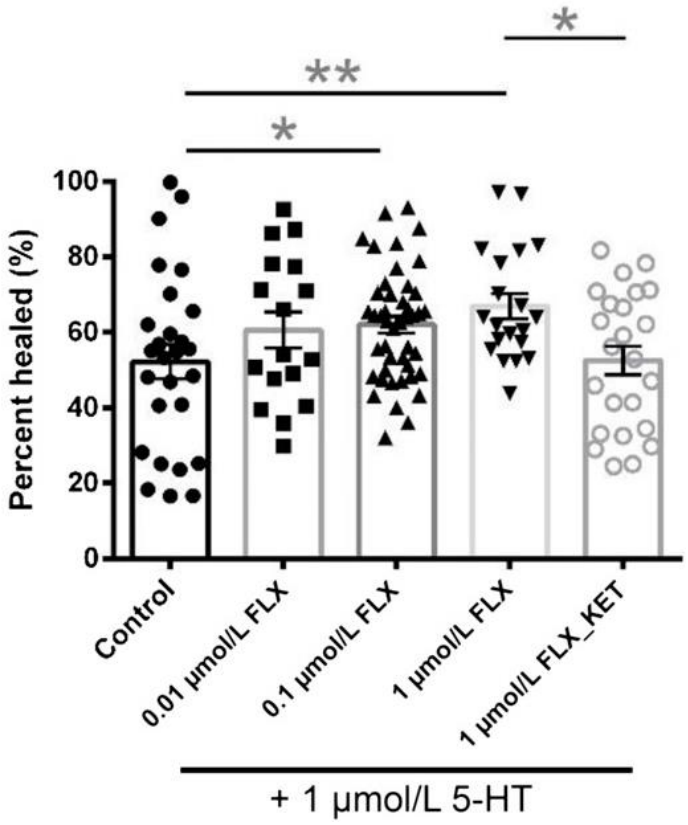

Figure 10. 5-HT and FLX increase re-epithelialization *in vitro*. Scratch wound assays were performed on confluent cultures of NHKs from three donors with different doses of FLX in the presence of 5-HT. HTR2A blocker KET was added to confirm the 5-HT-dependent mechanism. Data represented as mean ± SEM. Kolmogorov-Smirnov tests were performed to confirm normality in data distribution. Two-way ANOVAs with correction to multiple comparisons were used to assess statistical significance. *P≤0.05; **P≤0.01. n = 27/group

4.2.2. Fluoxetine promotes re-epithelialization in vivo

To test whether FLX promotes re-epithelialization in vivo, full-thickness excisional wounds in db/db diabetic mice, a model for impaired wound healing **(Park SA et al., 2014)**, were treated

with topically applied FLX, 5-HT, or vehicle control 5% w/v polyethylene glycol **(PEG)**. Wounds from mice treated with either 0.02% FLX or 2% 5-HT dissolved in 5% PEG showed less exudate compared with vehicle control counterparts at day 10 postwounding. Moreover, re-epithelialization was increased from an average of 39.6% in PEG-treated mice to 66.2% in mice treated with 0.2% FLX (P = 0.01) (**Figure 11**). Since the topical application of 5-HT did not result in statistically significant improvement in re-epithelialization, likely due to the short half-life of serotonin **(Udenfriend S et al., 1958)**, we did not further investigate its direct effects.

Fig. 11

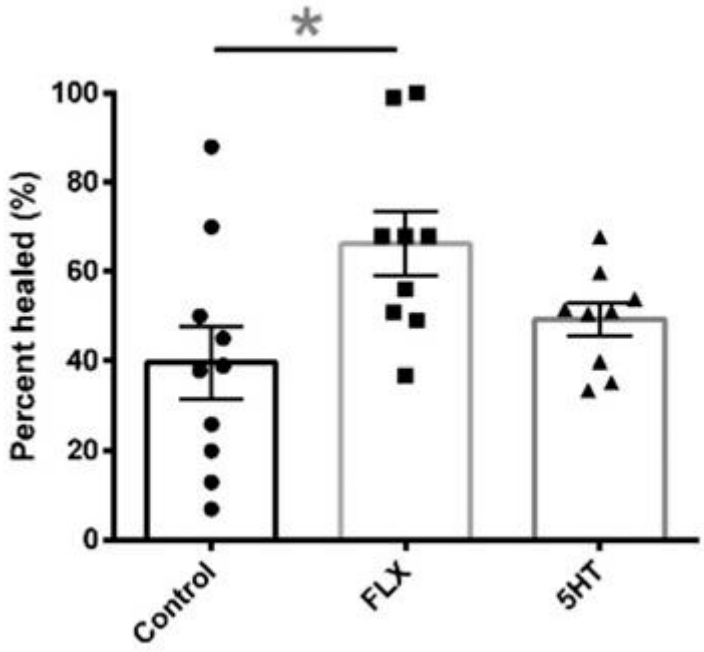

Figure 11. FLX increased wound closure *in vivo*. Average percent re-epithelialization per treatment group was quantified at day 10. Data represented as mean ± SEM. Kolmogorov-Smirnov tests were performed to confirm normality in data distribution. Student t tests were used to assessed statistical significance *P ≤ 0.05. n=9/group

4.2.3. Limited systemic effects of topically applied fluoxetine

For clinical translation of a topically administered drug, ideally, systemic absorption should be minimized to limit the side effect profile. After 10 days of daily dosing with topically applied 0.2% FLX, the levels of FLX in mouse plasma ranged from 23 to 64 ng/mL, with no change in plasma serotonin concentrations. The FLX levels measured are twofold lower than plasma levels in patients treated with oral FLX at therapeutic doses and are also significantly lower

than levels in mice treated with neurologically therapeutic doses of FLX, either orally or intraperitoneally administered **(Hodes GE et al., 2010, Dulawa SC et al., 2004)**. To further query if our topical FLX treatment induces psychological effects, we performed behavioral experiments on wounded diabetic mice treated with topically applied FLX and found that the animals treated with FLX did not exhibit significant changes in their behavior in the light/dark chamber box test, a measure of anxiety **(Bourin M et al., 2003)** (**Fig. 14C**), or in the novel object recognition test, a measure of cognition **(Ennaceur A 2010)** (**Figure 12A, 12B**). These findings indicate the potential of topically delivered FLX, contrasted to other delivery methods for improving healing with minimal systemic effects.

Fig. 12A

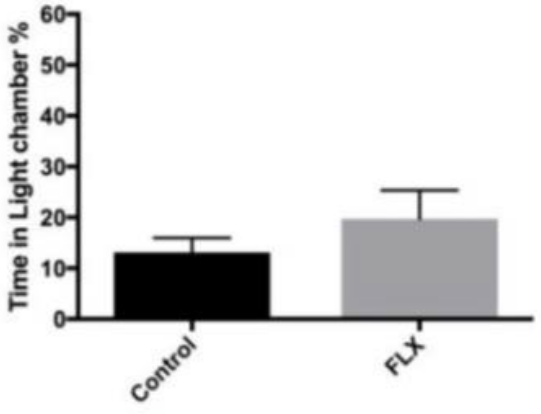

Fig. 12B

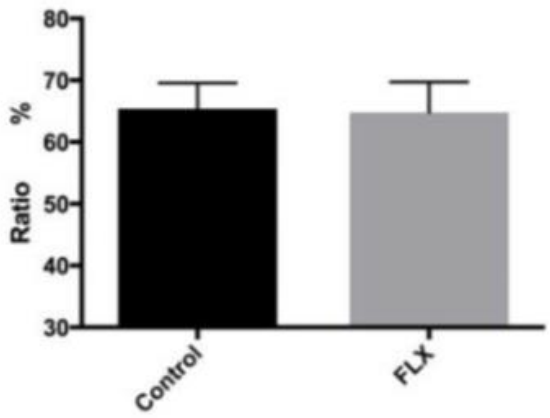

Figure 12. FLX does not alter behavior. On day 9, the time mice spent in light versus dark chambers was quantified. The results show no significant differences in the amount of time spent in the light compartment between the control and the FLX treated groups. All mice used in this study displayed a preference for the dark chamber (A). Exploration ratio, calculated as the frequency of exploration of a novel versus a known object in mice treated with vehicle control or FLX, was used to evaluate cognitive ability in mice (B). n=9/group

5. Discussion

Wounds of different type may considerably decrease the health-related quality of life and place substantial burden on healthcare system. Thus, there seems to be a need for novel therapeutic approaches accelerating the healing process. In our studies we investigated the effect of already marketed drugs - DA, a muscle-relaxant and FLX, an antidepressant - on wound healing. Our study has revealed that DA, an inhibitor of RyRs, promotes macroscopic wound closure *in vivo* and the histological examination has confirmed that this agent contributes to the process of epithelialization. Furthermore, the *in vitro* experiments have shown faster closure of the keratinocyte layer after application of DA. Regeneration of the epithelium requires tightly regulated spatiotemporal process of proliferation, migration and differentiation. Calcium signals seem to have a role in these processes. Epidermis displays a characteristic calcium gradient, with low calcium levels in the lower, basal, and spinous epidermal layers, and increasing calcium levels towards the stratum granulosum **(Menon GK et al., 1985)** that contributes to keratinocyte differentiation **(Elias PM et al., 2002)**. It has also been described that extracellular calcium triggers an increase in the level of intracellular free calcium which subsequently promotes cell differentiation **(Sharpe GR et al., 1989, Bikle DD et al., 1996)**. Since epidermal injuries disturb the calcium gradient and RyRs are known to be major mediators of calcium-induced calcium release, it seemed to be presumptive that influence of these receptors may affect wound healing. Denda *et al.,* (have shown that activation of RyRs delays the barrier regeneration while inhibition of RyRs by means of topical DA accelerates the barrier recovery **(Denda S et al., 2012)**. In the mentioned study, the injury was confined to the uppermost layer of the skin. A novelty of our investigation is the demonstration of the efficacy of DA in full thickness dermal wounds. According to our findings, inhibition of RyR contributes to the healing process via different ways. By means of immunostaining for Ki-67, we have not found significantly higher proliferation rate after application of DA. Thus, it can be assumed that increased cell migration can be responsible for the accelerated wound closure. Migration may be regulated by calcium dependent processes, but this question requires further investigation. However, our *in vivo* experiments have identified another important factor playing role in the regeneration.

The results obtained by means of IVM have shown that local application of DA led to a considerable increase in RBCV in the capillaries of the wound edge. This elevation may originate in the vasodilation of the arterioles and the relaxation of the precapillary sphincters. Measurement of vessel diameters has proven the vasodilation and the laser Doppler flowmetry

has also confirmed the elevated blood flow after inhibition of RyR. It is known that RyRs are expressed in vessels of different calibres in several organs, e.g. renal resistance arterioles, mesenteric arteries, cremaster arterioles, large cerebral arteries and in cerebral microcirculation, as well **(Arendshorst WJ et al., 2009, Borisova L et al., 2009, Westcott EB et al., 2011, Dabertrand F et al., 2013)**. RyRs play a pivotal role in the regulation of vascular tone but their effect may be diverse in different organs. Pharmacological induction of RyRs leads to contraction in the smooth muscle of guinea pig mesenteric artery **(Itoh T et al., 1981)**. The RyR antagonist ryanodine results in vasoconstriction in hamster cremaster muscle feed arteries **(Westcott EB et al., 2011)** and rat cerebral arteries **(Knot HJ et al., 1998)** while DA prevents the vasoconstriction induced by serotonin in rat basilar and femoral arteries **(Salomone S et al., 2009)**. In human, DA attenuates cerebral vasoconstriction without altering systemic physiological parameters **(Muehlschlegel S et al., 2009)**. However, the role of RyRs in the dermal microcirculation has not been known before. Our results have demonstrated that DA considerably elevates the vessel diameter and the RBCV. The increased perfusion of the wound area may thus result in a better oxygen and nutrient supply hereby contributing to a faster regeneration.

The present study has also revealed that DA has an impact on inflammation accompanying wounds. Inflammation is known to be the first phase of wound repair **(Clark RAF 1996)** and plays an important role in healing. However, an excessive inflammatory reaction may lead to chronic wound **(Schafer M et al., 2008)** and contribute to scar formation **(Reinke JM et al., 2012)**. Inflammation can be characterized with different factors e.g., inflammatory cell accumulation and production of reactive oxygen species (ROS). MPO, which is a lysosomal protein highly expressed in neutrophil granulocytes and macrophages, is a critical element of oxygen-dependent antimicrobial system in granulocytes **(Nauseef WM et al., 1995)** and can be used as a marker of inflammatory cell accumulation. XOR is a major source of ROS in macrophages, it can also be detected in keratinocytes and it is an important component of innate inflammatory signaling **(Ives A et al., 2015, Nakai K et al., 2006)**. During normal healing process, the expression of XOR is upregulated shortly after wounding **(Madigan MC et al., 2015)**. Although local application of DA has not influenced the leukocyte accumulation, it considerably moderated the ROS production. According to the literature, calcium seems to play a role in the regulation of ROS forming mechanisms. Barrier injury is followed by the release of various neurotransmitters from the epidermis e.g. ATP, dopamine and glutamate (Glut) **(Denda S et al., 2012)**. After wounding, Glut achieves high concentrations in the skin **(Albina JE et al., 1993)**. Accumulation of Glut stimulates NMDA receptors which increase the

intracellular calcium level triggering a ryanodine-gated calcium release from ER. Moreover, inhibition of NMDA receptors or RyRs suppresses ROS production in astrocytes **(Kuhlmann CR et al., 2009)**. The calcium influx may also lead to mitochondrial calcium overload which can enhance mitochondrial superoxide generation **(Hassoun SM et al., 2008)**. The mentioned processes seem to be self-propelling, because ROS-induced damage in the mitochondria leads to XO activation and further ROS production **(Gladden JD et al., 2011)**. Furthermore, exposure to ROS also activates the RyRs **(Csordas G et al., 2009)**. It can be assumed that restraining of intracellular calcium release by inhibition of RyRs results in a decrease of ROS formation.

The potential anti-inflammatory effect of DA has already been suggested by previous studies. In animal experiments, DA was found to suppress the production of pro-inflammatory cytokines (TNF-α, IL-12 and IFN-γ), to increase the quantity of anti-inflammatory cytokines (IL-10), to attenuate mitochondrial dysfunction and to improve survival in a murine model of endotoxemia **(Hassoun SM et al., 2008, Fischer DR et al., 2001, Nemeth ZH et al., 1998)**. On the other hand, activation of the RyRs with 4-CMC has not influenced the studied parameters, thus seems to have no effect on wound healing.

FLX has also been shown to exert anti-inflammatory and immunosuppressive effects. In a lipopolysaccharide-induced murine model of septic shock, FLX was found to reduce the expression of TNF-α and to improve survival **(Roumestan C et al., 2007)**. It has also been shown that FLX can suppress graft-versus-host disease **(Gobin V et al., 2013)**. Moreover, FLX has been found to reduce LPS-induced ROS/RNS generation in microglial cells and also in Huh7.5 cells stimulated with hepatitis C virus respectively **(Liu D et al., 2011, Young KC et al., 2014)**. Interestingly, a research on human T lymphocytes showed that FLX interferes with Ca^{2+} signaling by depleting Ca-stores, therefore leaving less Ca^{2+} available for release after IP3R or RyR activation, suggesting a possible mechanism behind the anti-infalmmatory effect of FLX **(Gobin M et al., 2015)**. The mentioned study also demonstrated that the depletion of Ca-stores is not 5-HT mediated. In accordance with previous studies, our analysis of wound beds by quantitative RT-PCR showed a decrease in TNF, IFN-γ, and IL-6 transcript, respectively, compared with the control group, indicating that FLX decreased inflammation in the wound bed (data not shown). In addition, our study revealed that FLX shifted the local immune milieu toward a less inflammatory phenotype in vivo by promoting the generation of pro-reparative M2 macrophages at the local wound environment (data not shown). These results are in consistent with the study by F. Su *et al*., that showed that FLX can inhibit M1 activation and improve M2 activation of microglia cells, the brain-specific macrophages **(Su F et al., 2015)**.

The present study has also revealed that signaling through serotonin pathways 5-HT in combination with FLX, improved keratinocyte migration *in vitro*. We discovered that 5-HT activated mitogen-activated protein kinase (MAPK) pathways in keratinocytes, evidenced by the increase in phosphorylation of ERK and its downstream signals STAT3 and NF-kB (data not shown). Furthermore, the *in vivo* impaired wound healing model has shown increased re-epithelialization after application of FLX.

According to our results topically applied FLX may interact with multiple pathways involved in wound healing.

In conclusion, our results have demonstrated that inhibition of calcium-induced calcium release by means of locally applied DA accelerates wound closure *in vivo* and *in vitro*. Moreover, DA increases the blood flow of the skin. We have also shown that inhibition of RyRs decreases XOR activity thereby diminishes ROS production. While there are a variety of materials available for wound care, such as dexpanthenol, sodium hyaluronate or zinc hyaluronate, which can promote wound healing by increasing fibroblast proliferation and accelerating re-epithelialization, to our knowledge there are no other agents for topical use which can additionally promote wound healing by increasing perfusion of the wound area. However, we have to mention that DA is an expensive compound, but in a previous experiment the dose-response evaluation of DA demonstrated a maximal effect in the concentration of 100 μM, which is much lower compared to dexpanthenol- or sodium hyaluronate-containing creams and ointments, which makes the final product cheaper.

In the diabetic mouse model of impaired wound healing, we have demonstrated that topical FLX improves wound healing through local effects on multiple cell types within the wound. The beneficial effects of FLX in our study appear to be independent of psychological changes. Our work has demonstrated the potential of repurposing DA, as a RyR antagonist, and FLX, an SSRI, as safe and promising therapeutic tools in order to promote dermal wound healing via different pathways.

6. Summary and new findings

Our in vivo investigation and in vitro experiments were focused on unraveling the roles of RyRs and HTR in the process of wound healing.

We have revealed that inhibition of RyRs has beneficial effects on wound healing with action on multiple targets:

- DA accelerates wound closure in vivo
- wound closure of HaCaT cells is accelerated by DA
- DA elevates the vessel diameter and the red blood cell velocity
- inhibition of RyRs decreases XOR activity thereby diminishing ROS production

We demonstrated that FLX as a topically applied drug:

- accelerates the wound closure of NHK cells in the presence of 5-HT
- FLX promotes re-epithelialization in vivo
- topically applied FLX has limited systemic effects

Hence, these topically applied drugs represent a safe alternative for the challenging clinical problem of chronic, nonhealing wounds.

7. Acknowledgements

Firstly, I wish to express my sincere gratitude to Professor Lajos Kemény for initiating my scientific career and for providing me with the opportunity to perform my scientific work at the Department of Dermatology and Allergology and for his valuable scientific guidance and help. I would like to express my special appreciation and thanks to my advisor Dr. Gábor Erős, I could not have imagined having a better advisor and mentor. His guidance helped me in all the time of research and writing of this thesis.

The authors are grateful to Mrs. Éva Sztanyik and Mrs. Kitti Gyuris for their excellent assistance in the implementation of the experiments. They thank Mrs. Erika Függ for her contribution to histology and Mr. Gábor Tax for the help in the work with cells.

The authors acknowledge Chuong Minh Nguyen, Danielle Marie Tartar, Michelle Dawn Bagood, Michelle So, Alan Vu Nguyen, Anthony Gallegos, Daniel Fregoso, Jorge Serrano, Duc Nguyen, Andrew Adams, Benjamin Harouni, Jaime Joel Fuentes, Melanie G. Gareau, Robert William Crawford, Athena M. Soulika, and Roslyn Rivkah Isseroff at the University of California, Davis, for the *in vitro* and *in vivo* experiments.

The authors acknowledge Alexander D. Borowsky and the Immunohistochemistry Laboratory at the Mouse Biology Program at the University of California, Davis, for immunohistochemical staining.

This study was funded by a California Institute for Regenerative Medicine (CIRM) Preclinical Development Award (PC1-08118), a CIRM doctoral training grant (TG2-01163), a National Institutes of Health (National Institute of General Medical Sciences) T32 pharmacology training grant (T32GM099608), and a University of California, Davis, Department of Dermatology Seed Grant.

This research was supported by the project nr. EFOP-3.6.2-16-2017-00009, titled Establishing and Internationalizing the Thematic Network for Clinical Research. The project has been supported by the European Union, co-financed by the European Social Fund and the budget of Hungary. The work was also supported by Hungarian research grant GINOP-2.3.2-15-2016-00015.

8. References

Singer A.J., Clark R.A.F.: Cutaneous wound healing. CutaneoupradSep. (1999) 341(10), 738-746.

Clark RA.: Fibrin is a many splendored thing. *J Invest Dermatol.* (2003) 121, xxi–xxii.

He L., Marneros A.G.: Macrophages are essential for the early wound healing response and the formation of a fibrovascular scar. *Am J Pathol.* (2013) 182, 2407–2417.

Slauch JM.: How does the oxidative burst of macrophages kill bacteria? Still an open question. *Mol Microbiol.* (2011) 80, 580–583.

Martin P.: Wound healing–aiming for perfect skin regeneration. *Science.* (1997) 276, 75–81.

Savill J., Fadok V.: Corpse clearance defines the meaning of cell death. *Nature.* (2000) 407, 784–788.

Galli S.J., Borregaard N., Wynn T.A.: Phenotypic and functional plasticity of cells of innate immunity: macrophages, mast cells and neutrophils. *Nat Immunol.* (2011) 12, 1035–1044.

Leibovich S.J., Polverini P.J., Shepard H.M., et al.: Macrophage- induced angiogenesis is mediated by tumour necrosis factor-alpha. *Nature.* (1987) 329, 630–632.

Eilken H.M., Adams R.H.: Dynamics of endothelial cell behavior in sprouting angiogenesis. *Curr Opin Cell Biol.* (2010) 22, 617–625.

Rodrigues M., Kosaric N., Bonham C.A., et al.: Wound Healing: A Cellular Perspective. *Physiol Rev.* (2019) 99(1), 665-706.

Gurtner G.C., Werner S., Barrandon Y., et al.: Wound repair and regeneration. *Nature.* (2008) 453, 314–321.

Fonder MA, Lazarus GS, Cowan DA. Treating the chronic wound: A practical approach to the care of nonhealing wounds and wound care dressings. *J Am Acad Dermatol.* (2008) 58(2), 185-206.

Jung K., Covington S., Sen C.K., et al.: Rapid identification of slow healing wounds. *Wound Repair Regen.* (2016) 24, 181–188.

Powers J.G., Higham C., Broussard K., et al.: Wound healing and treating wounds: chronic wound care and management. *J Am Acad Dermatol.* (2016) 74, 607–625.

Leena P., Nicholas D.A., Frank W.: LoGerfo and Aristidis Veves, “Molecular Targets for Promoting Wound Healing in Diabetes”, Recent Patents on Endocrine. *Metabolic & Immune Drug Discovery.* (2007) 1, 1.

Otero-Viñas M., Falanga V.: Mesenchymal stem cells in chronic wounds: the spectrum from basic to advanced therapy. *Adv Wound Care (New Rochelle).* (2016) 5, 149–163.

Cordeiro J.V., Jacinto A.: The role of transcription-independent damage signals in the initiation of epithelial wound healing. *Nat Rev Mol Cell Biol.* (2013) 14(4), 249–262.

Nixon G.F., Mignery G. A., Somlyo A. V.: Immunogold localization of inositol 1,4,5-trisphosphate receptors and characterization of ultrastructural features of the sarcoplasmic reticulum in phasic and tonic smooth muscle. *J Muscle Res Cell Motil.* (1994) 15, 682-700.

Otsu K., Willard H. F., Khanna V. K., et al.: Molecular cloning of cDNA encoding the Ca2+ release channel (ryanodine receptor) of rabbit cardiac muscle sarcoplasmic reticulum. *J Biol Chem.* (1990) 265, 13472-13483.

Zucchi R., Ronca-Testoni S.: The sarcoplasmic reticulum Ca2+ channel/ryanodine receptor: modulation by endogenous effectors, drugs and disease states. *Pharmacol Rev.* (1997) 49, 1-51.

Kushnir A., Betzenhauser M. J., Marks A. R.: Ryanodine receptor studies using genetically engineered mice. *FEBS Lett.* (2010) 584, 1956-1965.

Denda S., Kumamoto J., Takei K., et al.: Ryanodine receptors are expressed in epidermal keratinocytes and associated with keratinocyte differentiation and epidermal permeability barrier homeostasis. *J Invest Dermatol.* (2012) 132, 69-75.

Graham D.M., Huang L., Robinson K. R., et al.: Epidermal keratinocyte polarity and motility require Ca(2)(+) influx through TRPV1. *J Cell Sci.* (2013) 126, 4602-4613.

Tu C.L., Bikle D. D.: Role of the calcium-sensing receptor in calcium regulation of epidermal differentiation and function. *Best Pract Res Clin Endocrinol Metab.* (2013) 27, 415-427.

Denda M., Fuziwara S., Inoue K.: Influx of calcium and chloride ions into epidermal keratinocytes regulates exocytosis of epidermal lamellar bodies and skin permeability barrier homeostasis. *J Invest Dermatol.* (2003) 121, 362-367.

Denda M., Inoue K., Fuziwara S., et al.: P2X purinergic receptor antagonist accelerates skin barrier repair and prevents epidermal hyperplasia induced by skin barrier disruption. *J Invest Dermatol.* (2002) 119, 1034-1040.

Fuziwara S., Inoue K., Denda M.: NMDA-type glutamate receptor is associated with cutaneous barrier homeostasis. *J Invest Dermatol.* (2003) 120, 1023-1029.

Denda M., Fujiwara S., Hibino T.: Expression of voltage-gated calcium channel subunit alpha1C in epidermal keratinocytes and effects of agonist and antagonists of the channel on skin barrier homeostasis. *Exp Dermatol.* (2006) 15, 455-460.

Slominski A, Pisarchik A, Zbytek B, et al.: Functional activity of serotoninergic and melatoninergic systems expressed in the skin. *J Cell Physiol.* (2003) 196, 144–153.

Slominski A, Pisarchik A, Semak I, et al.: Serotoninergic and melatoninergic sys- tems are fully expressed in human skin. *FASEB J.* (2002) 16, 896-898.

Slominski A, Wortsman J, Tobin D.J.: The cutaneous serotoninergic/melatoninergic system: securing a place under the sun. *FASEB J.* (2005) 19, 176-194.

Ahern G.P.: 5-HT and the immune system. *Curr Opin Pharmacol.* (2011) 11, 29-33.

Shah A., Amini-Nik S.: The role of serotoninergic system in skin healing. *Int J Drug Res Tech.* (2017) 7, 8.

Duerschmied D., Suidan G.L., Demers M., et al.: Platelet serotonin promotes the recruitment of neutrophils to sites of acute inflammation in mice. *Blood.* (2013) 121, 1008-1015.

de Las Casas-Engel M., Corbi A. L.: Serotonin modulation of macrophage polarization: inflammation and beyond. *Adv Exp Med Biol.* (2014) 824, 89–115.

Lofdahl A, Rydell-Tormanen K, Muller C, et al.: 5-HT2B receptor antagonists attenuate myofibroblast differentiation and subsequent fibrotic responses in vitro and in vivo. *Physiol Rep.* (2016) 4.

Mann D.A., Oakley F.: Serotonin paracrine signaling in tissue fibrosis. *Biochim Biophys Acta*. (2013) 1832, 905-910.

Gobin V., Van Steendam K., Fevery S., et al.: Fluoxetine reducesmurine graft-versus-host disease by induction of T cell immunosuppression. *J Neuroimmune Pharmacol.* (2013) 8, 934–943.

Gobin M., De Bock B.J.G., Broeckx M., et al.: Fluoxetine suppresses calcium signaling in human T lymphocytes through depletion of intracellular calcium stores. *Cell Calcium.* (2015) 58(3), 254-263.

Kilkenny C., Browne W., Cuthill I. C., et al.: Animal research: reporting in vivo experiments: the ARRIVE guidelines. *Br J Pharmacol.* (2010) 160, 1577-1579.

McGrath J.C., Lilley E.: Implementing guidelines on reporting research using animals (ARRIVE etc.): new requirements for publication in BJP. *Br J Pharmacol.* (2015) 172, 3189-3193.

Park S.A., Teixeira L.B., Raghunathan V.K., et al.: Full-thickness splinted skin wound healing models in db/db and heterozygous mice: implications for wound healing impairment. *Wound Repair Regen.* (2014) 22, 368–380.

Sorg H., Krueger C., Vollmar B.: Intravital insights in skin wound healing using the mouse dorsal skin fold chamber. *J Anat.* (2007) 211, 810-818.

Erős G., Kurgyis Z., Németh I.B., et al.: The irritant effects of pharmaceutically applied surfactants. *Journal of Surfactant and Detergens.* (2014) 17, 67-70.

Jarabin J., Bere Z., Hartmann P., et al.: Laser-Doppler microvascular measurements in the peri-implant areas of different osseointegrated bone conductor implant systems. *Eur Arch Otorhinolaryngol.* (2015) 272, 3655-3662.

Zografos G.C., Martis K., Morris D.L.: Laser Doppler flowmetry in evaluation of cutaneous wound blood flow using various suturing techniques. *Ann Surg.* (1992) 215, 266-268.

Beckman J.S., Parks D.A., Pearson J.D., et al.: A sensitive fluorometric assay for measuring xanthine dehydrogenase and oxidase in tissues. *Free Radic Biol Med.* (1989) 6, 607-615.

Kuebler W.M., Abels C., Schuerer L., et al.: Measurement of neutrophil content in brain and lung tissue by a modified myeloperoxidase assay. *Int J Microcirc Clin Exp.* (1996) 16, 89-97.

Varga G., Erces D., Fazekas B., et al.: N-Methyl-D-aspartate receptor antagonism decreases motility and inflammatory activation in the early phase of acute experimental colitis in the rat. *Neurogastroenterol Motil.* (2010) 22, 217-225, e68.

Safferling K., Sutterlin T., Westphal K., et al.: Wound healing revised: a novel reepithelialization mechanism revealed by in vitro and in silico models. *J Cell Biol.* (2013) 203, 691-709.

Matsuura K., Kuratani T., Gondo T., et al.: Promotion of skin epithelial cell migration and wound healing by a 2-benzazepine derivative. *Eur J Pharmacol.* (2007) 563, 83-87.

Isseroff R.R., Ziboh V.A., Chapkin R.S., et al.: *J. Lipid Res.* (1987) 28, 1342–1349.

Rheinwald J. G., Green H.: Serial cultivation of strains of human epidermal keratinocytes: the formation of keratinizing colonies from single cells. *Cell.* (1975) 6, 331–343.

Pullar C.E., Grahn J.C., Liu W., et al.: Beta2-adrenergic receptor activation delays wound healing. *FASEB J.* (2006) 20, 76–86.

Crawley J.N., Goodwin F.K.: Preliminary report of a simple animal behaviour for the anxiolytic effects of benzodiazepines. *Pharmacol Biochem Behav.* (1980) 13, 167–170.

Bourin M., Hascoet M.: The mouse light/dark box test. *Eur J Pharmacol.* (2003) 463, 55–65.

Ennaceur A.: One-trial object recognition in rats and mice: Methodological and theoretical issues. *Behav Brain Res.* (2010) 215(2), 244-254.

Berlyne D.: Novelty and curiosity as determinants of exploratory behavior. *Br J Psychol.* (1950) 41(1-2), 68-80.

Gareau M.G, Wine E., Rodrigues D.M., et al.: Bacterial infection causes stressinduced memory dysfunction in mice. *Gut.* (2011) 60, 307–317.

Curtis M.J., Bond R. A., Spina D., et al.: Experimental design and analysis and their reporting: new guidance for publication in BJP. *Br J Pharmacol.* (2015) 172, 3461-3471.

Slominski A., Pisarchik A., Johansson O., et al.: Tryptophan hydroxylase expression in human skin cells. *Biochim Biophys Acta.* (2003) 1639, 80–86.

Udenfriend S., Weissbach H.: Turnover of 5-hydroxytryptamine (serotonin) in tissues. *Proc Soc Exp Biol Med.* (1958) 97, 748–751.

Hodes G.E., Hill-Smith T.E., Suckow R.F., et al.: Sex-specific effects of chronic fluoxetine treatment on neuroplasticity and pharmacokinetics in mice. *J Pharmacol Exp Ther.* (2010) 332, 266–273.

Dulawa S.C., Holick K.A., Gundersen B., et al.: Effects of chronic fluoxetine in animal models of anxiety and depression. *Neuropsychopharmacology.* (2004) 29, 1321–1330

Menon G.K., Grayson S., Elias P.M.: Ionic calcium reservoirs in mammalian epidermis: ultrastructural localization by ion-capture cytochemistry. *J Invest Dermatol.* (1985) 84, 508-512.

Elias P.M., Ahn S.K., Denda M., et al.: Modulations in epidermal calcium regulate the expression of differentiation-specific markers. *J Invest Dermatol.* (2002) 119, 1128-1136.

Sharpe G.R., Gillespie J.I., Greenwell J.R., et al.: An increase in intracellular free calcium is an early event during differentiation of cultured human keratinocytes. *FEBS Lett.* (1989) 254, 25-28.

Bikle D.D., Ratnam A., Mauro T., et al.: Changes in calcium responsiveness and handling during keratinocyte differentiation. Potential role of the calcium receptor. *J Clin Invest.* (1996) 97, 1085-1093.

Arendshorst W.J., Thai T. L.: Regulation of the renal microcirculation by ryanodine receptors and calcium-induced calcium release. *Curr Opin Nephrol Hypertens.* (2009) 18, 40-49.

Borisova L., Wray S., Eisner D.A., et al.: How structure, Ca signals, and cellular communications underlie function in precapillary arterioles. *Circ Res.* (2009) 105, 803-810.

Westcott E.B., Jackson W.F.: Heterogeneous function of ryanodine receptors, but not IP3 receptors, in hamster cremaster muscle feed arteries and arterioles. *Am J Physiol Heart Circ Physiol.* (2011) 300, H1616-H1630.

Dabertrand F., Nelson M.T., Brayden J.E.: Ryanodine receptors, calcium signaling, and regulation of vascular tone in the cerebral parenchymal microcirculation. *Microcirculation.* (2013) 20, 307-316.

Itoh T., Kuriyama H., Suzuki H.: Excitation--contraction coupling in smooth muscle cells of the guinea-pig mesenteric artery. *J Physiol.* (1981) 321, 513-535.

Knot H.J., Standen N.B., Nelson M.T.: Ryanodine receptors regulate arterial diameter and wall [Ca2+] in cerebral arteries of rat via Ca2+-dependent K+ channels. *J Physiol.* (1998) 508, 211-221.

Salomone S., Soydan G., Moskowitz M.A., et al.: Inhibition of cerebral vasoconstriction by dantrolene and nimodipine. *Neurocrit Care.* (2009) 10, 93-102.

Muehlschlegel S., Rordorf G., Bodock M., et al.: Dantrolene mediates vasorelaxation in cerebral vasoconstriction: a case series. *Neurocrit. Care.* (2009) 10, 116-121.

Clark R.A.F.: Wound repair; overview and general considerations. In The Molecular and Cellular Biology of Wound Repair. (1996) 3-50. Plenum Press, London.

Schafer M., Werner S.: Oxidative stress in normal and impaired wound repair. *Pharmacol Res.* (2008) 58, 165-171.

Reinke J.M., Sorg H.: Wound repair and regeneration. *Eur Surg Res.* (2012) 49, 35-43.

Nauseef W.M., McCormick S.J., Clark R.A.: Calreticulin functions as a molecular chaperone in the biosynthesis of myeloperoxidase. *J Biol Chem.* (1995) 270, 4741-4747.

Ives A., Nomura J., Martinon F., et al.: Xanthine oxidoreductase regulates macrophage IL1beta secretion upon NLRP3 inflammasome activation. *Nat Commun.* (2015) 6, 6555.

Nakai K., Kadiiska M.B., Jiang J.J., et al.: Free radical production requires both inducible nitric oxide synthase and xanthine oxidase in LPS-treated skin. *Proc Natl Acad Sci USA.* (2006) 103, 4616-4621.

Madigan M.C., McEnaney R.M., Shukla A.J., et al.: Xanthine Oxidoreductase Function Contributes to Normal Wound Healing. *Mol Med.* (2015) 21, 313-322.

Albina J.E., Abate J. A., Mastrofrancesco B.: Role of ornithine as a proline precursor in healing wounds. *J Surg Res.* (1993) 55, 97-102.

Kuhlmann C.R., Zehendner C.M., Gerigk M., et al.: MK801 blocks hypoxic blood-brain-barrier disruption and leukocyte adhesion. *Neurosci Lett.* (2009) 449, 168-172.

Hassoun S.M., Marechal X., Montaigne D., et al.: Prevention of endotoxin-induced sarcoplasmic reticulum calcium leak improves mitochondrial and myocardial dysfunction. *Crit Care Med.* (2008) 36, 2590-2596.

Gladden J.D., Zelickson B.R., Wei C.C., et al.: Novel insights into interactions between mitochondria and xanthine oxidase in acute cardiac volume overload. *Free Radic Biol Med.* (2011) 51, 1975-1984.

Csordas G., Hajnoczky G.: SR/ER-mitochondrial local communication: calcium and ROS. *Biochim Biophys Acta.* (2009) 1787, 1352-1362.

Fischer D.R., Sun X., Williams A.B., et al.: Dantrolene reduces serum TNFalpha and corticosterone levels and muscle calcium, calpain gene expression, and protein breakdown in septic rats. *Shock.* (2001) 15, 200-207.

Nemeth Z.H., Hasko G., Szabo, C., et al.: Calcium channel blockers and dantrolene differentially regulate the production of interleukin-12 and interferon-gamma in endotoxemic mice. *Brain Res Bull.* (1998) 46, 257-261.

Roumestan C, Michel A, Bichon F, et al.: Antiinflammatory properties of desipramine and fluoxetine. *Respir Res.* (2007) 8, 35.

Liu D., Wang Z., Liu S., et al.: Anti-inflammatory effects of fluoxetine in lipopolysaccharide (LPS)-stimulated microglial cells. *Neuropharmacology.* (2011) 61, 592-599.

Young K.C., Bai C.H., Su H.C., et al.: Fluoxetine a novel anti-hepatitis C virus agent via ROS, JNK, and PPARβ/γ-dependent pathways. *Antiviral Res.* (2014) 110, 158-167.

Su F., Yi H., Xu L., et al.: Fluoxetine and S-citalopram inhibit M1 activation and promote M2 activation of microglia in vitro. *Neuroscience.* (2015) 294, 60-68.

I.

Toxicology and Applied Pharmacology 366 (2019) 17–24

Contents lists available at ScienceDirect

Toxicology and Applied Pharmacology

journal homepage: www.elsevier.com/locate/taap

A novel target for the promotion of dermal wound healing: Ryanodine receptors

Döníz Degovics[a,*], Petra Hartmann[b], István Balázs Németh[a], Noémi Árva-Nagy[a], Enikő Kaszonyi[a], Edit Szél[a], Gerda Strifler[b], Balázs Bende[a], László Krenács[c], Lajos Kemény[a,d], Gábor Erős[a]

[a] Department of Dermatology and Allergology, University of Szeged, Szeged, Hungary
[b] Institute of Surgical Research, University of Szeged, Szeged, Hungary
[c] Laboratory of Tumour Pathology and Molecular Diagnostics, Szeged, Hungary
[d] MTA-SZTE Dermatological Research Group, Szeged, Hungary

ARTICLE INFO

Keywords:
Ryanodine receptor
Calcium channel
Wound healing
Skin fold chamber

ABSTRACT

Ryanodine receptors have an important role in the regulation of intracellular calcium levels in the nervous system and muscle. It has been described that ryanodine receptors influence keratinocyte differentiation and barrier homeostasis. Our goal was to examine the role of ryanodine receptors in the healing of full-thickness dermal wounds by means of *in vitro* and *in vivo* methods.

The effect of ryanodine receptors on wound healing, microcirculation and inflammation was assessed in an *in vivo* mouse wound healing model, using skin fold chambers in the dorsal region, and in HaCaT cell scratch wound assay *in vitro*. SKH-1 mice were subjected to sterile saline (n = 36) or ryanodine receptor agonist 4-chloro-m-cresol (0.5 mM) (n = 42) or ryanodine receptor antagonist dantrolene (100 μM) (n = 42).

Application of ryanodine receptor agonist 4-chloro-m-cresol did not influence the studied parameters significantly, whereas ryanodine receptor antagonist dantrolene accelerated the wound closure. Inhibition of the calcium channel also increased the vessel diameters in the wound edges during the process of healing and increased the blood flow in the capillaries at all times of measurement. Furthermore, application of dantrolene decreased xanthine-oxidoreductase activity during the inflammatory phase of wound healing.

Inhibition of ryanodine receptor-mediated effects positively influence wound healing. Thus, dantrolene may be of therapeutic potential in the treatment of wounds.

1. Introduction

As a major secondary messenger, intracellular Ca^{2+} is involved in various intracellular signalling pathways *e.g.* excitation-contraction coupling. The main intracellular Ca^{2+} stores are the endoplasmic reticulum (ER)/sarcoplasmic reticulum (SR) and the mitochondrion. There are two major receptors regulating the Ca^{2+} release from the SR/ER, the inositol 1,4,5-triphosphate receptors (IP3Rs) (Nixon et al., 1994) and the ryanodine receptors (RyRs) (Otsu et al., 1990). In mammalian tissues, three genes encode three RyR isoforms and many types of cells express each of them. RyR1 (skeletal muscle type) and RyR2 (cardiac type) are primarily expressed in the skeletal and the cardiac muscle and they are pivotal for excitation–contraction coupling, whereas RyR3 (brain type) contributes to the intracellular calcium regulation in the brain (Zucchi and Ronca-Testoni, 1997; Kushnir et al., 2010). Recently the functional existence of RyR in epidermal keratinocytes has been demonstrated (Denda et al., 2012).

Intracellular Ca^{2+} signalling in keratinocytes is essential for cellular processes, including migration, proliferation, differentiation, barrier homeostasis and release of proinflammatory cytokines (Graham et al., 2013; Tu and Bikle, 2013; Denda et al., 2003). It has been previously shown that activation of excitatory receptors, such as *N*-methyl-D-aspartate receptor (NMDA), nicotinic acetylcholine receptor, P2X purinergic receptor, and RyR induces elevation of intracellular calcium concentration and delays barrier recovery of the skin (Denda et al., 2002; Denda et al., 2003; Fuziwara et al., 2003). On the other hand, the

Abbreviations: ER, endoplasmic reticulum; SR, sarcoplasmic reticulum; IP3R, inositol 1,4,5-triphosphate receptor; RyR, ryanodine receptor; NMDA, *N*-methyl-D-aspartate receptor; P2X, P2X purinergic receptor; 4-CMC, 4-chloro-m-cresol; DA, dantrolene; IVM, intravital videomicroscopy; XOR, xanthine-oxidoreductase; MPO, myeloperoxidase; RBCV, the red blood cell velocity; VD, vessel diameter; ROS, reactive oxygen species; Glut, glutamate

* Corresponding author at: Department of Dermatology and Allergology, University of Szeged, Korányi fasor 6, 6720 Szeged, Hungary.
E-mail address: degovics.doniz@med.u-szeged.hu (D. Degovics).

https://doi.org/10.1016/j.taap.2019.01.021
Received 3 October 2018; Received in revised form 11 January 2019; Accepted 23 January 2019
Available online 23 January 2019
0041-008X/

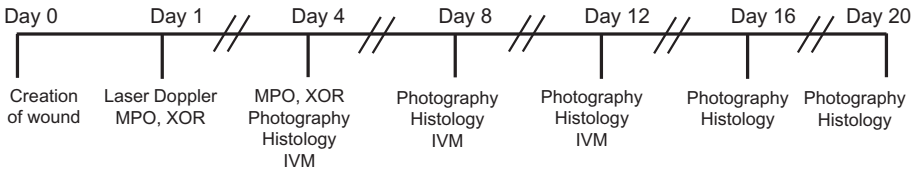

Fig. 1. Experimental protocol.

inhibition of calcium channels, such as voltage-gated calcium channel, P2X receptor, and RyR accelerate barrier recovery (Denda et al., 2002; Denda et al., 2006; Denda et al., 2012). However, no information is available concerning the effects of RyRs on the healing of full-thickness dermal wounds.

In the present study, we first examined the effect of induction and inhibition of RyRs on full-thickness wounds in SKH-1 mice. We evaluated the rate of wound closure by means of photographic imaging and histological analysis. We examined the effects of these modulators on keratinocyte proliferation, and monitored different parameters of the microcirculation in the wound edges with intravital videomicroscopy and laser Doppler flowmeter. Finally, we studied the effects of the topical agents on the inflammation process of the healing.

2. Methods

2.1. Animals

The experiments were performed on 12–15-week-old male SKH-1 hairless mice (body weight: 36–44 g). The animals were housed in plastic cages in a thermoneutral environment with a 12 h light-dark cycle and had access to standard laboratory chow and water *ad libitum*. All interventions were in full accordance with the NIH guidelines. The procedures and protocols applied were approved by the Ethical Committee for the Protection of Animals in Scientific Research at the University of Szeged. (Permit number: V./145/2013.) Animal studies are reported in compliance with the ARRIVE guidelines (Kilkenny et al., 2010; McGrath and Lilley, 2015).

2.2. Implantation of dorsal skin fold chamber

The animals were carefully examined. Mice with any type of injury or apparent sign of disorder were discarded. Prior to intervention the animals were anesthetized with a mixture of ketamine (90 mg/kg body weight) and xylazine (25 mg/kg body weight) administered intraperitoneally. The surgery was performed as described elsewhere (Sorg et al., 2007). Briefly, two holding stitches were inserted in the dorsal midline and moderate tension was exerted in order to form a skin fold. Two symmetrical titanium frames (IROLA GmbH, Schonach, Germany) were then applied to sandwich the extended double layer of the skin. The skin fold was fixed to the metal frames with sutures and sandwiched securely between the frames by means of three nuts and bolts. A circular full-thickness wound was formed on one side of the skin fold. A stamp with a diameter of 4 mm was used to determine the line of incision. The complete skin and the musculus panniculus carnosus were removed. The non-wounded skin of the opposite side still consisted of epidermis, dermis and striated skin muscle. The wounded side was treated topically with one or other of the test solutions and was then covered with a removable glass coverslip incorporated in the titanium frame. The covering glasses were removed only for the times of treatments and measurements.

2.3. Groups and treatments

The mice were divided into 3 treatment groups: (1) wounds were treated with sterile saline (pH = 7.4); (2) wounds were treated with 4-CMC (0.5 mM, pH = 6.5); (3) wounds were treated with DA (100 μM, pH = 7.1). Photographs were taken every 4 days (4, 8, 12, 16 and 20), then the animals were euthanized with an overdose of ketamine and tissue samples were taken for histological analysis.

Monitoring of the microcirculation with intravital videomicroscopy (IVM) was performed on days 4, 8 and 12. In a separate group of mice laser Doppler flowmetry was performed on wounds treated with either 4-CMC or DA.

Xanthine-oxidoreductase (XOR) and myeloperoxidase (MPO) activity were measured during the inflammatory phase on days 1 and 4. 6 mice were assigned to each group and time point.

Concerning treatments, the mice were restrained with a plastic cylinder into which they were inserted. The titanium frames were fixed to an aperture on the cylinder, hereby free access was provided to the wounds. The covering glasses were removed and sterile saline, the formulation of 4-CMC or the solution of DA was administered to the wounds with micropipette (100 μL). The covering glasses were then rapidly returned. Daily one treatment was applied in all groups. The experimental setup is shown in Fig. 1. Groups and treatments are summarized in Table 1.

2.4. Measurement of wound area

The animals were anesthetized before measurement, as described above. They were placed on a heating pad in a lateral position and the covering glass was removed. Photographs were taken with a camera (DiMage A200, KonicaMinolta). Photographing was performed under standard circumstances: the same light sources were used in a dark room and the camera was fixated to a stand in order to standardize the distance. The resolution of the images was 3264 × 2448. Planimetric analysis of the images was performed by means of a software (modification of the ImageJ) (DermAssess©) developed by our working group. This software can be utilized for the determination of an area and for the quantification of colour intensity (*e.g.* grade of erythema), as

Table 1
Summary of research methods.

Group	Treatment	Observation period (days)	Method	n
1	4-CMC	1	Laser Doppler	6
2	DA			6
3	NaCl	1	MPO, XOR	6
4	4-CMC			6
5	DA			6
6	NaCl	4	MPO, XOR photography	6
7	4-CMC		Histology	6
8	DA		IVM	6
9	NaCl	8	Photography	6
10	4-CMC		Histology	6
11	DA		IVM	6
12	NaCl	12	Photography	6
13	4-CMC		Histology	6
14	DA		IVM	6
15	NaCl	16	Photography	6
16	4-CMC		Histology	6
17	DA			6
18	NaCl	20	Photography	6
19	4-CMC		Histology	6
20	DA			6

DA, dantrolene; 4-CMC, 4-chloro-m-cresol; MPO, myeloperoxidase; XOR, xanthine-oxidoreductase; IVM, intravital videomicroscopy.

it has been reported in a recent study (Erős et al., 2014). The area of the wound was measured by two investigators independently and referred to the area determined on day 0 in order to calculate the rate of wound closure.

2.5. Intravital videomicroscopy (IVM)

The microcirculation was visualized with a fluorescence intravital videomicroscope equipped with a 100 W mercury lamp (Axiotech vario, Zeiss, Jena, Germany). The anesthetized mice received a retrobulbar injection of 80 μL 2% fluorescein isothiocyanate-labeled dextran (molecular weight 150 kD; Sigma Chemicals, USA). After this injection, a blue (450–490 nm) filter set allowed analysis of the microcirculation by the epi-illumination technique, using an Acroplan 20× water immersion objective. During examinations, the tissue was superfused with 37 °C saline. The intravital microscopic images were recorded with a charge-coupled device video camera (AVT-BC 12, AVT Horn, Aalen, Germany) attached to an S-VHS video recorder (Panasonic AG-MD830) and a personal computer. Quantitative assessment of the microcirculatory parameters was performed offline with frame-to-frame analysis, using image analysis software (IVM, Pictron Ltd., Budapest, Hungary). The following parameters were examined: the red blood cell velocity (RBCV, μm/s) was measured in the capillaries of wound edges. At least 2 separate fields of view were visualized in all quadrants of the circular wound and measurements were performed in at least 6 capillaries of all fields of view. Vessel diameter (VD, μm) was assessed by measuring of all vessels in the given fields or view except those of < 6 μm.

2.6. Microcirculatory measurements

A non-invasive laser Doppler tissue flowmeter (PeriFlux System 5000, Perimed, Järfälla, Sweden) was used to evaluate the cutaneous microvascular blood flow. A standard pencil probe producing laser beam was placed on the surface of the wound edge. The method is based on the reflection of a beam of laser light (780 nm). The coherent, monochromatic laser beam penetrates into the tissues and scattered by moving and stationary tissue cells. The photons scattered by red blood cells are Doppler-shifted, and the reflected light is collected by fibers coupled to a photodetector. The number of blood cells and their velocities within the measured skin volume are linearly correlated with the skin blood flow and expressed in perfusion unit (P.U.) (Jarabin et al., 2015; Zografos et al., 1992). We formed circular wounds as big as the probe head. We measured the flow 24 h after the surgery. First, we measured the baseline flow, and then the wounds were treated. 10 min later we repeated the measurements. The signal was registered for 20 s.

2.7. Tissue XOR activity

Skin biopsies kept on ice were homogenized in phosphate buffer (pH 7.4) containing 50 mM Tris–HCl (Reanal, Budapest, Hungary), 0.1 mM EDTA, 0.5 mM dithiotreitol, 1 mM phenylmethylsulfonyl fluoride, 10 μg/mL soybean trypsin inhibitor and 10 μg/mL leupeptin. The homogenate was centrifuged at 4 °C for 20 min at 24,000 g and the supernatant was loaded into centrifugal concentrator tubes. The activity of XOR was determined in the ultrafiltered supernatant by fluorometric kinetic assay based on the conversion of pterine to isoxanthopterine in the presence (total XOR) or absence (XO activity) of the electron acceptor methylene blue (Beckman et al., 1989).

2.8. Tissue MPO activity

The activity of MPO, a marker of tissue leukocyte infiltration, was measured from homogenized skin biopsies by the modified method of Kuebler et al. (Kuebler et al., 1996). Briefly, the pellet was resuspended in K_3PO_4 buffer (0.05 mol L^{-1}; pH 6.0) containing 0.5% hexa-1,6-bisdecyltriethylammonium bromide. After 3-times repeated freeze-thaw procedures, the material was centrifuged at 4 °C for 20 min at 24,000 g and the supernatant was used for MPO determination. During the measurements, 0.15 mL of 3,3′,5,5′-tetramethylbenzidine (dissolved in DMSO; 1.6 mmol L^{-1}) and 0.75 mL of hydrogen peroxide (dissolved in K_3PO_4 buffer; 0.6 mmol L^{-1}) were added to 0.1-mL samples. The reaction causes the hydrogen peroxide-dependent oxidation of tetramethylbenzidine, which can be detected spectrophotometrically at 450 nm (UV-1601 spectrophotometer; Shimadzu, Kyoto, Japan). The MPO activities of the samples were measured at 37 °C; the reaction was stopped after 5 min with 0.2 mL of H_2SO_4 (2 mol L^{-1}) and the data were referred to the protein content (Varga et al., 2010).

2.9. Routine histology and immunohistochemistry

The tissue in the window of the titanium chamber was excised. The biopsies were fixed in a 4% buffered solution of formaldehyde and embedded in paraffin. One slide was stained with haematoxylin-eosin (H&E), while the other was used for immunohistochemical detection of Ki-67 (Biocare Medical, Cat#: PRM 325 AA, rabbit monoclonal, prediluted) positive cells. Retrieval was performed at pH = 6 at 100 °C for 20 min. The antibody was applied overnight. A Bond Polymer Refine Detection Kit (Leica Biosystems) was then used; the sections were exposed to 3,3′-diaminobenzidine (DAB) for 10 min, followed by counterstaining with haematoxylin.

The sections were subjected to histological examination with the Pannoramic Viewer software (3DHISTECH Ltd., Budapest, Hungary). In the H&E-stained sections, we measured the diameter of the wound and the length of the growing epithelial tissue on both sides. The sum of the growing epithelial tissue was referred to the initial diameter of the wound. In the Ki-67-stained slides, tissue samples were separated into 100 μm long regions. The wound area was divided into 1–4 regions, depending on the length of the growing epithelial tissue, whereas unwounded areas surrounding the wound were divided into 4 regions at each side of the wound. To analyse the epidermal proliferation in response to the treatments, we calculated the epidermal proliferation index; the amount of Ki-67-expressing basal keratinocytes were divided by the whole number of basal keratinocytes, to determine the percentage of proliferating cells as an indicator for proliferative activity (Safferling et al., 2013).

2.10. Cell culture and scratch test

Human HaCaT keratinocytes, kindly provided by Dr. N. E. Fusenig (Heidelberg, Germany), were cultured in Dulbecco's modified Eagle's medium (DMEM) containing 10% foetal bovine serum (FBS) until reaching confluency. HaCaT keratinocytes were grown at 37 °C in a 5% CO_2 atmosphere. For the experiments cells were seeded into 24-well plates. 3 different treatments were applied by using 6 samples for each case.

Scratch wounding was performed with a cell scraper of 4 mm width, according to a well-established *in vitro* wound-healing assay (Matsuura et al., 2007). The cells were treated once daily with either 4-CMC (0.3 mM), or DA (45 μM), while the control group was left untreated. The entire area of a well was imaged using a Nikon Eclipse TS100 inverted routine microscope (Nikon Incorporation, Melville, USA) fitted with a Nikon Coolpix 4500 camera (Nikon Incorporation, Melville, USA) at the time of wounding (time 0), at 24 h, 48 h, and 72 h post-wounding. DermAssess© software was used to measure the width of the scratch.

2.11. Statistical analysis

Data analysis was performed with SigmaStat for Windows (Jandel Scientific, Erkrath, Germany). Since the normality test (Shapiro-Wilk) failed in few cases, nonparametric test was chosen. Differences between

groups were analysed with Kruskal-Wallis one-way analysis of variance on ranks, followed by Dunn method for pairwise multiple comparison. In the Figures, median values with 25th and 75th percentiles are given, $P < .05$ was considered statistically significant. The data and statistical analysis comply with the recommendations on experimental design and analysis in pharmacology (Curtis et al., 2015).

2.12. Materials

A ryanodine receptor (RyR) agonist, 4-chloro-m-cresol (4-CMC, 0.5 mM), or a RyR antagonist, dantrolene sodium salt (DA, 100 μM) was applied on the wounds of the animals. The drugs were dissolved in sterile saline. Immortalized human keratinocytes from the HaCaT-cell line after scratching were treated with 4-CMC (0.3 mM) or DA (45 μM). The drugs were dissolved in purified water before added to the culture medium. The solutions were vortexed and sonicated until dantrolene and 4-CMC were completely dissolved. 4-CMC and DA were purchased from Sigma-Aldrich.

3. Results

3.1. Inhibition of RyRs accelerates wound closure in vivo

Planimetric analysis of the wound area on digital images showed a continuous increase in epithelialization with approximately 20% wound coverage on day 4, 50% on day 8, and 80% on day 12 in the group treated with DA (Fig. 2A, B). At the end of the experiment, on day 20 all of the calcium antagonist treated wounds achieved a complete wound closure, while the 4-CMC treated animals did not.

The macroscopic finding of increased rate of wound closure in the group treated with DA was confirmed by routine histology. The growing epithelial tongues of the edges of the wounds were found significantly longer on days 4 and 8, compared to the control animals. From day 12 to 20, no significant difference was found between the groups (Fig. 3A, B).

To determine whether the accelerated wound closure can be attributed to increased proliferation, we quantified the proliferative activity of the epidermis by analysing Ki-67-stained sections. The epidermal proliferation index was calculated on days 4, 8, 12, 16 and 20 but our results did not show significant difference temporally or spatially between the groups (data not shown).

3.2. Wound closure of HaCaT cells is accelerated by dantrolene

We investigated the effect of DA and 4-CMC on wound closure in HaCaT cell monolayers. Fig. 4A shows the evolution of the scratch on the cell culture. The experimental results showed that the scratch closure occurred at a significantly faster rate in the presence of DA compared to the control, and the scratch area was completely closed after 72-h culture. In contrast, in cultures treated with 4-CMC the gap closure was delayed by 72 h (Fig. 4B).

3.3. Dantrolene elevates the vessel diameter and the red blood cell velocity

The analysis of the IVM video records revealed that the vessel diameters did not display a change within the 4-CMC and the control groups during the observation period, while the calcium channel antagonist increased the vessel diameters by 25% on day 4 compared to the control group. This significant difference was also observed on day 8 (17%) and on day 12 (22%) as well (Fig. 5A).

It has also been shown that inhibition of the RyRs increased the red blood cell velocity in the capillaries at all times of measurements by approximately 25%, while there were no difference between the 4-CMC and the control group (Fig. 5B). The findings of laser Doppler flowmetry have confirmed the data obtained from IVM. The flow curves demonstrated consistent significant increases in the blood flow from baseline levels to posttreatment levels with an average of 15-fold increase in the group treated with DA (Fig. 6).

3.4. Inhibition of RyRs decreases XOR activity thereby diminishing ROS production

MPO activity, a commonly used index of inflammatory cell accumulation, was measured during the inflammatory phase of wound healing on the first and the fourth days post-wounding. According to our results no significant difference was found between the groups (data not shown). In contrast, significant reductions of XOR activity, a critical source of ROS production, were observed in the group treated with DA on days 1 and 4 as compared with the control group, while 4-CMC did not alter the enzyme activity (Fig. 7).

4. Discussion

Wounds of different type may considerably decrease the health-related quality of life and place substantial burden on healthcare system. Thus, there seems to be a need for novel therapeutic approaches accelerating the healing process. Our study has revealed that DA, an inhibitor of RyRs, promotes macroscopic wound closure *in vivo* and the histological examination has confirmed that this agent contributes to the process of epithelialization. Furthermore, the *in vitro* experiments have shown faster closure of the keratinocyte layer after application of DA. Regeneration of the epithelium requires tightly regulated spatiotemporal process of proliferation, migration and differentiation. Calcium signals seem to have a role in these processes. Epidermis displays a characteristic calcium gradient, with low calcium levels in the lower, basal, and spinous epidermal layers, and increasing calcium levels towards the stratum granulosum (Menon et al., 1985) that contributes to keratinocyte differentiation (Elias et al., 2002). It has also been described that extracellular calcium triggers an increase in the level of intracellular free calcium which subsequently promotes cell differentiation (Sharpe et al., 1989; Bikle et al., 1996). Since epidermal injuries disturb the calcium gradient and RyRs are known to be major mediators of calcium-induced calcium release, it seemed to be presumptive that influence of these receptors may affect wound healing. Denda et al., have shown that activation of RyRs delays the barrier regeneration while inhibition of RyRs by means of topical DA accelerates the barrier recovery (Denda et al., 2012). In the mentioned study, the injury was confined to the uppermost layer of the skin. A novelty of our investigation is the demonstration of the efficacy of DA in full thickness dermal wounds. According to our findings, inhibition of RyR contributes to the healing process *via* different ways. By means of immunostaining for Ki-67, we have not found significantly higher proliferation rate after application of DA. Thus, it can be assumed that increased cell migration can be responsible for the accelerated wound closure. Migration may be regulated by calcium dependent processes but this question requires further investigation. However, our *in vivo* experiments have identified another important factor playing role in the regeneration.

The results obtained by means of IVM have shown that local application of DA led to a considerable increase in RBCV in the capillaries of the wound edge. This elevation may originate in the vasodilation of the arterioles and the relaxation of the precapillary sphincters. Measurement of vessel diameters has proven the vasodilation and the laser Doppler flowmetry has also confirmed the elevated blood flow after inhibition of RyR. It is known that RyRs are expressed in vessels of different calibres in several organs, *e.g.* renal resistance arterioles, mesenteric arteries, cremaster arterioles, large cerebral arteries and in cerebral microcirculation, as well (Arendshorst and Thai, 2009; Borisova et al., 2009; Westcott and Jackson, 2011; Dabertrand et al., 2013). RyRs play a pivotal role in the regulation of vascular tone but their effect may be diverse in different organs. Pharmacological induction of RyRs leads to contraction in the smooth muscle of guinea pig

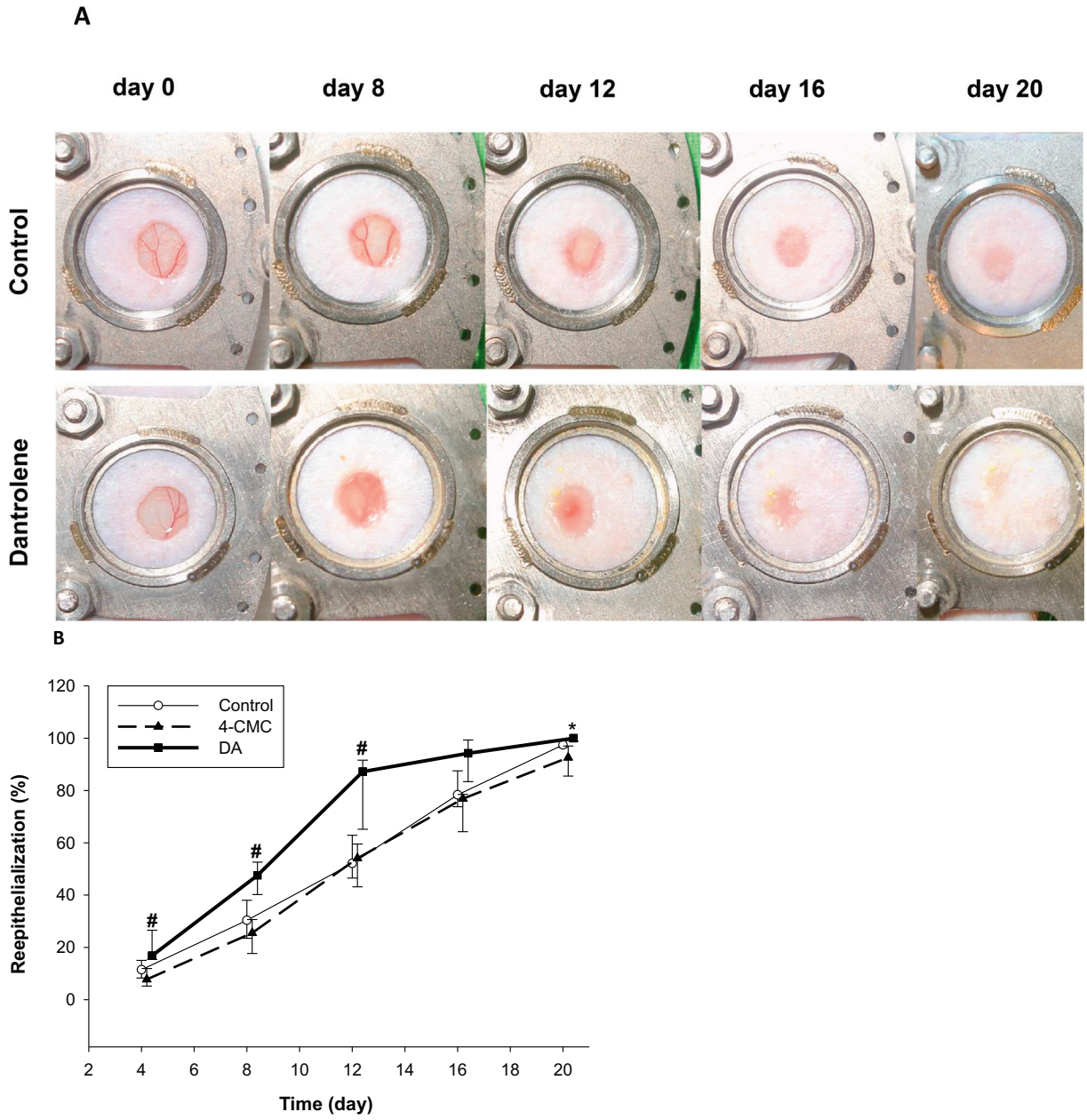

Fig. 2. Inhibition of ryanodine receptors accelerates wound closure *in vivo*. Full-thickness excisional skin wounds were created on the backs of SKH-1 mice, topically treated with DA or 4-CMC or saline daily. Wounds were digitally photographed every 4 days. Image is representative of a healing wound in the control and the DA-treated groups (A). The extent of wound closure was expressed as the increasing coverage of the wound area referred to the size of the wound on day 0 (B). # Indicates significant differences in DA treated mice compared to control, * indicates significant differences in DA treated mic compared to 4-CMC. n = 6.

mesenteric artery (Itoh et al., 1981). The RyR antagonist ryanodine results in vasoconstriction in hamster cremaster muscle feed arteries (Westcott and Jackson, 2011) and rat cerebral arteries (Knot et al., 1998) while DA prevents the vasoconstriction induced by serotonin in rat basilar and femoral arteries (Salomone et al., 2009). In human, DA attenuates cerebral vasoconstriction without altering systemic physiological parameters (Muehlschlegel et al., 2009). However, the role of RyRs in the dermal microcirculation has not been known before. Our results have demonstrated that DA considerably elevates the vessel diameter and the RBCV. The increased perfusion of the wound area may thus result in a better oxygen and nutrient supply hereby contributing to a faster regeneration.

The present study has also revealed that DA has an impact on inflammation accompanying wounds. Inflammation is known to be the first phase of wound repair (Clark, 1996) and plays an important role in healing. However, an excessive inflammatory reaction may lead to chronic wound (Schafer and Werner, 2008) and contribute to scar formation (Reinke and Sorg, 2012). Inflammation can be characterized with different factors *e.g.* inflammatory cell accumulation and production of reactive oxygen species (ROS). MPO, which is a lysosomal protein highly expressed in neutrophil granulocytes and macrophages, is a critical element of oxygen-dependent antimicrobial system in granulocytes (Nauseef et al., 1995) and can be used as a marker of inflammatory cell accumulation. XOR is a major source of ROS in macrophages, it can also be detected in keratinocytes and it is an important component of innate inflammatory signalling (Ives et al., 2015; Nakai et al., 2006). During normal healing process, the expression of XOR is upregulated shortly after wounding (Madigan et al., 2015). Although local application of DA has not influenced the leukocyte accumulation, it considerably moderated the ROS production. According

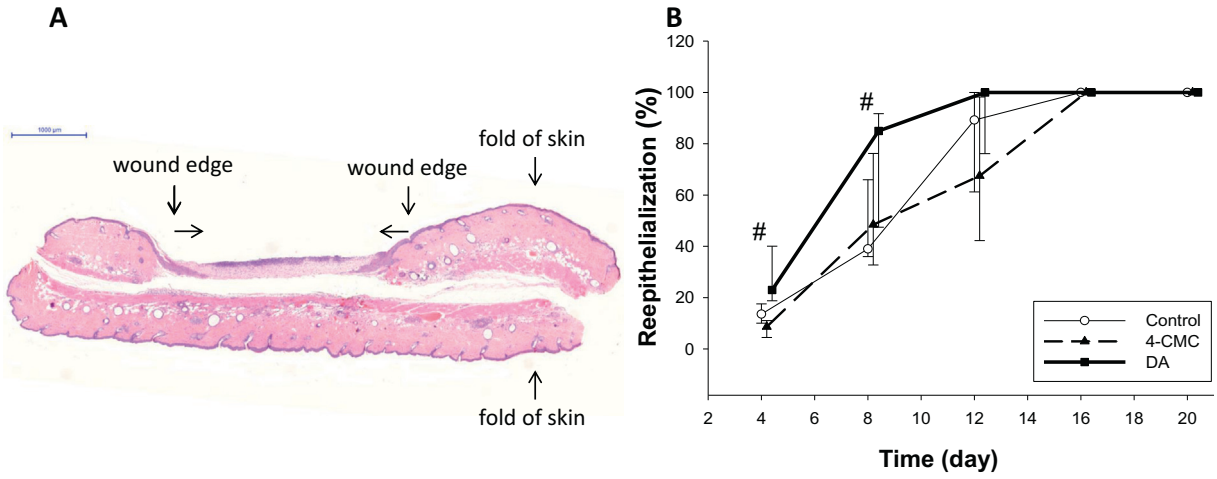

Fig. 3. Analysis of histological sections shows accelerated reepithelialization after dantrolene treatment. Image is representative of a histological section stained with haematoxylin and eosin at day 4. Scale bar is 1000 µm, and arrows indicate the two folds of the sandwiched skin, the wound edges and the growing epithelial tissue (A). Wound closure rate during 20 days was calculated as a percentage of that at 0 h (0%) until total closure of the wound (100%) and is shown in (B). # Indicates significant differences in DA treated wounds compared to the control group. n = 6.

to the literature, calcium seems to play a role in the regulation of ROS forming mechanisms. Barrier injury is followed by the release of various neurotransmitters from the epidermis *e.g.* ATP, dopamine and glutamate (Glut) (Denda et al., 2012). After wounding, Glut achieves high concentrations in the skin (Albina et al., 1993). Accumulation of Glut stimulates NMDA receptors which increase the intracellular calcium level triggering a ryanodine-gated calcium release from ER. Moreover, inhibition of NMDA receptors or RyRs suppresses ROS production in astrocytes (Kuhlmann et al., 2009). The calcium influx may also lead to mitochondrial calcium overload which can enhance mitochondrial superoxide generation (Hassoun et al., 2008). The mentioned processes seem to be self-propelling, because ROS-induced damage in the mitochondria leads to XO activation and further ROS production (Gladden et al., 2011). Furthermore, exposure to ROS also activates the RyRs (Csordas and Hajnoczky, 2009). It can be assumed that restraining of intracellular calcium release by inhibition of RyRs results in a decrease of ROS formation.

The potential anti-inflammatory effect of DA has already been suggested by previous studies. In animal experiments, DA was found to suppress the production of pro-inflammatory cytokines (TNF-α, IL-12 and IFN-γ), to increase the quantity of anti-inflammatory cytokines (IL-10), to attenuate mitochondrial dysfunction and to improve survival in a murine model of endotoxemia (Hassoun et al., 2008; Fischer et al., 2001; Nemeth et al., 1998). On the other hand, activation of the RyRs with 4-CMC has not influenced the studied parameters, thus seems to have no effect on wound healing.

In conclusion, our results have demonstrated that inhibition of calcium-induced calcium release by means of locally applied DA accelerates wound closure *in vivo* and *in vitro*. Moreover, DA increases the blood flow of the skin. We have also shown that inhibition of RyRs decreases XOR activity thereby diminishes ROS production. While there are a variety of materials available for wound care, such as dexpanthenol, sodium hyaluronate or zinc hyaluronate, which can promote wound healing by increasing fibroblast proliferation and accelerating re-epithelialization, to our knowledge there are no other agents for topical use which can additionally promote wound healing by

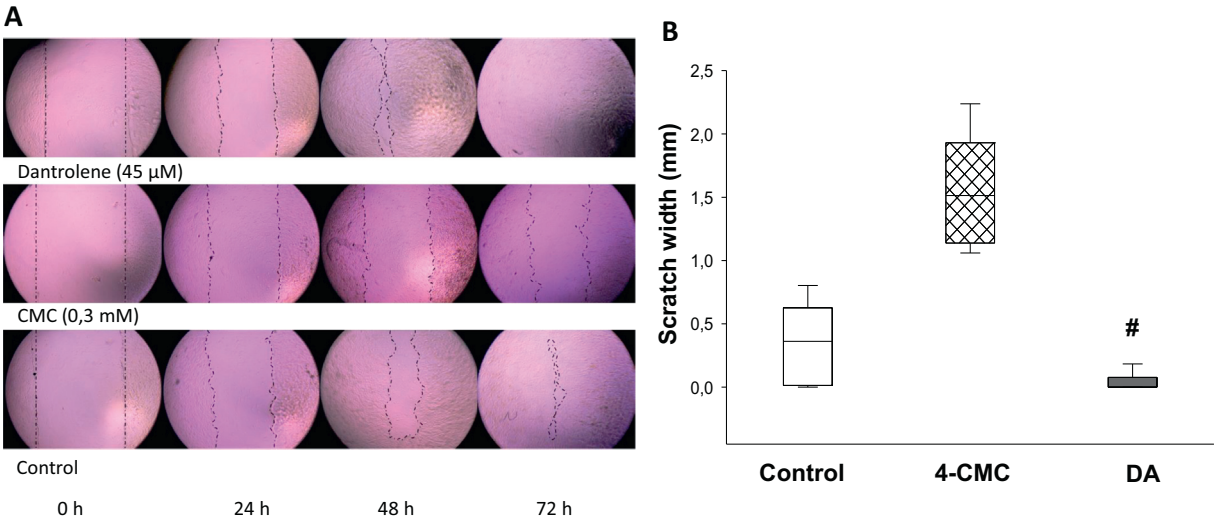

Fig. 4. Wound closure of HaCaT cells is accelerated by dantrolene. Representative microscopic images of scratch wounds at 0 h, 24, 48, and 72 h. The migrating edges were outlined using black dashed/dotted lines (A). The gap width was measured in mm at the time of wounding (time 0 h), at 24 h, 48 h, and 72 h post-wounding. Epithelialization rate of cultures treated with DA is significantly higher than those treated with sterile saline at 72 h (B). All data are representative of three independent experiments with n = 6 per group. # Indicates significant differences in DA-treated cultures compared with control.

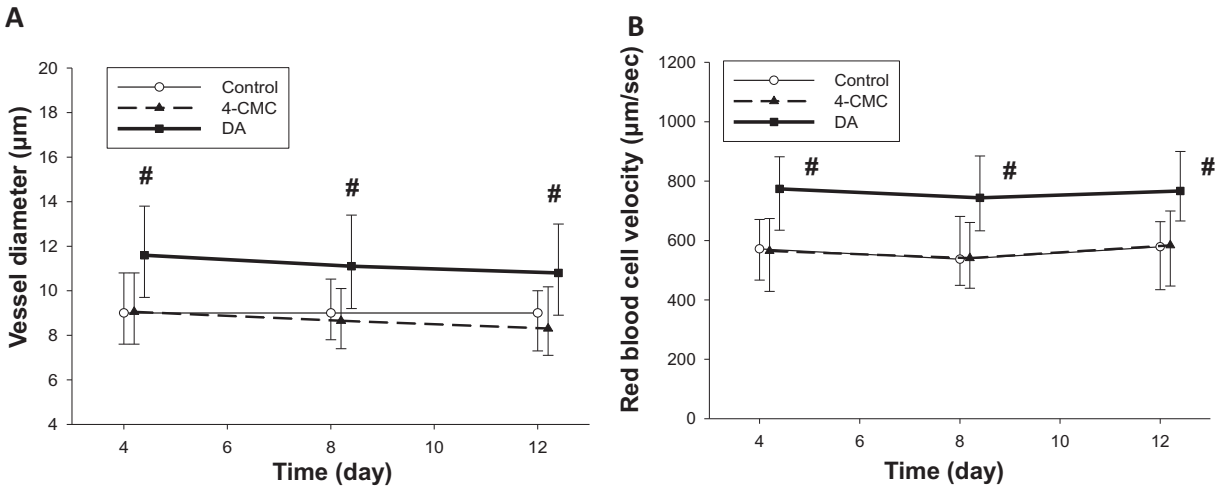

Fig. 5. Dantrolene elevates the vessel diameter and the red blood cell velocity. Microcirculatory parameters were determined from fluorescein isothiocyanate-labeled dextran perfused vessels in the dorsal skin-fold. Quantitative analysis of their diameters (µm) during regeneration at days 4, 8, and 12 post wounding shows a significant increase in caliber in the DA treated mice compared to the control group (A). Red blood cell velocity in the microvasculature of calcium antagonist treated mice reached 800 µm/s significantly differ to values in the control group (B). #Indicates significant differences. n = 6.

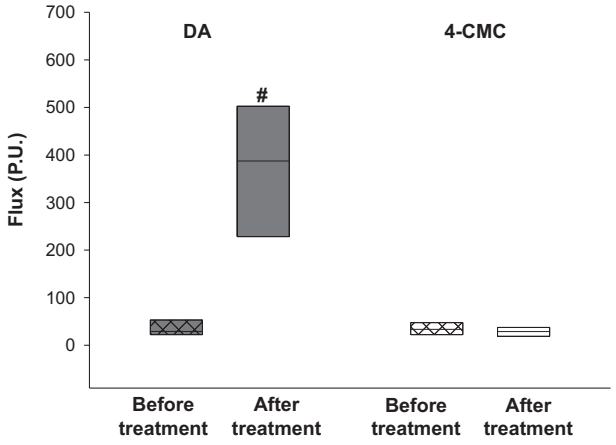

Fig. 6. Laser-Doppler microvascular measurements show increased flow after dantrolene treatment. Blood flow in the calcium antagonist treated mice 10 min post-treatment ranged between 200 P.U. and 500 P.U. significantly differ to baseline values, ranging between 20 P.U. and 30 P.U. n = 6.

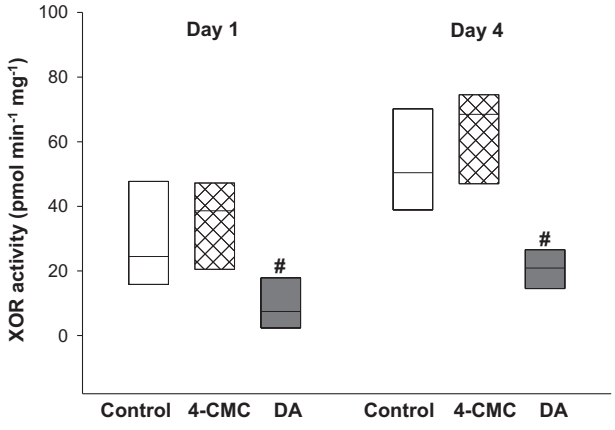

Fig. 7. Inhibition of ryanodine receptors decreases XOR activity. Wounds were harvested on days 1 and 4 post-wounding. Animals were treated once a day with 4-CMC (0.5 mM, pH = 6.5) or DA (100 µM, pH = 7.1) or saline (control). Compared to the control group, DA produced a significant decrease in XOR activity during the inflammatory phase of wound healing in all six tissues studied at each time point. # Indicates significant differences in DA treated mice compared to control. n = 6.

increasing perfusion of the wound area. However, we have to mention that DA is an expensive compound, but in a previous experiment the dose–response evaluation of DA demonstrated a maximal effect in the concentration of 100 µM, which is much lower compared to dexpanthenol- or sodium hyaluronate-containing creams and ointments, which makes the final product cheaper. Accordingly, DA, as a RyR-antagonist, seems to be a promising novel therapeutic tool in order to promote dermal wound healing *via* different pathways.

Acknowledgements

This research was supported by the project nr. EFOP-3.6.2-16-2017-00009, titled Establishing and Internationalizing the Thematic Network for Clinical Research. The project has been supported by the European Union, co-financed by the European Social Fund and the budget of Hungary. The work was also supported by Hungarian research grant GINOP-2.3.2-15-2016-00015. The authors are grateful to Mrs. Éva Sztanyik and Mrs. Kitti Gyuris for their excellent assistance in the implementation of the experiments. They thank Mrs. Erika Függ for her contribution to histology and Mr. Gábor Tax for the help in the work with cells.

Conflict of interest statement

The authors declare no conflicts of interest.

References

Albina, J.E., Abate, J.A., Mastrofrancesco, B., 1993. Role of ornithine as a proline precursor in healing wounds. J. Surg. Res. 55, 97–102.
Arendshorst, W.J., Thai, T.L., 2009. Regulation of the renal microcirculation by ryanodine receptors and calcium-induced calcium release. Curr. Opin. Nephrol. Hypertens. 18, 40–49.
Beckman, J.S., Parks, D.A., Pearson, J.D., Marshall, P.A., Freeman, B.A., 1989. A sensitive fluorometric assay for measuring xanthine dehydrogenase and oxidase in tissues. Free Radic. Biol. Med. 6, 607–615.
Bikle, D.D., Ratnam, A., Mauro, T., Harris, J., Pillai, S., 1996. Changes in calcium responsiveness and handling during keratinocyte differentiation. Potential role of the calcium receptor. J. Clin. Invest. 97, 1085–1093.
Borisova, L., Wray, S., Eisner, D.A., Burdyga, T., 2009. How structure, Ca signals, and cellular communications underlie function in precapillary arterioles. Circ. Res. 105, 803–810.
Clark, R.A.F., 1996. Wound repair; overview and general considerations. In: Clark, R.A.F. (Ed.), The Molecular and Cellular Biology of Wound Repair. Plenum Press, London,

pp. 3–50.
Csordas, G., Hajnoczky, G., 2009. SR/ER-mitochondrial local communication: calcium and ROS. Biochim. Biophys. Acta 1787, 1352–1362.
Curtis, M.J., Bond, R.A., Spina, D., Ahluwalia, A., Alexander, S.P., Giembycz, M.A., Gilchrist, A., Hoyer, D., Insel, P.A., Izzo, A.A., Lawrence, A.J., MacEwan, D.J., Moon, L.D., Wonnacott, S., Weston, A.H., McGrath, J.C., 2015. Experimental design and analysis and their reporting: new guidance for publication in BJP. Br. J. Pharmacol. 172, 3461–3471.
Dabertrand, F., Nelson, M.T., Brayden, J.E., 2013. Ryanodine receptors, calcium signaling, and regulation of vascular tone in the cerebral parenchymal microcirculation. Microcirculation 20, 307–316.
Denda, M., Inoue, K., Fuziwara, S., Denda, S., 2002. P2X purinergic receptor antagonist accelerates skin barrier repair and prevents epidermal hyperplasia induced by skin barrier disruption. J. Invest. Dermatol. 119, 1034–1040.
Denda, M., Fuziwara, S., Inoue, K., 2003. Influx of calcium and chloride ions into epidermal keratinocytes regulates exocytosis of epidermal lamellar bodies and skin permeability barrier homeostasis. J. Invest. Dermatol. 121, 362–367.
Denda, M., Fujiwara, S., Hibino, T., 2006. Expression of voltage-gated calcium channel subunit alpha1C in epidermal keratinocytes and effects of agonist and antagonists of the channel on skin barrier homeostasis. Exp. Dermatol. 15, 455–460.
Denda, S., Kumamoto, J., Takei, K., Tsutsumi, M., Aoki, H., Denda, M., 2012. Ryanodine receptors are expressed in epidermal keratinocytes and associated with keratinocyte differentiation and epidermal permeability barrier homeostasis. J. Invest. Dermatol. 132, 69–75.
Elias, P.M., Ahn, S.K., Denda, M., Brown, B.E., Crumrine, D., Kimutai, L.K., Komuves, L., Lee, S.H., Feingold, K.R., 2002. Modulations in epidermal calcium regulate the expression of differentiation-specific markers. J. Invest. Dermatol. 119, 1128–1136.
Erős, G., Kurgyis, Z., Németh, I.B., Csizmazia, E., Berkó, S., Szabó-Révész, P., Kemény, L., Csányi, E., 2014. The irritant effects of pharmaceutically applied surfactants. J. Surfactant and Deterg. 17, 67–70.
Fischer, D.R., Sun, X., Williams, A.B., Gang, G., Pritts, T.A., James, J.H., Molloy, M., Fischer, J.E., Paul, R.J., Hasselgren, P.O., 2001. Dantrolene reduces serum TNFalpha and corticosterone levels and muscle calcium, calpain gene expression, and protein breakdown in septic rats. Shock 15, 200–207.
Fuziwara, S., Inoue, K., Denda, M., 2003. NMDA-type glutamate receptor is associated with cutaneous barrier homeostasis. J. Invest. Dermatol. 120, 1023–1029.
Gladden, J.D., Zelickson, B.R., Wei, C.C., Ulasova, E., Zheng, J., Ahmed, M.I., Chen, Y., Bamman, M., Ballinger, S., Darley-Usmar, V., Dell'Italia, L.J., 2011. Novel insights into interactions between mitochondria and xanthine oxidase in acute cardiac volume overload. Free Radic. Biol. Med. 51, 1975–1984.
Graham, D.M., Huang, L., Robinson, K.R., Messerli, M.A., 2013. Epidermal keratinocyte polarity and motility require Ca(2)(+) influx through TRPV1. J. Cell Sci. 126, 4602–4613.
Hassoun, S.M., Marechal, X., Montaigne, D., Bouazza, Y., Decoster, B., Lancel, S., Neviere, R., 2008. Prevention of endotoxin-induced sarcoplasmic reticulum calcium leak improves mitochondrial and myocardial dysfunction. Crit. Care Med. 36, 2590–2596.
Itoh, T., Kuriyama, H., Suzuki, H., 1981. Excitation—contraction coupling in smooth muscle cells of the Guinea-pig mesenteric artery. J. Physiol. 321, 513–535.
Ives, A., Nomura, J., Martinon, F., Roger, T., LeRoy, D., Miner, J.N., Simon, G., Busso, N., So, A., 2015. Xanthine oxidoreductase regulates macrophage IL1beta secretion upon NLRP3 inflammasome activation. Nat. Commun. 6, 6555.
Jarabin, J., Bere, Z., Hartmann, P., Toth, F., Kiss, J.G., Rovo, L., 2015. Laser-Doppler microvascular measurements in the peri-implant areas of different osseointegrated bone conductor implant systems. Eur. Arch. Otorhinolaryngol. 272, 3655–3662.
Kilkenny, C., Browne, W., Cuthill, I.C., Emerson, M., Altman, D.G., 2010. Animal research: reporting in vivo experiments: the ARRIVE guidelines. Br. J. Pharmacol. 160, 1577–1579.
Knot, H.J., Standen, N.B., Nelson, M.T., 1998. Ryanodine receptors regulate arterial diameter and wall [Ca2+] in cerebral arteries of rat via Ca2+-dependent K+ channels. J. Physiol. 508 (Pt 1), 211–221.
Kuebler, W.M., Abels, C., Schuerer, L., Goetz, A.E., 1996. Measurement of neutrophil content in brain and lung tissue by a modified myeloperoxidase assay. Int. J. Microcirc. Clin. Exp. 16, 89–97.
Kuhlmann, C.R., Zehendner, C.M., Gerigk, M., Closhen, D., Bender, B., Friedl, P., Luhmann, H.J., 2009. MK801 blocks hypoxic blood-brain-barrier disruption and leukocyte adhesion. Neurosci. Lett. 449, 168–172.
Kushnir, A., Betzenhauser, M.J., Marks, A.R., 2010. Ryanodine receptor studies using genetically engineered mice. FEBS Lett. 584, 1956–1965.
Madigan, M.C., McEnaney, R.M., Shukla, A.J., Hong, G., Kelley, E.E., Tarpey, M.M., Gladwin, M., Zuckerbraun, B.S., Tzeng, E., 2015. Xanthine oxidoreductase function contributes to normal wound healing. Mol. Med. 21, 313–322.
Matsuura, K., Kuratani, T., Gondo, T., Kamimura, A., Inui, M., 2007. Promotion of skin epithelial cell migration and wound healing by a 2-benzazepine derivative. Eur. J. Pharmacol. 563, 83–87.
McGrath, J.C., Lilley, E., 2015. Implementing guidelines on reporting research using animals (ARRIVE etc.): new requirements for publication in BJP. Br. J. Pharmacol. 172, 3189–3193.
Menon, G.K., Grayson, S., Elias, P.M., 1985. Ionic calcium reservoirs in mammalian epidermis: ultrastructural localization by ion-capture cytochemistry. J. Invest. Dermatol. 84, 508–512.
Muehlschlegel, S., Rordorf, G., Bodock, M., Sims, J.R., 2009. Dantrolene mediates vasorelaxation in cerebral vasoconstriction: a case series. Neurocrit. Care. 10, 116–121.
Nakai, K., Kadiiska, M.B., Jiang, J.J., Stadler, K., Mason, R.P., 2006. Free radical production requires both inducible nitric oxide synthase and xanthine oxidase in LPS-treated skin. Proc. Natl. Acad. Sci. U. S. A. 103, 4616–4621.
Nauseef, W.M., McCormick, S.J., Clark, R.A., 1995. Calreticulin functions as a molecular chaperone in the biosynthesis of myeloperoxidase. J. Biol. Chem. 270, 4741–4747.
Nemeth, Z.H., Hasko, G., Szabo, C., Salzman, A.L., Vizi, E.S., 1998. Calcium channel blockers and dantrolene differentially regulate the production of interleukin-12 and interferon-gamma in endotoxemic mice. Brain Res. Bull. 46, 257–261.
Nixon, G.F., Mignery, G.A., Somlyo, A.V., 1994. Immunogold localization of inositol 1,4,5-trisphosphate receptors and characterization of ultrastructural features of the sarcoplasmic reticulum in phasic and tonic smooth muscle. J. Muscle Res. Cell Motil. 15, 682–700.
Otsu, K., Willard, H.F., Khanna, V.K., Zorzato, F., Green, N.M., MacLennan, D.H., 1990. Molecular cloning of cDNA encoding the Ca2+ release channel (ryanodine receptor) of rabbit cardiac muscle sarcoplasmic reticulum. J. Biol. Chem. 265, 13472–13483.
Reinke, J.M., Sorg, H., 2012. Wound repair and regeneration. Eur. Surg. Res. 49, 35–43.
Safferling, K., Sutterlin, T., Westphal, K., Ernst, C., Breuhahn, K., James, M., Jager, D., Halama, N., Grabe, N., 2013. Wound healing revised: a novel reepithelialization mechanism revealed by in vitro and in silico models. J. Cell Biol. 203, 691–709.
Salomone, S., Soydan, G., Moskowitz, M.A., Sims, J.R., 2009. Inhibition of cerebral vasoconstriction by dantrolene and nimodipine. Neurocrit. Care. 10, 93–102.
Schafer, M., Werner, S., 2008. Oxidative stress in normal and impaired wound repair. Pharmacol. Res. 58, 165–171.
Sharpe, G.R., Gillespie, J.I., Greenwell, J.R., 1989. An increase in intracellular free calcium is an early event during differentiation of cultured human keratinocytes. FEBS Lett. 254, 25–28.
Sorg, H., Krueger, C., Vollmar, B., 2007. Intravital insights in skin wound healing using the mouse dorsal skin fold chamber. J. Anat. 211, 810–818.
Tu, C.L., Bikle, D.D., 2013. Role of the calcium-sensing receptor in calcium regulation of epidermal differentiation and function. Best. Pract. Res. Clin. Endocrinol. Metab. 27, 415–427.
Varga, G., Erces, D., Fazekas, B., Fulop, M., Kovacs, T., Kaszaki, J., Fulop, F., Vecsei, L., Boros, M., 2010. N-Methyl-D-aspartate receptor antagonism decreases motility and inflammatory activation in the early phase of acute experimental colitis in the rat. Neurogastroenterol. Motil. 22, 217–25, e68.
Westcott, E.B., Jackson, W.F., 2011. Heterogeneous function of ryanodine receptors, but not IP3 receptors, in hamster cremaster muscle feed arteries and arterioles. Am. J. Physiol. Heart Circ. Physiol. 300, H1616–H1630.
Zografos, G.C., Martis, K., Morris, D.L., 1992. Laser Doppler flowmetry in evaluation of cutaneous wound blood flow using various suturing techniques. Ann. Surg. 215, 266–268.
Zucchi, R., Ronca-Testoni, S., 1997. The sarcoplasmic reticulum Ca2+ channel/ryanodine receptor: modulation by endogenous effectors, drugs and disease states. Pharmacol. Rev. 49, 1–51.

II.

Topical Fluoxetine as a Novel Therapeutic That Improves Wound Healing in Diabetic Mice

Chuong Minh Nguyen,[1] Danielle Marie Tartar,[1,2] Michelle Dawn Bagood,[1] Michelle So,[1] Alan Vu Nguyen,[1] Anthony Gallegos,[1] Daniel Fregoso,[1] Jorge Serrano,[1] Duc Nguyen,[1] Doniz Degovics,[1] Andrew Adams,[1] Benjamin Harouni,[1] Jaime Joel Fuentes,[3] Melanie G. Gareau,[4] Robert William Crawford,[3] Athena M. Soulika,[1,5] and Roslyn Rivkah Isseroff[1,2]

Diabetes 2019;68:1499–1507 | https://doi.org/10.2337/db18-1146

Diabetic foot ulcers represent a significant source of morbidity in the U.S., with rapidly escalating costs to the health care system. Multiple pathophysiological disturbances converge to result in delayed epithelialization and persistent inflammation. Serotonin (5-hydroxytryptamine [5-HT]) and the selective serotonin reuptake inhibitor fluoxetine (FLX) have both been shown to have immunomodulatory effects. Here we extend their utility as a therapeutic alternative for nonhealing diabetic wounds by demonstrating their ability to interact with multiple pathways involved in wound healing. We show that topically applied FLX improves cutaneous wound healing in vivo. Mechanistically, we demonstrate that FLX not only increases keratinocyte migration but also shifts the local immune milieu toward a less inflammatory phenotype in vivo without altering behavior. By targeting the serotonin pathway in wound healing, we demonstrate the potential of repurposing FLX as a safe topical for the challenging clinical problem of diabetic wounds.

Chronic wounds represent a significant source of morbidity, with more than 6 million people suffering in the U.S. alone and expenditures of ~$9.7 billion annually (1). With standard of care, only 50% of patients with diabetic foot ulcers heal, and to date, no single therapeutic agent has been successful in improving the healing rate above 50–60% (2). During the wound healing process, the initial postwounding inflammatory phase, influx of neutrophils and macrophages, is critical for normal healing but, if persistent, results in a chronically inflamed wound that does not heal (1).

Our early finding of high levels of serotonin (5-hydroxytryptamine [5-HT]) generated by cultured human bone marrow mesenchymal stem cells (3), cells important for tissue repair, prompted this investigation into the utility of serotonin, or selective serotonin reuptake inhibitors (SSRIs) that increase extracellular serotonin, to improve wound healing. Serotonin receptors are widely expressed on many tissues, including cells present within the skin (4). A clinical trial of the effects of 5-HT in wounds demonstrated that ketanserin (a 5-HT receptor 2A [HTR2A] inhibitor) had no effects on healing of the normal surgical wound (5); however, it did improve healing in patients with venous or ischemic ulcers (6). Unfortunately, the study did not conform to current Consolidated Standards of Reporting Trials (CONSORT) guidelines for randomization method, exclusion of rapid healers, size limitations, and mixed wound etiologies, so conclusions are limited (5,6). Ketanserin may improve wound healing by blocking the vasoconstrictive effects of 5-HT on HTR2A (6). Intriguingly, we found that 5-HT itself appears to be beneficial in an in vivo animal model of impaired healing. We set out to determine additional targets of serotonin signaling that may mediate the observed improvement in healing.

Fluoxetine (FLX) is an SSRI that is used to treat psychiatric disorders. Interestingly, prior studies have shown that FLX has immune-modulatory properties (7).

[1]Department of Dermatology, University of California, Davis, Sacramento, CA
[2]Dermatology Section, VA Northern California Health Care System, Mather, CA
[3]Department of Biological Sciences, California State University, Sacramento, CA
[4]Department of Anatomy, Physiology, and Cell Biology, University of California, Davis, Sacramento, CA
[5]Shriners Hospitals for Children, Northern California, Sacramento, CA
Corresponding author: Roslyn Rivkah Isseroff, rrisseroff@ucdavis.edu
Received 26 October 2018 and accepted 14 April 2019

This article contains Supplementary Data online at http://diabetes.diabetesjournals.org/lookup/suppl/doi:10.2337/db18-1146/-/DC1.

D.D. is currently affiliated with the Department of Dermatology and Allergology, University of Szeged, Szeged, Hungary.

For example, lymphocytes are activated in patients with depression with dysfunctional serotonergic systems, and FLX administration reduces their proliferation and immune function (8). Therefore, examining SSRI local effects on the stalled inflammatory phase that characterizes chronic wounds is reasonable.

Here we demonstrate the utility of repurposing FLX as a topically applied drug to improve healing, with action on multiple targets of wound healing, including improved re-epithelialization and decreased inflammation.

RESEARCH DESIGN AND METHODS

Protocols Approved

Both institutional review board and institutional animal care and use committee approval were obtained for all human tissue and animal experiments.

Primary Neonatal Human Keratinocyte Isolation and Scratch Wound Assays

Neonatal human keratinocytes (NHKs) were isolated from human foreskin, and assays were performed as previously reported (9).

Time-lapse images of wounded cultures were captured every 30 min for 6 h. Healing was calculated as follows:

$$\%\ \text{healed} = \frac{SA_{t=0} - SA_{t=6}}{SA_{t=0}}$$

SA represents surface area of the scratch wound gap at the 0-h (t = 0) or 6-h time point.

In Vivo Wounding

Mice were randomly assigned to control or treatment groups to limit bias. Diabetic (*db/db*) mice (age 11 weeks, blood glucose >300 mg/dL) received two full-thickness 8-mm splinted circular excisional wounds as previously described (10). Daily treatments as indicated were applied topically. Day 10 wound tissue was fixed, sectioned, and stained for hematoxylin-eosin or immunohistochemistry.

To limit potential bias in scoring results of scratch wound assays and histological evaluation of wound re-epithelialization, images were captured, coded, and scored by investigators blinded to the treatment group. To limit potential bias in the measurement of wound re-epithelialization, wounds were bisected through the center of the lesion and multiple sections obtained in order to score the section with the largest wound diameter. In a prior publication (10), we reported on the experimental conditions that can affect outcomes in interpretation of healing of splinted wounds in mice and have incorporated the optimized conditions in the work reported here.

Flow Cytometry

Wound tissues were dissociated mechanically (Tissue Tearor; BioSpec Products) and enzymatically (Dispase II, Collagenase D, DNase I; Sigma-Aldrich). Flow was performed with the following monoclonal antibodies: peridinin chlorophyll protein complex (PerCP)–conjugated anti-CD45 (30-F11), BV711-conjugated anti-CD11b (M1/70), phycoerythrin-conjugated anti-Ly6C (Hk1.4), FITC-conjugated anti-Ly6G (1A8), phycoerythrin-Cy7–conjugated anti-CD11c (N418), APC-conjugated anti-F4/80 (BM8), APC-Fire–conjugated anti-MHC II (M5/114.15.2), and BV421-conjugated anti-CD206 (C068C2) (all from BioLegend, San Diego, CA). Data were acquired using an Attune NxT Flow Cytometer (Invitrogen by Thermo Fisher Scientific) and were analyzed using FlowJo software (Tree Star Inc.).

Multiplex Assays

Wound lysates were assayed according to the manufacturer's protocol (Millipore Multiplex Assay; MILLIPLEX MAP 48-680MAG).

RT-PCR

RNA was extracted from wound tissue using Qiazol (Qiagen) followed by RNeasy Miniprep (Qiagen). RNA was reverse transcribed to cDNA using iScript Reverse Transcription Supermix (Bio-Rad). RT-PCR was performed using PowerUp SYBR Green Master Mix (Thermo/Applied Biosystems). Data were analyzed and normalized using the ΔΔCt method with GAPDH, Tbp, and 18S rRNA as housekeeping genes. Fold change is shown relative to the healthy unwounded skin.

Statistical Analysis

Kolmogorov-Smirnov tests were performed to verify normal distribution of each data set. For data that do not deviate from normal distribution, Student t test was used to compare each individual treatment group to the control; ANOVA was used to determine statistical significance when there were three or more groups of treatment. For data that did not pass the normality test, the nonparametric Mann-Whitney test was used to assess statistical significance. P values ≤0.05 were considered significant.

RESULTS

Wound re-epithelialization, needed for complete healing, requires migration of keratinocytes from the wound edge, a function that is stalled in chronic wounds (11). Using an in vitro scratch assay to evaluate keratinocyte migration and ability to re-epithelialize a wound, we found that serotonin (5-HT) enhanced migration in a dose-dependent manner (Fig. 1*A*). Control untreated cultures healed 41.5% of their scratch wound area compared with 52.2% in the 1 μmol/L 5-HT treatment group (P = 0.01) and 54.7% in the 10 μmol/L 5-HT treatment group (P = 0.001) (Fig. 1*A*). To explore the signaling that modulated migration in these cells, we probed relevant intracellular signaling pathways using protein multiplex assays. We discovered that 5-HT activated mitogen-activated protein kinase (MAPK) pathways in keratinocytes, evidenced by the increase in phosphorylation of ERK (1.34-fold, P = 0.004) and its downstream signals STAT3 (1.59-fold, P = 0.043) and NF-κB (1.66-fold, P = 0.035). There was no modulation

observed in PI3K/Akt pathways (Fig. 1*B*). Although human keratinocytes have been shown to express tryptophan hydroxylase gene (12), an enzyme in the rate-limiting step in 5-HT synthesis, we did not find any 5-HT produced by keratinocytes above our lower limit of detection of 9.8 nmol/L (Supplementary Fig. 1). Thus, endogenous generation of 5-HT by keratinocytes may be too low to enhance migratory speed in FLX-treated keratinocytes in the absence of exogenous 5-HT (Fig. 1*C*). In the presence of 5-HT, however, FLX improved healing in treated cultures: 60.6% in the 10 nmol/L treatment group, 62.0% in the 100 nmol/L treatment group ($P = 0.01$), and 67.0% healed wound area in the 1 μmol/L FLX group ($P = 0.001$), relative to the 52.2% healing in the control cultures (Fig. 1*D*). FLX-enhanced keratinocyte migration effect was consistent with what we found in keratinocytes derived from patients with type 2 diabetes (Supplementary Fig. 1). These data support the hypothesis that signaling through the serotonin pathway increases keratinocyte migration in vitro. To provide further evidence that FLX is working through 5-HT–dependent pathways, scratch wound assays were repeated in the presence of the HTR2A blocker ketanserin. The HTR2A blocker ketanserin reversed the effects of FLX on wound healing in vitro, again returning wound healing to the level of the untreated control group ($P = 0.948$). These data demonstrate not only that FLX increases keratinocyte migration in vitro but that this is dependent upon 5-HT signaling through HTR (Fig. 1*D*).

To test whether FLX promotes re-epithelialization in vivo, full-thickness excisional wounds in *db/db* diabetic mice, a model for impaired wound healing (10), were treated with topically applied FLX, serotonin, or vehicle control 5% w/v polyethylene glycol (PEG). Wounds from mice treated with either 0.02% FLX or 2% 5-HT dissolved in 5% PEG showed decreased wound area and less exudate compared with vehicle control counterparts at day 10 postwounding (Fig. 2*A*). Moreover, re-epithelialization was increased from an average of 39.6% in PEG-treated mice to 66.2% in mice treated with 0.2% FLX ($P = 0.01$) (Fig. 2*B* and *C*). Since the topical application of 5-HT did not result in statistically significant improvement in re-epithelialization, likely due to the short half-life of serotonin (13), we did not further investigate its direct effects.

Immunohistochemical analysis showed increased $CD31^+$ endothelial cells in the wound beds of mice treated topically with 0.2% FLX (133 cells/mm^2), with more visible scattered small blood vessels compared with control mice (67 cells/mm^2, $P = 0.045$) (Fig. 2*D* and *E*), suggesting increased angiogenesis and wound bed vascularity. Interestingly, there was a twofold increase in $CD11b^+$ immune cells within the wound bed at day 10 in control wounds compared with those treated with 0.2% FLX, indicating that inflammation persists in the absence of FLX treatment ($P = 0.006$) (Fig. 2*F* and *G*).

Since proreparative macrophages are known to mediate both wound healing and angiogenesis by acting as cellular chaperones, we hypothesized that the topically applied FLX could be promoting the generation of proreparative macrophages at the local wound environment. This seemed likely since 5-HT has previously been shown to modulate the polarization of macrophages toward an anti-inflammatory phenotype (14). Therefore, we immune phenotyped the FLX-treated wounds using flow cytometry.

Wounds were predominantly infiltrated by cells of myeloid lineage ($CD11^+CD45^+$). $CD11b^+CD45^+$ cells were fewer in FLX-treated compared with vehicle-treated wounds at day 10, from 5.25×10^6 to 1.53×10^6 ($P = 0.016$) (Fig. 3*A* and *B*), confirming the immunohistochemistry observations. Importantly, FLX treatment decreased $Ly6C^+Ly6G^-$ inflammatory monocyte/macrophage (mo/ma) numbers overall in the wound at day 10 from 3.2 to 0.5×10^6 cells ($P = 0.032$) (Fig. 3*C* and *D*). Although there was an increase in the percentage of neutrophils (due to a decrease in absolute numbers of mo/ma at the wounds), there was no difference in the absolute counts between the two groups (Fig. 3*E*), suggesting that wound neutrophils are not affected by FLX. Moreover, within the $Ly6C^+Ly6G^-$ inflammatory mo/ma, there was a notable decrease in proinflammatory $CD206^-MHCII^+$ macrophages (from 77.9 to 26.2%, $P = 0.008$), indicating a shift away from the proinflammatory phenotype (Fig. 3*F* and *G*).

Analysis of wound beds by quantitative RT-PCR (qRT-PCR; primer sequences listed in Table 1) on day 10 showed a 1.65-fold increase in arginase 1 (Arg-1), a marker for alternatively activated, prohealing macrophages ($P = 0.04$), and 5.6-fold decrease in inducible nitric oxide synthase (Nos2), a marker for classically activated, proinflammatory macrophages ($P = 0.007$), compared with the control group, supporting the notion of a more proreparative wound environment (Fig. 4*A* and *B*). FLX-treated wounds had a twofold, 2.4-fold, and 2.2-fold decrease in *Tnf, Ifng*, and *Il6* transcript, respectively, compared with the control group, indicating that FLX decreased inflammation in the wound bed (Fig. 4*C–E*). Topical application of FLX induced the expression of *Pdgfb* (1.8-fold, $P = 0.008$) and *Col3a1* (2.3-fold, $P = 0.004$), which are essential for granulation tissue formation and wound resolution (Fig. 4*F* and *G*). Interestingly, we found a significant increase (2.2-fold, $P = 0.009$) in the *Hspa1a* transcript (Fig. 4*H*), which encodes for the HSP70, an anti-inflammatory mediator, that is downregulated in diabetic mice postwounding (15). Serotonin has been shown to induce HSP expression in the absence of heat stress (16,17). Multiple studies have demonstrated that HSP70 induces Arg-1 (18) and downregulates tumor necrosis factor (Tnf) (19), interleukin 6 (Il6), nitric oxide (20), and interferon-γ (Ifng) (16) (Fig. 4*I*), consonant with the findings in the current study.

For clinical translation of a topically administered drug, ideally, systemic absorption should be minimized to limit the side effect profile. After 10 days of daily dosing with topically applied 0.2% FLX, the levels of FLX in mouse plasma ranged from 23 to 64 ng/mL (Supplementary Fig. 3*A* and *B*), with no change in plasma

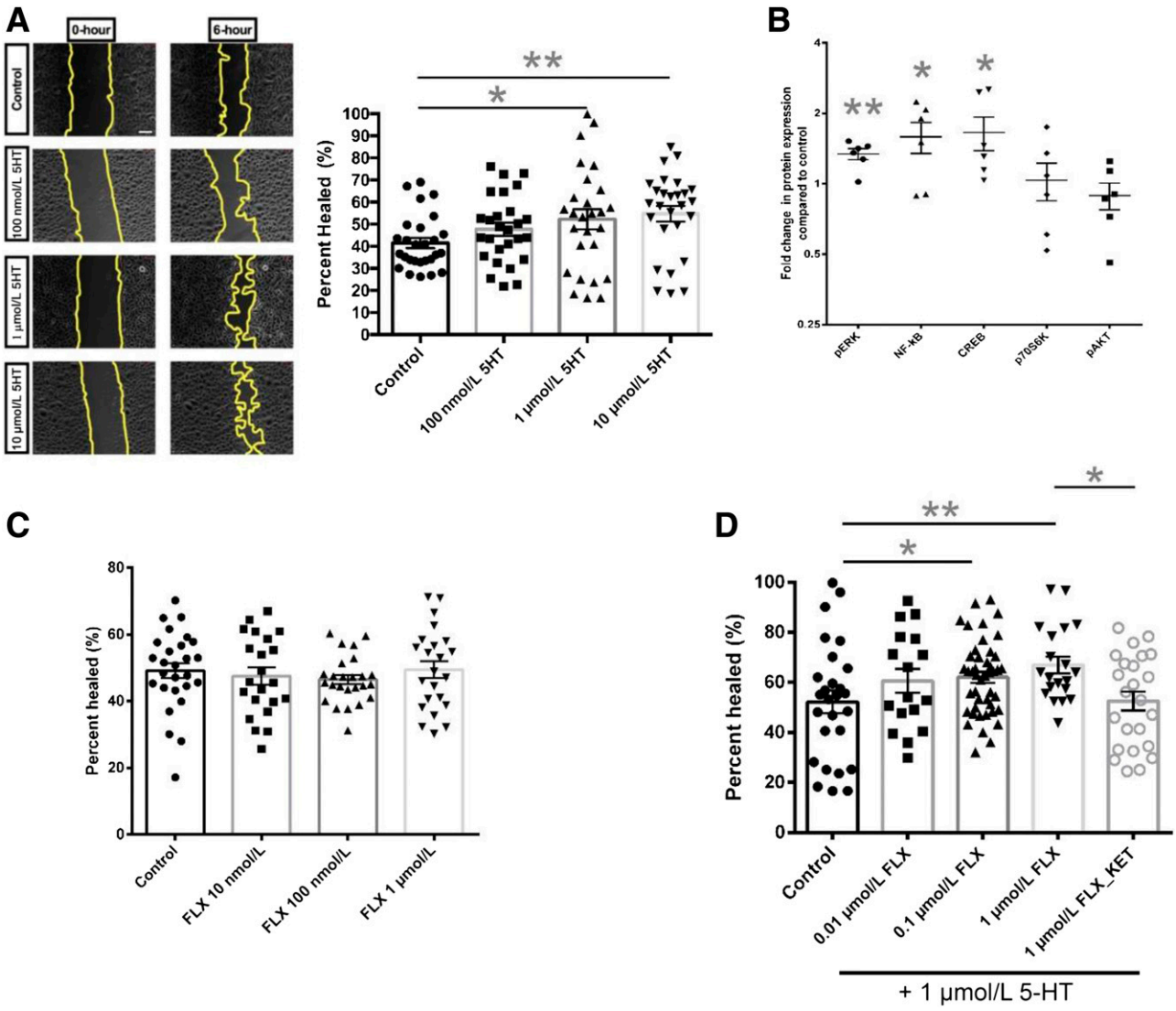

Figure 1—Serotonin and FLX increase re-epithelialization. Scratch wound assays were performed on confluent cultures of NHKs from three donors (n = 27/group) in the presence of varying doses of serotonin (5-HT). Scale bar = 100 μm (*A*). Intracellular signaling nine-plex assays; NHKs from three different donors were cultured in 100-mm dishes until 80% confluent and treated with 10 μM 5-HT for 6 h. Protein lysates (n = 6/group) were collected and quantified with Bradford assay before proceeding with Multiplex protocol as outlined in the RESEARCH DESIGN AND METHODS section. Results were normalized to total GAPDH protein expression. Fold change compared with nontreated control group were presented (*B*). Significant upregulation of phosphorylation of ERK, NF-κB, and CREB was identified. Scratch wound assays were repeated with different doses of FLX in the absence (*C*) and presence (*D*) of 5-HT. HTR2A blocker ketanserin (KET) was added to confirm the 5-HT–dependent mechanism. Data represented as mean ± SEM. Kolmogorov-Smirnov tests were performed to confirm normality in data distribution. Two-way ANOVAs with correction to multiple comparisons were used to assess statistical significance. *$P \leq 0.05$; **$P \leq 0.01$.

serotonin concentrations (Supplementary Fig. 4). The FLX levels measured are twofold lower than plasma levels in patients treated with oral FLX at therapeutic doses and are also significantly lower than levels in mice treated with neurologically therapeutic doses of FLX, either orally or intraperitoneally administered (21,22). To further query if our topical FLX treatment induces psychological effects, we performed behavioral experiments on wounded diabetic mice treated with topically applied FLX and found that the animals treated with FLX did not exhibit significant changes in their behavior in the light/dark chamber box test, a measure of anxiety (23) (Supplementary Fig. 3*C*), or in the novel object recognition test, a measure of cognition (24) (Supplementary Fig. 3*D*). These findings indicate the potential of topically delivered FLX, contrasted to other delivery methods for improving healing with minimal systemic effects.

DISCUSSION

Chronic nonhealing ulcers, commonly found in patients with diabetes, represent a significant source of morbidity and expense to both patients and the health care system in

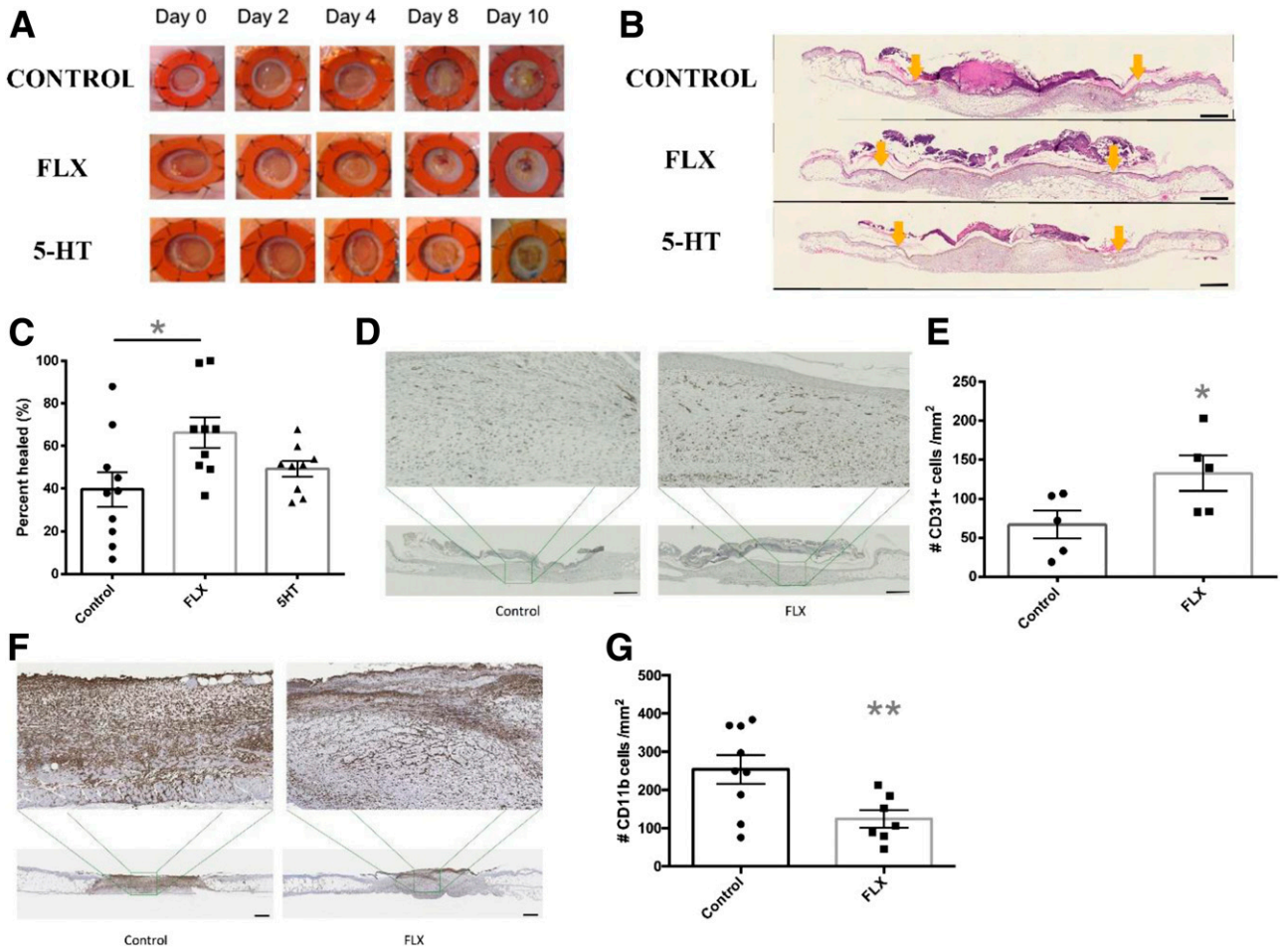

Figure 2— Representative wound images from day 0 to day 10 after excisional biopsy in *db/db* mice treated with topical PEG vehicle (control), topical 0.2% FLX, or topical serotonin (5-HT). Scale bar = 1 mm. *A*: Representative hematoxylin-eosin stains from each group for re-epithelialization analysis at day 10. Wound beds are demarcated by orange arrows (*B*). Average percent re-epithelialization per treatment group was quantified at day 10 (*C*). Immunohistochemical stainings of CD31 (*D*) and CD11b (*F*) on wound bed sections at day 10 postwounding. Average number of positive cells per treatment group was quantified (*E* and *G*). Data represented as mean ± SEM. Kolmogorov-Smirnov tests were performed to confirm normality in data distribution. Student *t* tests were used to assessed statistical significance $^{*}P \leq 0.05$; $^{**}P \leq 0.01$.

the U.S. Persistent inflammation and delayed epithelialization contribute to the stalled healing in these ulcers. Herein, we have illustrated the polypharmacological targeting in an impaired wound healing model, using a topical formulation of FLX that increases the availability of 5-HT.

Systemic administration of FLX has been shown to exhibit anti-inflammatory properties in microglia, splenocytes, and lymphocytes (8). However, the potential for local modulation of the inflammatory environment in a chronic wound by topical application of FLX has not yet been explored. Farahani et al. (25) showed that in psychologically stressed and nonstressed rats, systemically administered FLX improved healing of acute surgical wounds. However, such effects could have been due to anxiolytic and analgesic properties of FLX. In the diabetic mouse model of impaired wound healing, we have demonstrated that topical FLX improves wound healing through local effects on multiple cell types within the wound. The beneficial effects of FLX in our study appear to be independent of psychological changes.

There are some limitations to this study. Our in vivo studies are limited to only female diabetic mice. We have not taken into account the effects of sex hormones that may (26) or may not (27) impact the outcome of cutaneous wound healing. Intact male and female wild-type mice heal similarly, but gonadectomy revealed the inhibitory effects of androgens in males and the enhancing effects of estrogens (28). In humans, lower total testosterone levels commonly occur with type 2 diabetes (29), which may influence wound healing outcomes. Therefore, we chose to conduct our study in female mice only to limit potential confounding factors. Due to the limited tissue available for harvest from the wound, this study provides only gene expression data of the proposed

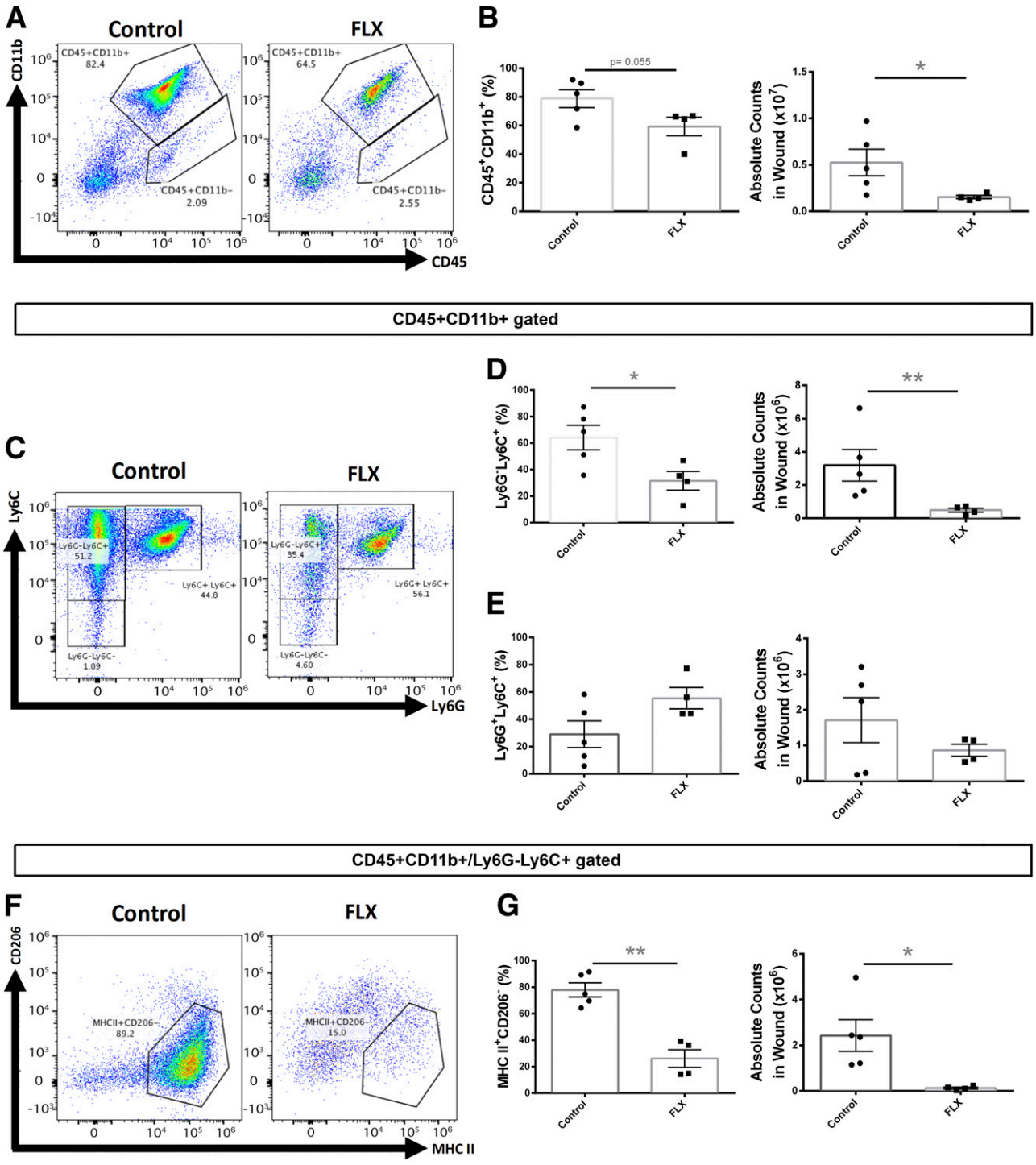

Figure 3—Topical FLX attenuates inflammation at wound site as shown by flow cytometry analysis. Wound cells were quantified based on percent, and cellularity $CD11b^+CD45^+$ myeloid cells are noted to be fewer (% and absolute number) (*A* and *B*). Within the $CD11b^+CD45^+$ population, the $Ly6C^+Ly6G^-$ inflammatory macrophages are decreased (*C* and *D*). No significant change in $Ly6C^+Ly6G^+$ neutrophil counts at wound site (*E*). Decreased numbers and percent of MHCII and $CD206^-$ cells within $Ly6C^+Ly6G$ inflammatory macrophage population (*F* and *G*). Data represented as mean ± SEM. Nonparametric Mann-Whitney *U* tests were performed to assess statistical significance. $^*P \leq 0.05$; $^{**}P \leq 0.01$.

signaling pathways at the wound site. Although gene expression is not always predictive of the protein level, it can be useful in the interpretation of the cellular and molecular events in the wound microenvironment (30,31).

Since FLX has undergone extensive toxicology profiling and safety evaluation, and postmarketing adverse event reporting, the path to translation to clinic for this novel indication could be shortened, and a therapeutic need filled rapidly. We believe that this topical therapeutic represents

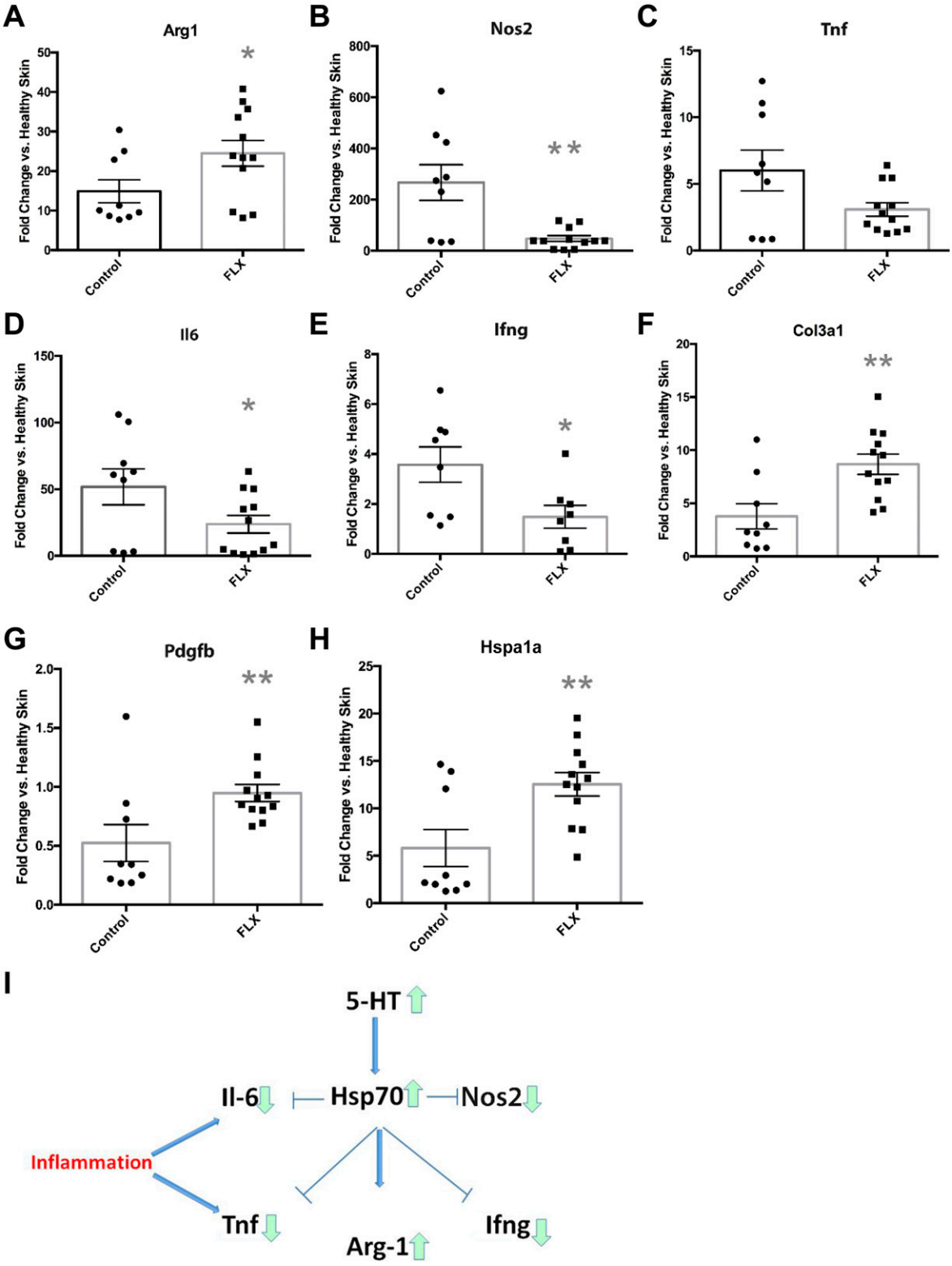

Figure 4—Topical FLX induces gene expression in Hsp70 signaling pathways. qRT-PCR was performed on RNA extracted from flash frozen skin tissues. Fold change in gene expression compared with healthy nonwounded skin was shown for Arg-1 (*A*), inducible NOS (iNOS; Nos2) (*B*), Tnf (*C*), Il6 (*D*), Ifng (*E*), collagen type III α (Col3a1) (*F*), platelet-derived growth factor β (Pdgfb) (*G*), and heat shock 70 kDa protein 1A (Hspa1a) (*H*). Taken together, a signaling pathway for serotonin in cutaneous inflammation was proposed (*I*). Data represented as mean ± SEM. Nonparametric Mann-Whitney *U* tests were performed to assess statistical significance. $^{*}P \leq 0.05$; $^{**}P \leq 0.01$.

Table 1—Primer sequences

Gene target	Forward	Size (bases)	Reverse	Size (bases)
Gapdh	AGGTCGGTGTGAACGGATTTG	21	TGTAGACCATGTAGTTGAGGTCA	23
18s	CCCAACTTCTTAGAGGGACAAG	22	GCTTATGACCCGCACTTACT	20
Tbp	GTTTCTGCGGTCGCGTCATTT	21	TGGGTTATCTTCACACACCATGAA	24
Arg-1	CTCCAAGCCAAAGTCCTTAGAG	22	AGGAGCTGTCATTAGGGACA	20
iNos	GTTCTCAGCCCAACAATACAAGA	23	GTGGACGGGTCGATGTCAC	19
Tnf	CCAGACCCTCACACTCAGATC	21	CACTTGGTGGTTTGCTACGAC	21
Il6	TAGTCCTTCCTACCCCAATTTCC	23	TTGGTCCTTAGCCACTCCTTC	21
Ifng	ATGAACGCTACACACTGCATC	21	CCATCCTTTTGCCAGTTCCTC	21
Col3a1	ACGTAGATGAATTGGGATGCAG	22	GGGTTGGGGCAGTCTAGTG	19
Pdgf-bb	AAGTGTGAGACAATAGTGACCCC	23	CATGGGTGTGCTTAAACTTTCG	22
Hsp70	TGGAGATCATCGCCAACGACC	21	TCCTCCACGAAGTGGCTCACC	21

a safe alternative for the challenging clinical problem of chronic, nonhealing wounds in patients with diabetes.

Acknowledgments. The authors acknowledge Alexander D. Borowsky and the Immunohistochemistry Laboratory at the Mouse Biology Program at the University of California, Davis, for immunohistochemical staining.

Funding. This study was funded by a California Institute for Regenerative Medicine (CIRM) Preclinical Development Award (PC1-08118), a CIRM doctoral training grant (TG2-01163), a National Institutes of Health (National Institute of General Medical Sciences) T32 pharmacology training grant (T32GM099608), and a University of California, Davis, Department of Dermatology Seed Grant.

Duality of Interest. C.M.N., D.M.T., and R.R.I. have a pending patent on the use of FLX in wound healing. No other potential conflicts of interest relevant to this article were reported.

Author Contributions. C.M.N. and D.M.T. proposed experiments, coordinated the work, and prepared the manuscript. C.M.N., D.M.T., M.D.B., M.S., D.F., J.S., and A.A. performed in vivo experiments. C.M.N., M.D.B., A.V.N., and A.M.S. performed flow cytometry experiments. C.M.N. and D.F. performed qRT-PCR experiments. C.M.N., D.N., and B.H. performed scratch wound assays. A.G. performed high-performance liquid chromatography and analyses. D.D. and M.G.G. performed behavioral experiments. J.J.F. and R.W.C. gave early critical input. R.R.I. conceived and oversaw the study and critically edited the manuscript. R.R.I. is the guarantor of this work and, as such, had full access to all the data in the study and takes responsibility for the integrity of the data and the accuracy of the data analysis.

Prior Presentation. This study was presented at the 29th Annual Meeting of the Wound Healing Society, San Diego, CA, 5–9 April 2017, and the 76th Annual Meeting of the Society of Investigative Dermatology, Portland, OR, 26–29 April 2017.

References

1. Powers JG, Higham C, Broussard K, Phillips TJ. Wound healing and treating wounds: chronic wound care and management. J Am Acad Dermatol 2016;74:607–625; quiz 625–626
2. Otero-Viñas M, Falanga V. Mesenchymal stem cells in chronic wounds: the spectrum from basic to advanced therapy. Adv Wound Care (New Rochelle) 2016;5:149–163
3. Nguyen C, Tartar D, So M, Nolta J, Isseroff R. 753 serotonin as a potential therapeutic target for mesenchymal stem cell–mediated improvement of wound healing. J Investig Dermatol 2016;136:S133
4. Slominski A, Pisarchik A, Zbytek B, Tobin DJ, Kauser S, Wortsman J. Functional activity of serotoninergic and melatoninergic systems expressed in the skin. J Cell Physiol 2003;196:144–153
5. Lawrence CM, Matthews JN, Cox NH. The effect of ketanserin on healing of fresh surgical wounds. Br J Dermatol 1995;132:580–586
6. Janssen PA, Janssen H, Cauwenbergh G, et al. Use of topical ketanserin in the treatment of skin ulcers: a double-blind study. J Am Acad Dermatol 1989;21:85–90
7. Di Rosso ME, Palumbo ML, Genaro AM. Immunomodulatory effects of fluoxetine: a new potential pharmacological action for a classic antidepressant drug? Pharmacol Res 2016;109:101–107
8. Fazzino F, Montes C, Urbina M, Carreira I, Lima L. Serotonin transporter is differentially localized in subpopulations of lymphocytes of major depression patients. Effect of fluoxetine on proliferation. J Neuroimmunol 2008;196:173–180
9. Dasu MR, Ramirez SR, La TD, et al. Crosstalk between adrenergic and toll-like receptors in human mesenchymal stem cells and keratinocytes: a recipe for impaired wound healing. Stem Cells Transl Med 2014;3:745–759
10. Park SA, Teixeira LB, Raghunathan VK, et al. Full-thickness splinted skin wound healing models in db/db and heterozygous mice: implications for wound healing impairment. Wound Repair Regen 2014;22:368–380.
11. Stojadinovic O, Brem H, Vouthounis C, et al. Molecular pathogenesis of chronic wounds: the role of beta-catenin and c-myc in the inhibition of epithelialization and wound healing. Am J Pathol 2005;167:59–69
12. Slominski A, Pisarchik A, Johansson O, et al. Tryptophan hydroxylase expression in human skin cells. Biochim Biophys Acta 2003;1639:80–86
13. Udenfriend S, Weissbach H. Turnover of 5-hydroxytryptamine (serotonin) in tissues. Proc Soc Exp Biol Med 1958;97:748–751
14. de las Casas-Engel M, Dominguez-Soto A, Sierra-Filardi E, et al. Serotonin skews human macrophage polarization through HTR2B and HTR7. J Immunol 2013;190:2301–2310.
15. McMurtry AL, Cho K, Young LJT, Nelson CF, Greenhalgh DG. Expression of HSP70 in healing wounds of diabetic and nondiabetic mice. J Surg Res 1999;86:36–41
16. Borges TJ, Wieten L, van Herwijnen MJ, et al. The anti-inflammatory mechanisms of Hsp70. Front Immunol 2012;3:95
17. Otaka M, Odashima M, Tamaki K, Watanabe S. Expression and function of stress (heat shock) proteins in gastrointestinal tract. Int J Hyperthermia 2009;25:634–640
18. Diao J, Yang X, Song X, et al. Exosomal Hsp70 mediates immunosuppressive activity of the myeloid-derived suppressor cells via phosphorylation of Stat3. Med Oncol 2015;32:453
19. Meng X, Harken AH. The interaction between Hsp70 and TNF-alpha expression: a novel mechanism for protection of the myocardium against post-injury depression. Shock 2002;17:345–353
20. Van Molle W, Wielockx B, Mahieu T, et al. HSP70 protects against TNF-induced lethal inflammatory shock. Immunity 2002;16:685–695
21. Hodes GE, Hill-Smith TE, Suckow RF, Cooper TB, Lucki I. Sex-specific effects of chronic fluoxetine treatment on neuroplasticity and pharmacokinetics in mice. J Pharmacol Exp Ther 2010;332:266–273
22. Dulawa SC, Holick KA, Gundersen B, and Hen R. Effects of chronic fluoxetine in animal models of anxiety and depression. Neuropsychopharmacology 2004;29:1321–1330.
23. Bourin M, Hascoët M. The mouse light/dark box test. Eur J Pharmacol 2003;463:55–65
24. Ennaceur A. One-trial object recognition in rats and mice: methodological and theoretical issues. Behav Brain Res 2010;215:244–254
25. Farahani RM, Sadr K, Rad JS, Mesgari M. Fluoxetine enhances cutaneous wound healing in chronically stressed Wistar rats. Adv Skin Wound Care 2007;20:157–165
26. Guo S, Dipietro LA. Factors affecting wound healing. J Dent Res 2010;89:219–229
27. Oyibo SO, Jude EB, Tarawneh I, et al. The effects of ulcer size and site, patient's age, sex and type and duration of diabetes on the outcome of diabetic foot ulcers. Diabet Med 2001;18:133–138
28. Gilliver SC, Ruckshanthi JP, Hardman MJ, Nakayama T, Ashcroft GS. Sex dimorphism in wound healing: the roles of sex steroids and macrophage migration inhibitory factor. Endocrinology 2008;149:5747–5757
29. Dhindsa S, Prabhakar S, Sethi M, Bandyopadhyay A, Chaudhuri A, Dandona P. Frequent occurrence of hypogonadotropic hypogonadism in type 2 diabetes. J Clin Endocrinol Metab 2004;89:5462–5468
30. Deonarine K, Panelli MC, Stashower ME, et al. Gene expression profiling of cutaneous wound healing. J Transl Med 2007;5:11
31. Pradhan L, Cai X, Wu S, et al. Gene expression of pro-inflammatory cytokines and neuropeptides in diabetic wound healing. J Surg Res 2011;167:336–342